Examples to verify and illustrate *ELPLA*

Determining
contact pressures, settlements, moments
and shear forces of slab foundations by the
method of finite elements

Version 2010

Program authors:

M. El Gendy
A. El Gendy

GEOTEC: GEOTEC Software Inc.
PO Box 14001 Richmond Road PO
Calgary AB, Canada T3E 7Y7

http://www.elpla.com
geotec@elpla.com

Contents

Introduction
Purpose of the examples

This book presents analysis of many foundation examples. These examples are presented in order to

- verify the mathematical models used in the program *ELPLA* by comparing *ELPLA* results with closed form or another published results

- illustrate how to use *ELPLA* for analyzing foundation by different subsoil models

The examples discussed in this chapter cover many practical problems. For each example discussed in this book, data files and some computed files are included in *ELPLA* software package. The file names, contents and short description of examples are listed below. Besides, a key figure of each problem that contains the main data concerning the foundation shape, loads and subsoil is also shown.

Examples can be run again by *ELPLA* to examine the details of the analysis or to see how the problem was defined or computed and to display, print or plot the results.

When ordering package *ELPLA*, a CD is delivered. It contains the programs and 29 project data files for test purposes, which are described in this book. Data are stored in 67 files. These data introduce some possibilities to analyze slab foundations by *ELPLA*.

Firstly, the numerical examples were carried out completely to show the influence of different subsoil models on the results. Furthermore, different calculation methods for the same subsoil model are applied to judge the computation basis and the accuracy of results. In some cases the influences of geological reloading, soil layers and also the structure rigidity are considered in the analysis. In addition, for applying *ELPLA* in the practice, typical problems are analyzed as follows:

- Stress in soil or plane stress
- Immediate settlement
- Final consolidation
- Ultimate bearing capacity of the soil
- Modulus of subgrade reaction
- Analysis of beams, grids or frames by FE method
- Floor slabs
- Soil settlement due to surcharge fills
- Flexible, elastic and rigid rafts

For this purpose, the following numerical examples introduce some possibilities to analyze foundations. Many different foundations are chosen, which are considered as some practical cases may be happened in practice. All analyses of foundations were carried out by *ELPLA*, which was developed by *M. El Gendy* / *A. El Gendy*.

Description of the calculation methods

A general computerized mathematical solution based upon the finite elements-method was developed to represent an analysis for foundations on the real subsoil model, and it is capable of analyzing foundations of arbitrarily shape considering holes within the slabs and the interaction of external foundations. The developed computer program is also capable of analyzing different types of subsoil models, especially a three dimensional continuum model that considers any number of irregular layers. Additionally, the program can be used to represent the effect of structural rigidity on the soil foundation system and the influence of temperature change on the slab. In *ELPLA*, there are 9 different numerical methods considered for the analysis of slab foundations as follows:

1. Linear contact pressure
2. Constant modulus of subgrade reaction
3. Variable modulus of subgrade reaction
4. Modification of modulus of subgrade reaction by iteration
5. Modulus of compressibility method for elastic raft on half-space soil medium
6. Modulus of compressibility method for elastic raft (Iteration)
7. Modulus of compressibility method for elastic raft (Elimination)
8. Modulus of compressibility method for rigid raft
9. Modulus of compressibility method for flexible foundation

Besides the above 9 main methods, *ELPLA* can also be used to analyze

- System of flexible, elastic or rigid foundations
- Floor slabs, beams, grids, plane trusses, plane frames and plane stress

File names, contents and short description of examples

File	Content	Foundation shape, loads, subsoil, ... etc.
str	Stress on soil	a) b) 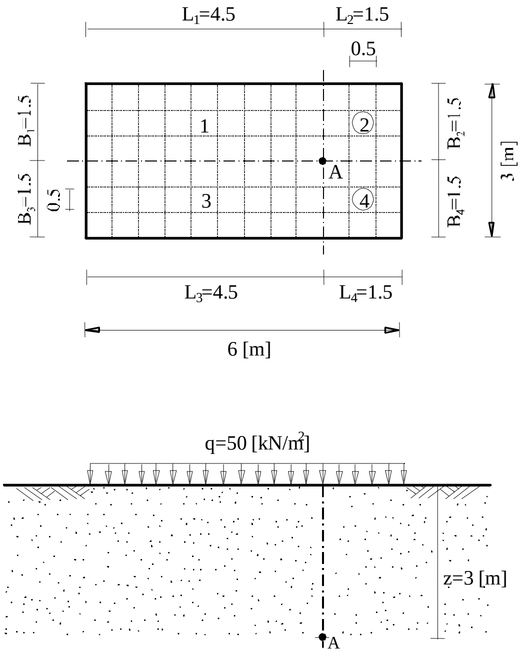
Example 1:	Verifying stress on soil under a rectangular loaded area	

File	Content	Foundation shape, loads, subsoil, ... etc.
cir	Stress on soil	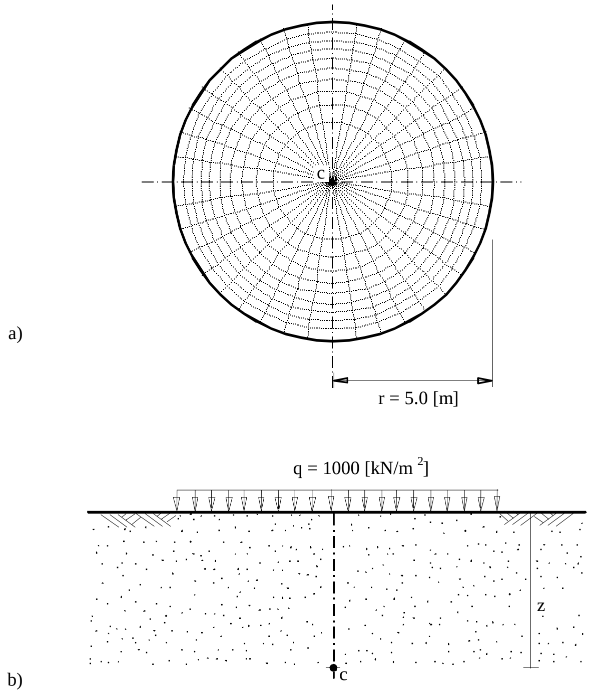

Example 2: Verifying stress on soil under a circular loaded area

File	Content	Foundation shape, loads, subsoil, ... etc.
circ	Circular area	
rec	Rectangular area	
squ	Square area	

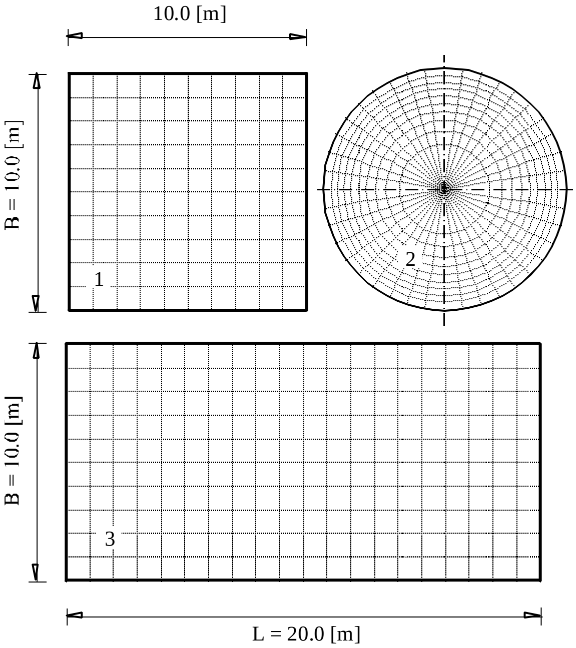

Example 3: Verifying immediate settlement under a loaded area on Isotropic elastic half-space medium

File	Content	Foundation shape, loads, subsoil, … etc.
rec	Immediate settlement	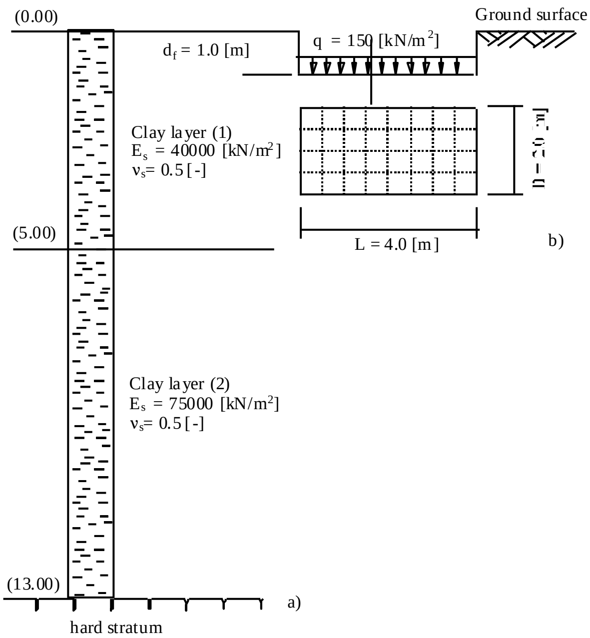

Example 4: Verifying immediate settlement under a rectangular loaded area on layered subsoil

File	Content	Foundation shape, loads, subsoil, ... etc.
tan1	One layer	
tan2	Three layers	

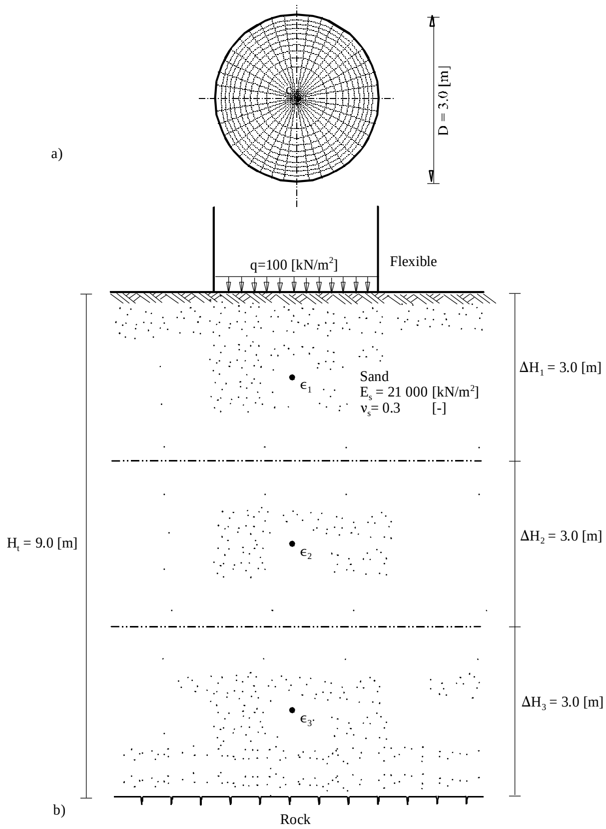

Example 5: Verifying immediate settlement under a circular tank on layered subsoil

File	Content	Foundation shape, loads, subsoil, ... etc.
Cons	Consolidation settlement	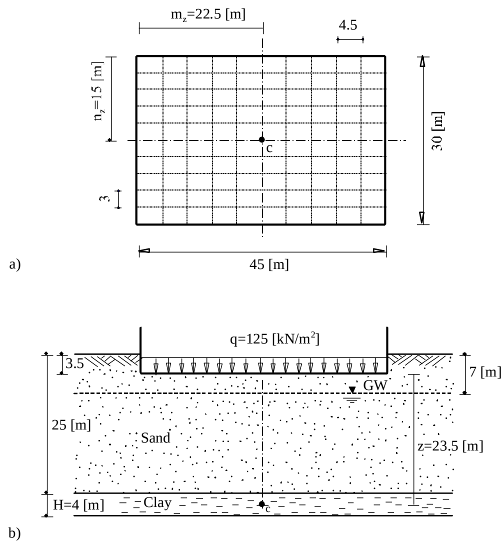

Example 6: Verifying consolidation settlement under a rectangular raft

File	Content	Foundation shape, loads, subsoil, ... etc.
scc	Consolidation settlement	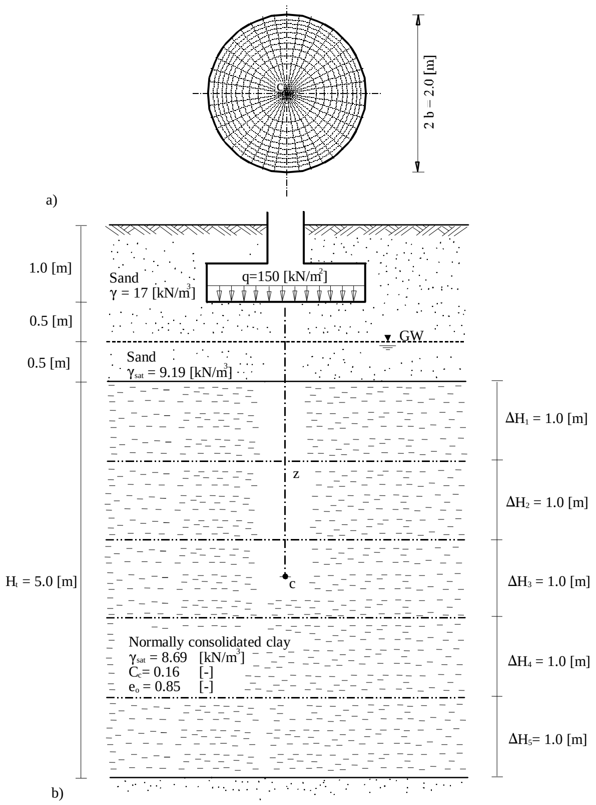

Example 7: Verifying consolidation settlement under a circular footing

File	Content	Foundation shape, loads, subsoil, ... etc.

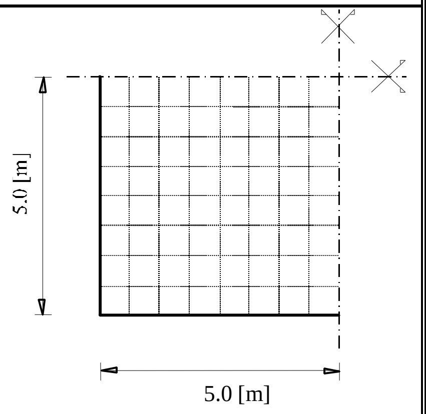

rf2 Raft with 2 * 2 net
rf4 Raft with 4 * 4 net
rf6 Raft with 6 * 6 net
rf8 Raft with 8 * 8 net
rf12 Raft with 12 * 12 net
rf16 Raft with 16 * 16 net
rf20 Raft with 20 * 20 net
rf24 Raft with 24 * 24 net
rf32 Raft with 32 * 32 net
rf48 Raft with 48 * 48 net

Example 8: Verifying rigid square raft on Isotropic elastic half-space medium

rig Rigid raft

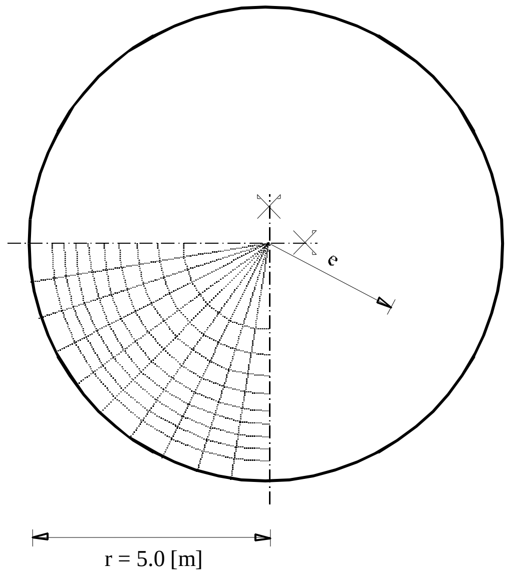

Example 9: Verifying rigid circular raft on Isotropic elastic half-space medium

File	Content	Foundation shape, loads, subsoil, ... etc.
fle rig	Flexible raft Rigid raft	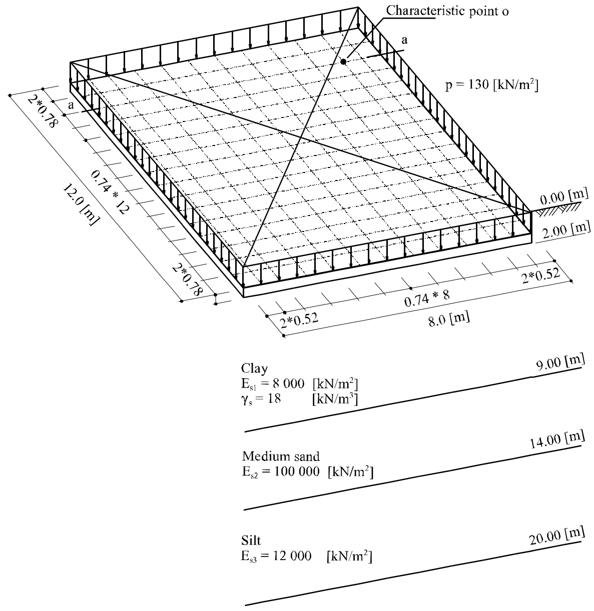
Example 10:	Verifying flexible foundation and rigid raft on layered subsoil	
bea	Ultimate bearing capacity	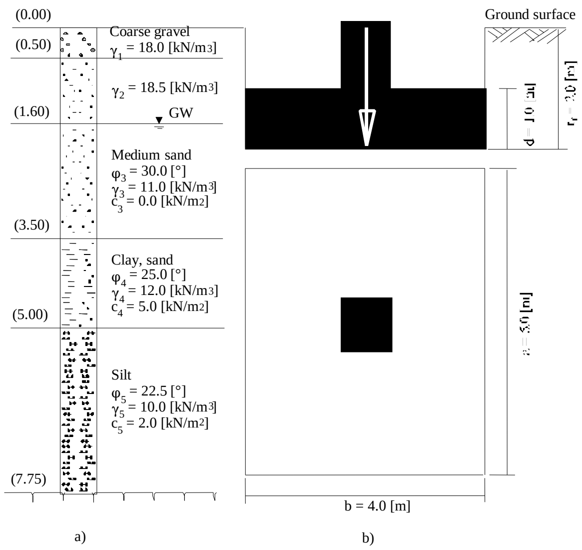
Example 11:	Verifying ultimate bearing capacity for a footing on layered subsoil	

File	Content	Foundation shape, loads, subsoil, ... etc.
lin	Simple assumption model	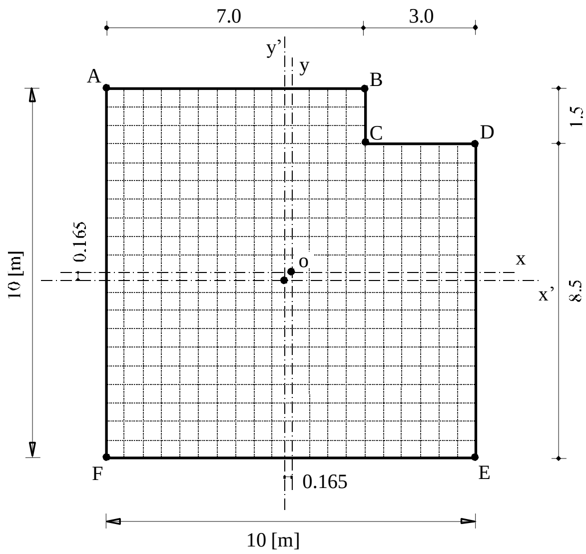

Example 12: Verifying simple assumption model for irregular raft

File	Content	
be1	Modulus of subgrade reaction	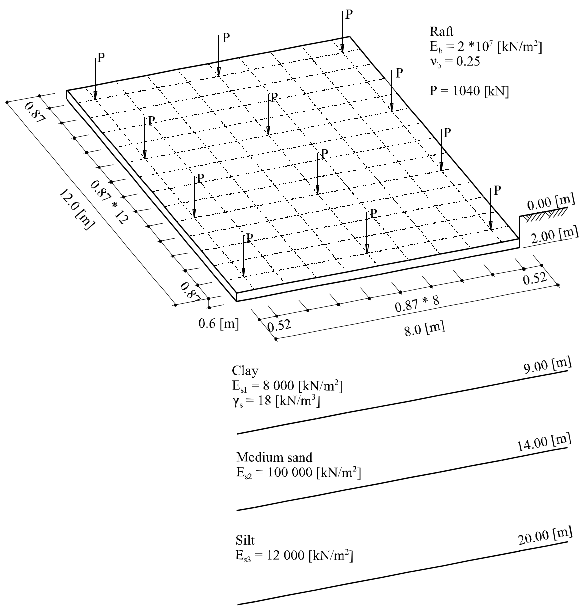

Example 13: Verifying main modulus of subgrade reaction k_{sm}

File	Content	Foundation shape, loads, subsoil, ... etc.

bea Beam foundation

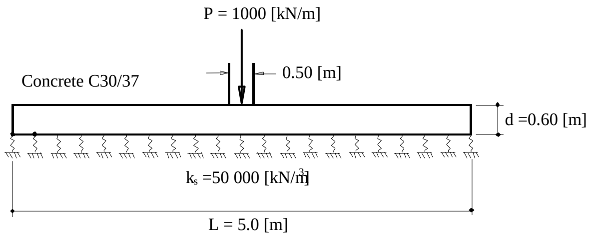

Example 14: Verifying beam foundation on elastic springs

gri grid foundation

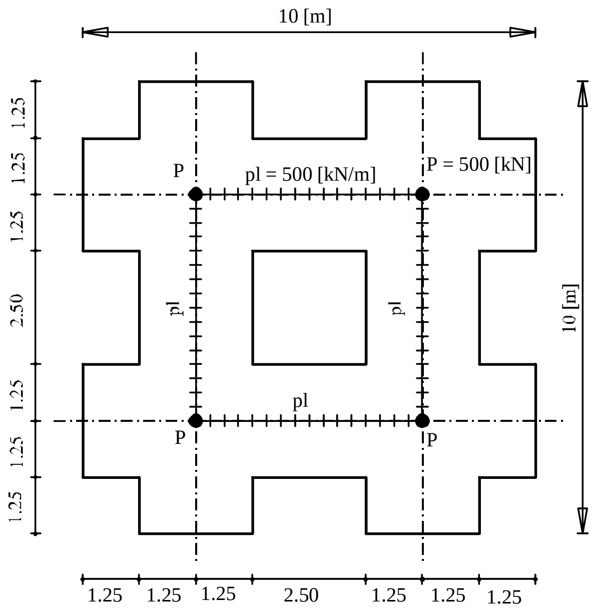

Example 15: Verifying grid foundation on elastic springs

File	Content	Foundation shape, loads, subsoil, ... etc.
ma1	$k_B = \pi/30$, d = 18.5 [cm]	
ma2	$k_B = \pi/10$, d = 26.7 [cm]	
ma3	$k_B = \pi/3$, d = 40 [cm]	

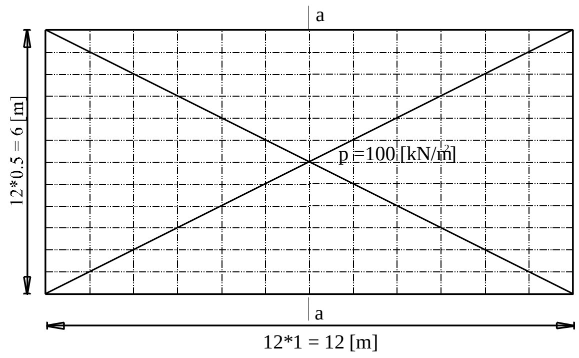

Example 16: Verifying elastic raft on Isotropic elastic half-space soil medium

File	Content	
win	*Winkler's* model	
iso	Half-space soil medium	

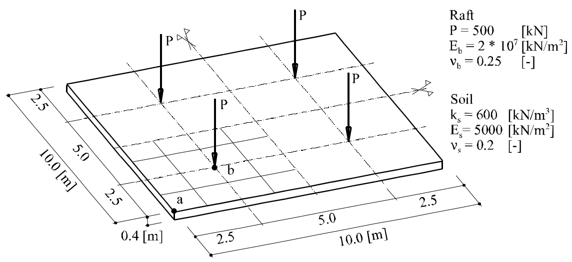

Example 17: Verifying *Winkler's* model and Isotropic elastic half-space soil medium

File	Content	Foundation shape, loads, subsoil, ... etc.
ne1	Slab with 1 element	
ne4	Slab with 4 elements	
ne9	Slab with 9 elements	
ne16	Slab with 16 elements	

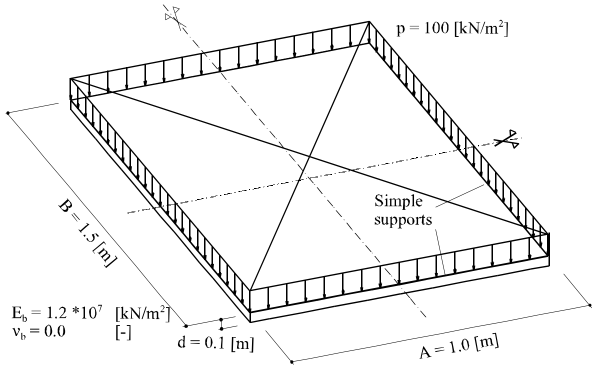

Example 18: Verifying simply supported slab

File	Content	
au1	Method 4	
au2	Method 6	
au3	Method 7	

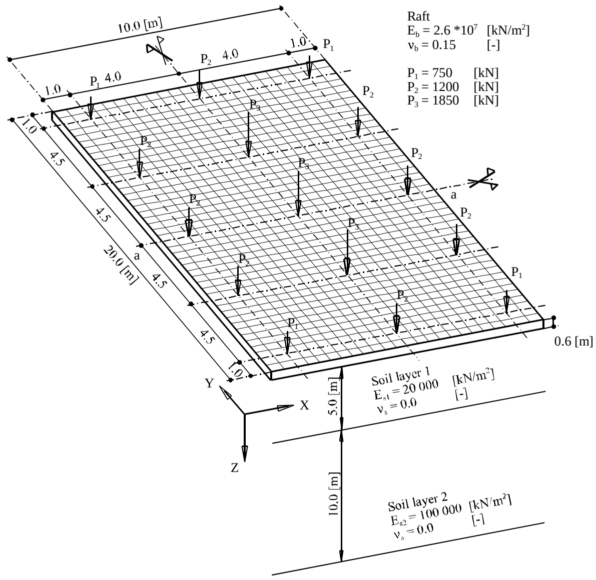

Example 19: Evaluation of iteration methods

File Content Foundation shape, loads, subsoil, ... etc.

vo1 $W_s = E_s$
vo2 W_s = 900 000 000 [kN/m^2]
vo3 $W_s = 3 * E_s$

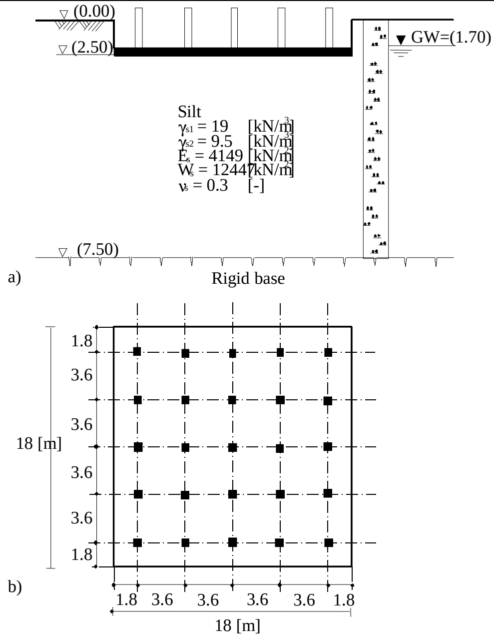

Example 20: Examination of influence of overburden pressure

Load geometry a
qa1 Linear contact pressure method
qa2 Modulus of subgrade reaction method
qa3 Isotropic elastic half-space
qa4 Modulus of compressibility method
qa5 Rigid slab

Load geometry b
qb1 Linear contact pressure method
qb2 Modulus of subgrade reaction method
qb3 Isotropic elastic half-space
qb4 Modulus of compressibility method
qb5 Rigid slab

Load geometry c
qc1 Linear contact pressure method
qc2 Modulus of subgrade reaction method
qc3 Isotropic elastic half-space
qc4 Modulus of compressibility method
qc5 Rigid slab

Load geometry d
qd1 Linear contact pressure method
qd2 Modulus of subgrade reaction method
qd3 Isotropic elastic half-space
qd4 Modulus of compressibility method
qd5 Rigid slab

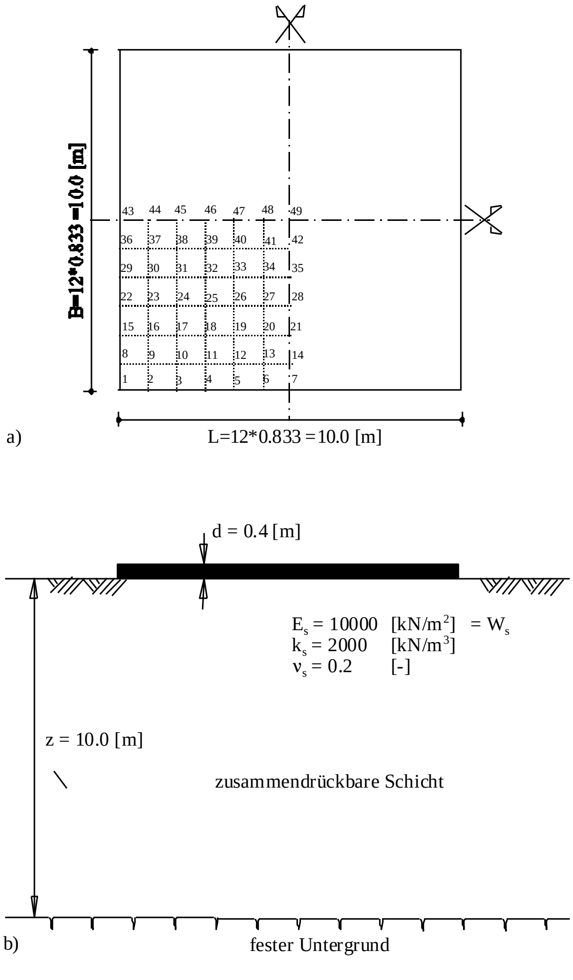

Example 21: Examination of influence of load geometry		
File	Content	Foundation shape, loads, subsoil, ... etc.
flex	Settlement calculation	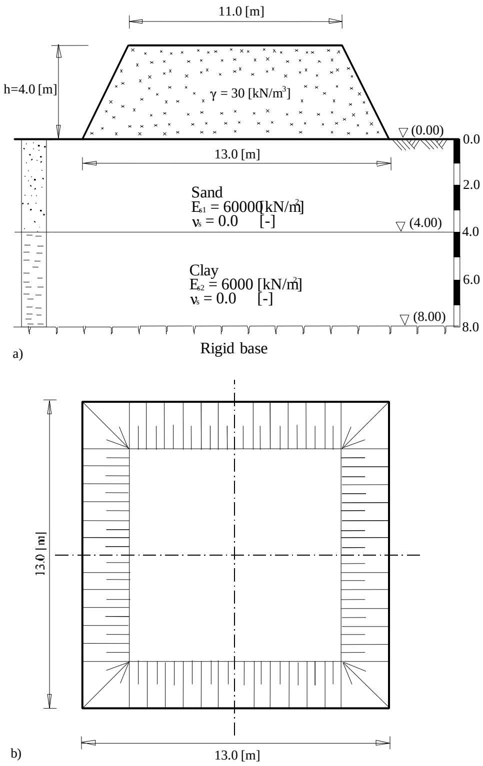

Example 22: Settlement calculation under flexible foundation of an ore heap

File	Content	Foundation shape, loads, subsoil, ... etc.
sta	Rigid raft	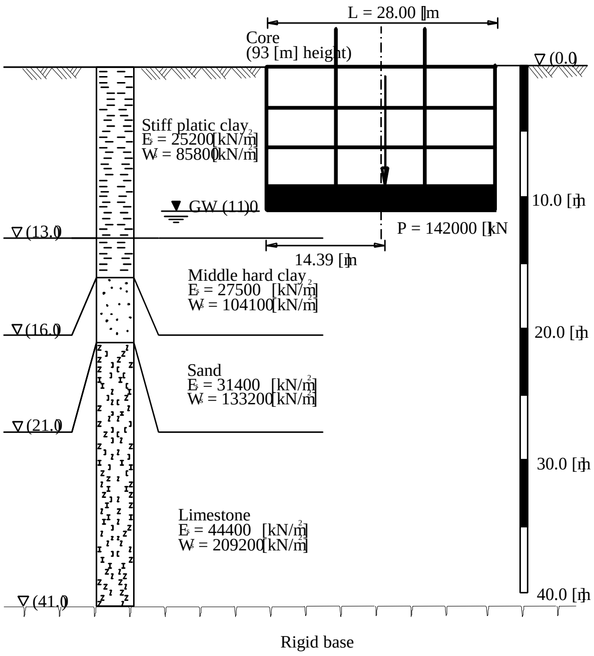
Example 23:	Settlement calculation for a rigid raft subjected to an eccentric load	
Plane Stress 10 10	Mesh size 10 * 10 [cm^2]	
Plane Stress 15 15	Mesh size 15 * 15 [cm^2]	
Plane Stress 20 20	Mesh size 20 * 20 [cm^2]	
Plane Stress 30 30	Mesh size 30 * 30 [cm^2]	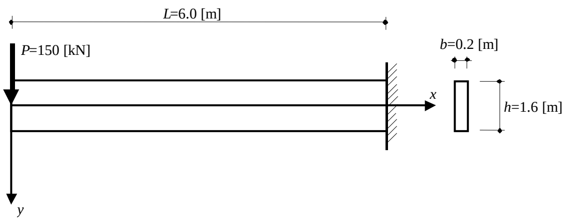
Example 24:	Verifying deflection of a thin cantilever beam	

File	Content	Foundation shape, loads, subsoil, ... etc.
Forces in piles	Pile group	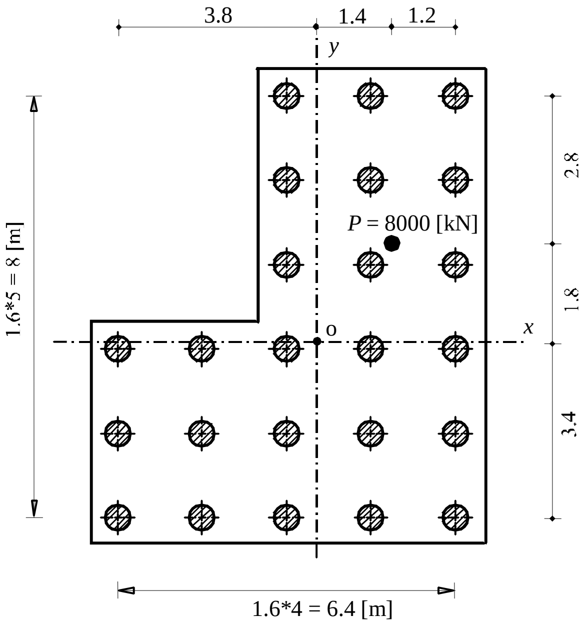
Example 25: Verifying forces in piles of a pile group		
Case a Case b Case c	Case a Case b Case c	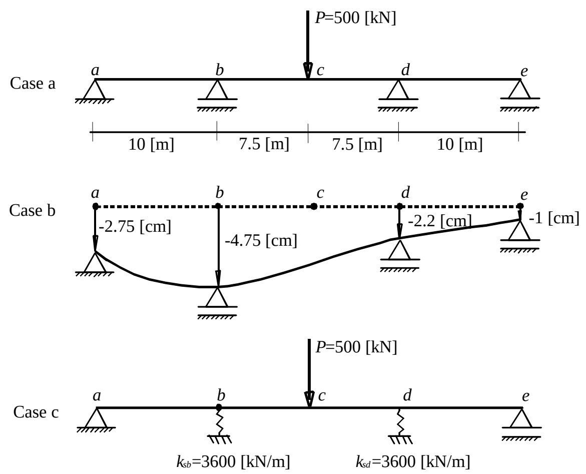
Example 26: Verifying continuous beam		

<table>
<tr><th>File</th><th>Content</th><th>Foundation shape, loads, subsoil, ... etc.</th></tr>
<tr><td>Frame</td><td>Closed frame</td><td>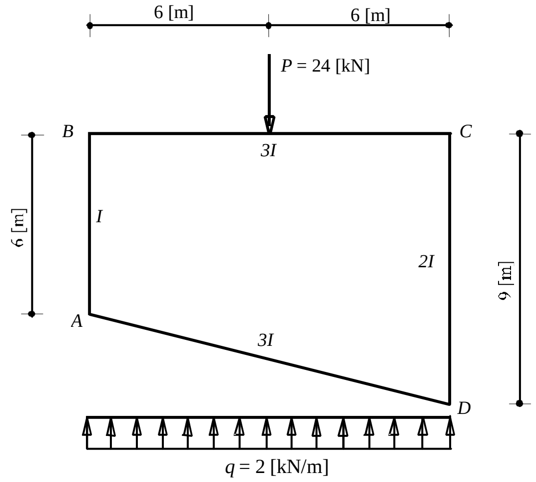
</td></tr>
<tr><td>Example 27:</td><td colspan="2">Verifying moments in an unsymmetrical closed frame</td></tr>
<tr><td>Plane Truss</td><td>Plane Truss</td><td>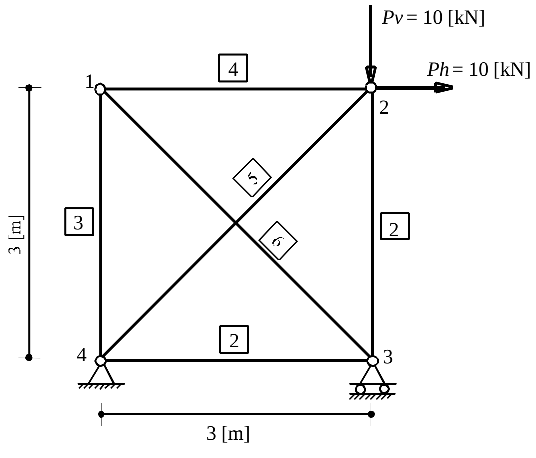
</td></tr>
<tr><td>Example 28:</td><td colspan="2">Verifying plane truss</td></tr>
</table>

File	Content	Foundation shape, loads, subsoil, ... etc.
poi	Settlement calculation	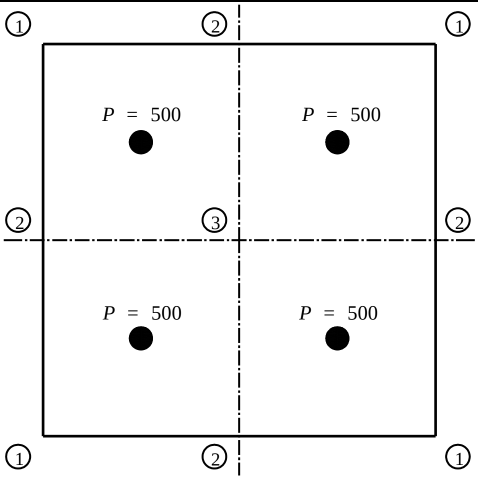

Example 29: Influence of *Poisson's* ratio

Example 1: Verifying stress on soil under a rectangular loaded area

1 Description of the problem

To verify the vertical stress at any point *A* below a rectangular loaded area, the stress on soil obtained by *Das* (1983), Example 6.3, page 370, using influence coefficients of *Newmark* (1935) is compared with that obtained by *ELPLA*.

A distributed load of q = 50 [kN/m^2] acts on a flexible rectangular area 6 [m] × 3 [m] as shown in Figure 1. It is required to determine the vertical stress at a point *A*, which is located at a depth of z = 3 [m] below the ground surface.

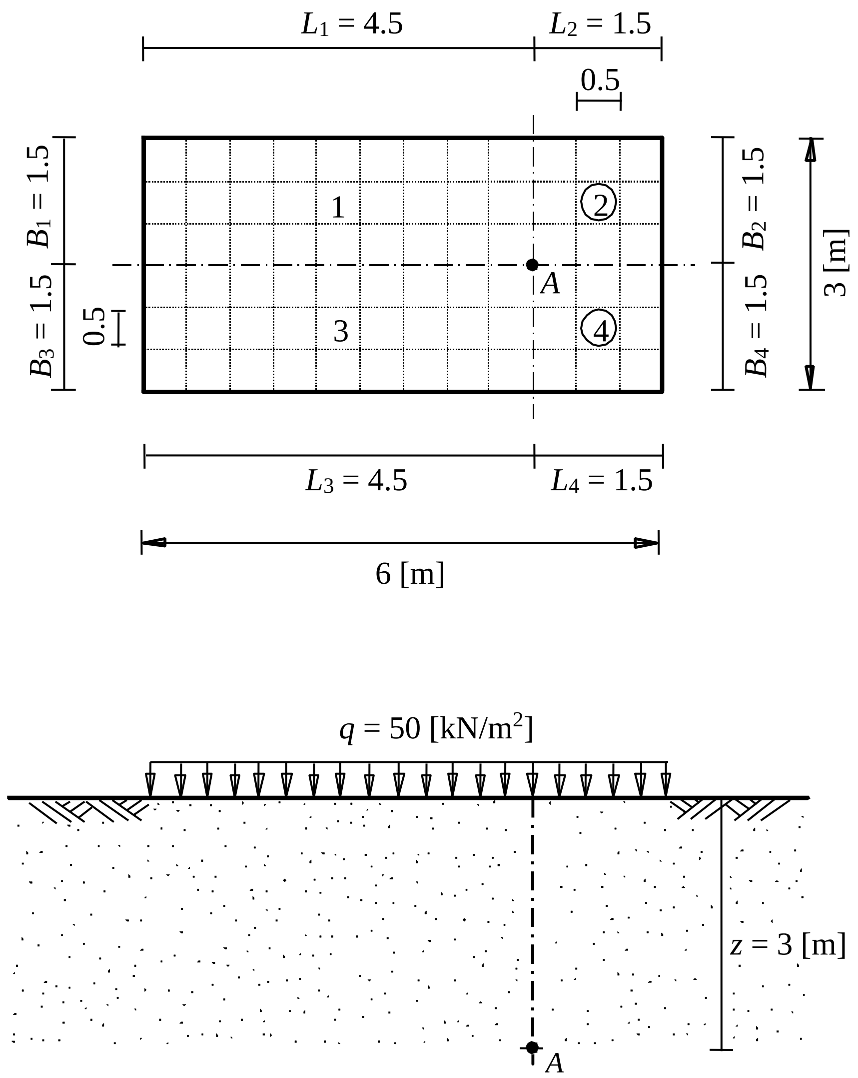

a)

b)

Figure 1 a) Plan of the loaded area with dimensions and FE-Net

b) Cross section through the soil under the loaded area

2 Hand calculation of stress on soil

According to *Das* (1983), the stress on soil can be obtained by hand calculation as follows:

Newmark (1935) has shown that the stress on soil σ_z at a depth z below the corner of a uniformly loaded rectangular area $L \times B$ is given by

$$\sigma_z = q\, I_\sigma \ [\text{kN/m}^2] \qquad (1)$$

where I_σ [-] is the influence coefficient of the soil stress and is given by

m^2

where $m = B/z;\ n = L/z$ [-]

The soil stress σ_z at a point *A* may be evaluated by assuming the stresses contributed by the four rectangular loaded areas using the principle of superposition as shown in Figure 1. Thus,

$$\sigma_z = q(\ I_{\sigma 1} + I_{\sigma 2} + I_{\sigma 3} + I_{\sigma 4}) \ [\text{kN/m}^2] \qquad (2)$$

The determination of influence coefficients for the four rectangular areas is shown in Table 1.

Table 1 Determination of influence coefficients for the four rectangular areas

Area No.	B [m]	L [m]	z [m]	$m = B/z$ [-]	$n = L/z$ [-]	I_σ [-]
1	1.5	4.5	3.0	0.5	1.5	0.131
2	1.5	1.5	3.0	0.5	0.5	0.085
3	1.5	4.5	3.0	0.5	1.5	0.131
4	1.5	1.5	3.0	0.5	0.5	0.085

The stress on soil is given by

$$\sigma_z = 50(\ 0.131 + 0.085 + 0.131 + 0.085) = 21.6 \ [\text{kN/m}^2]$$

3 Stress on soil by *ELPLA*

The contact pressure in this example is known and distributed uniformly on the ground surface. Therefore, the available method "Flexible foundation 9" in *ELPLA* may be used here to determine the stress on soil due to a uniformly rectangular loaded area at the surface. This can be carried out by choosing the option "Determination of limit depth", where the limit depth calculation requires to know the stress on soil against the depth under the foundation. The location of the stress on soil under the loaded area can be defined at any position in *ELPLA*. Here the position of the point A is defined by coordinates x = 4.5 [m] and y = 1.50 [m]. In this example only the stress on soil is required. Therefore, any reasonable soil data may be defined. A net of square elements is chosen. Each element has a side of 0.5 [m] as shown in Figure 1a.

The stress on soil obtained by *ELPLA* under the loaded area at depth 3 [m] below the ground surface is σ_z = 21.5 [kN/m²] and nearly equal to that obtained by hand calculation.

Example 2: Stress on soil under a circular loaded area

1 Description of the problem

To verify the vertical stress at point *c* below the center of a circular loaded area, the influence coefficients of stress I_z below the center of a uniformly loaded area at the surface obtained by *Scott* (1974), Table 12.2, page 287, are compared with those obtained by *ELPLA*.

Figure 2 shows a distributed load of q = 1000 [kN/m^2] that acts on a flexible circular area of radius r = 5 [m]. It is required to determine the vertical stress under the center *c* of the area at different depths *z* up to 10 [m] below the ground surface.

a)

b)

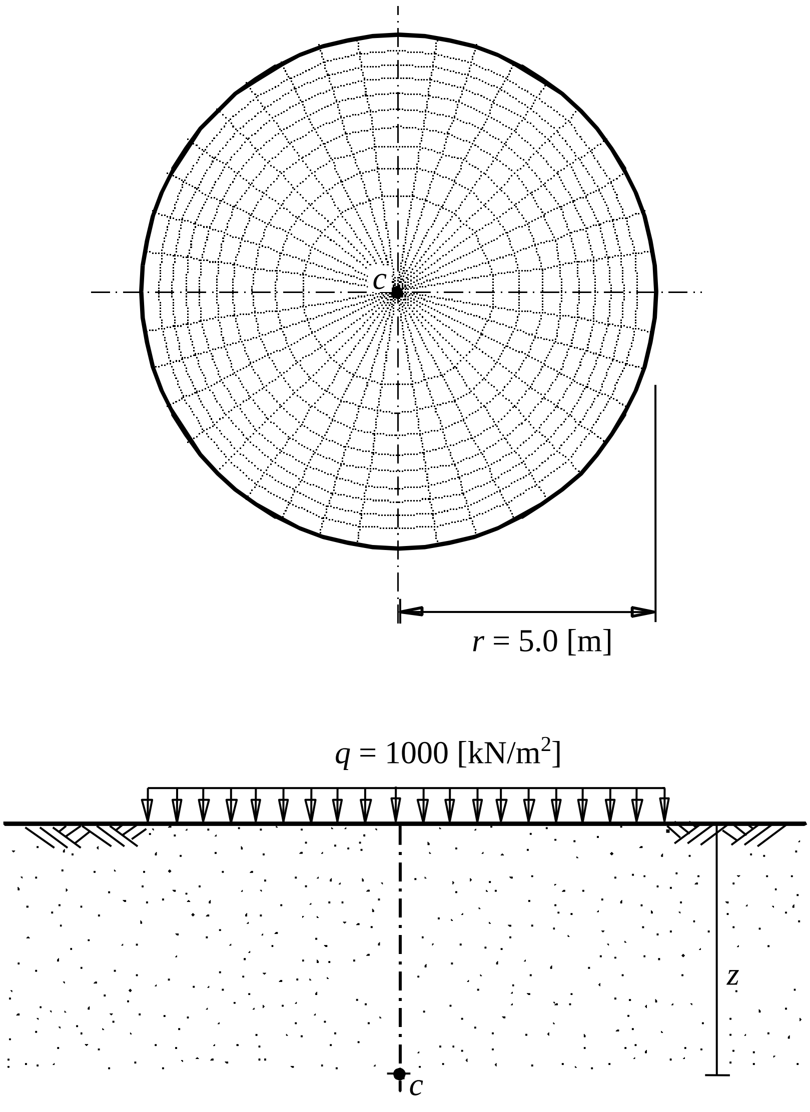

Figure 2 a) Plan of the loaded area with dimensions and FE-Net

b) Cross section through the soil under the loaded area

2 Hand calculation of stress on soil

According to *Scott* (1974), the stress on soil below the center of a uniformly loaded circular area at the surface may be determined by integrating *Boussinesq's* expressions over the relevant area. The stress σ_z [kN/m²] at a depth z [m] under the center of a circular loaded area q [kN/m²] of radius r [m] is given by

$$\sigma_z = q\, I_\sigma \ [\text{kN/m}^2] \qquad (3)$$

where I_σ [-] is the influence coefficient of the soil stress and is given by

$$I_\sigma = 1 - \frac{1}{\left[1+\left(\frac{r}{z}\right)^2\right]^{3/2}}$$

3 Stress on soil by *ELPLA*

The contact pressure in this example is known and distributed uniformly on the ground surface. Therefore, the available method "Flexible foundation 9" in *ELPLA* may be used here to determine the stress on soil due to a uniformly loaded circular area at the surface. This can be carried out by choosing the option "Determination of limit depth", where the limit depth calculation requires to know the stress on soil against the depth under the foundation. The location of the stress on soil under the loaded area can be defined at any position in *ELPLA*. In this example only the stress on soil is required. Therefore, any reasonable soil data may be defined.

The influence coefficients I_σ of the soil stress below the center of a uniformly loaded circular area at the surface are shown in Table 2. From this table, it can be observed that the influence coefficients obtained by *ELPLA* under the loaded circular area at different depths below the ground surface are nearly equal to those obtained by hand calculation from Eq. 3 with maximum difference of Δ = 0.50 [%].

Table 2 Influence coefficient I_σ [-] of the soil stress below the center of a uniformly loaded circular area

z/r [-]	I_σ [-]		Diff. Δ [%]	*z/r* [-]	I_σ [-]		Diff. Δ [%]
	Scott (1974)	*ELPLA*			*Scott* (1974)	*ELPLA*	
0.0	1.000	1.000	0.00	1.3	0.502	0.501	0.20
0.1	0.999	0.999	0.00	1.4	0.461	0.460	0.22
0.2	0.992	0.992	0.00	1.5	0.424	0.423	0.24
0.3	0.976	0.976	0.00	1.6	0.390	0.389	0.26
0.4	0.949	0.949	0.00	1.7	0.360	0.359	0.28
0.5	0.911	0.910	0.11	1.8	0.332	0.331	0.30
0.6	0.864	0.863	0.12	1.9	0.307	0.306	0.33
0.7	0.811	0.811	0.00	2.0	0.284	0.284	0.00
0.8	0.756	0.755	0.13	2.1	0.264	0.263	0.38
0.9	0.701	0.700	0.14	2.2	0.246	0.245	0.41
1.0	0.646	0.645	0.15	2.3	0.229	0.228	0.44
1.1	0.595	0.594	0.17	2.4	0.214	0.213	0.47
1.2	0.547	0.546	0.18	2.5	0.200	0.199	0.50

Example 3: Immediate settlement under a loaded area on Isotropic elastic half-space medium

1 Description of the problem

To verify the mathematical model of *ELPLA* for computing the immediate (elastic) settlement under a loaded area on Isotropic elastic half-space medium, the results of immediate settlement calculations obtained by *Bowles* (1977), Table 5-4, page 157, are compared with those obtained by *ELPLA*.

The vertical displacement *s* under an area carrying a uniform pressure *p* on the surface of Isotropic elastic half-space medium can be expressed as

$$s = \frac{pB\left(1-\nu_s^2\right)}{E_s} I \qquad (4)$$

where:

ν_s	*Poisson's* ratio of the soil [-]
E_s	*Young's* modulus of the soil [kN/m^2]
B	lesser side of a rectangular area or diameter of a circular area [m]
I	Settlement influence factor depending on the shape of the loaded area [-]
p	Load intensity [kN/m^2]

Eq. 4 can be used to estimate the immediate (elastic) settlement of soils such as unsaturated clays and silts, sands and gravels both saturated and unsaturated, and clayey sands and gravels.

Different loaded areas on Isotropic elastic half-space soil medium are chosen as shown in Figure 3. The loaded areas are square, rectangular and circular shapes. Load intensity, dimension of areas and the elastic properties of the soil are chosen to make the first term from Eq. 4 equal to 1.0, hence:

Area side or diameter	B	= 10	[m]
uniform load on the raft	p	= 1000	[kN/m^2]
Young's modulus of the soil	E_s	= 7500	[kN/m^2]
Poisson's ratio of the soil	ν_s	= 0.5	[-]

2 Analysis of the problem

The Isotropic elastic half-space medium for flexible foundation is available in the method "Flexible foundation 9".

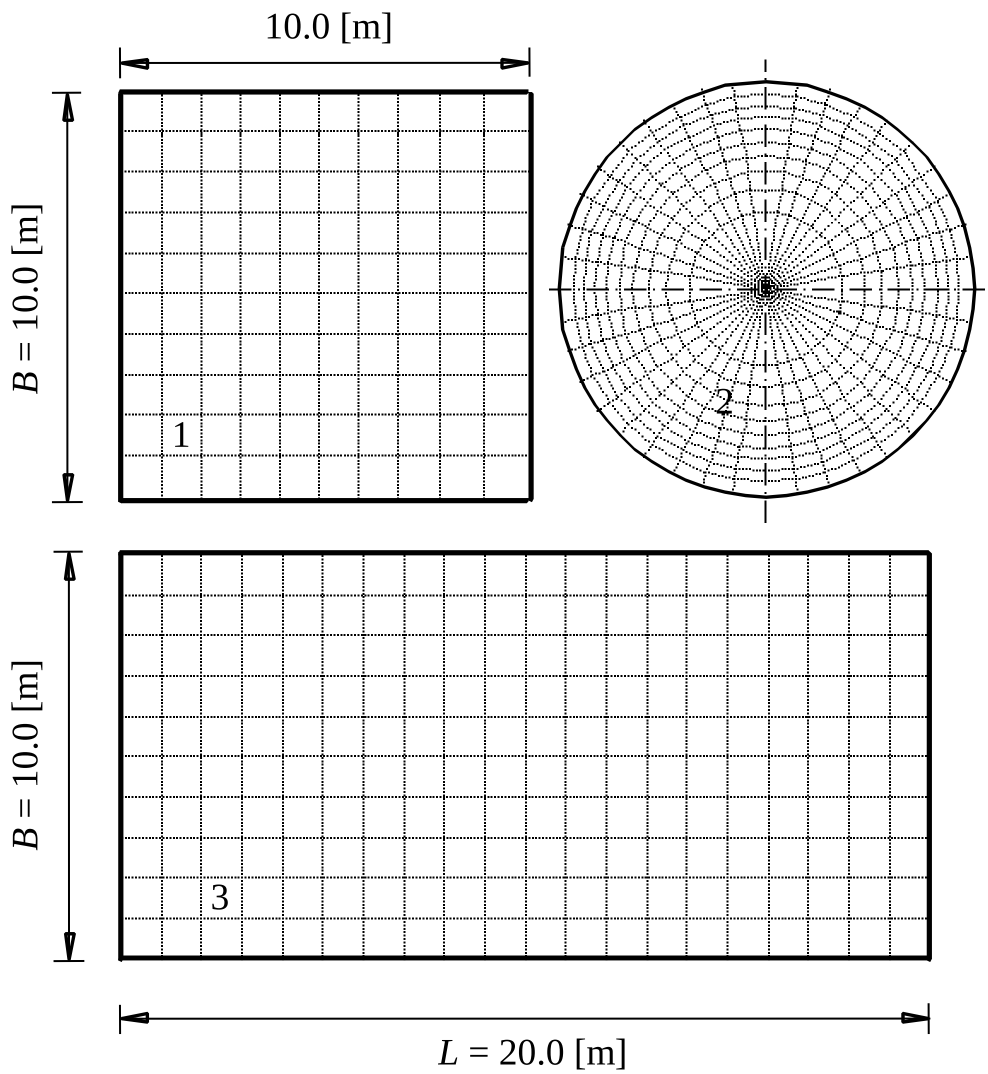

Figure 3 Various loaded areas with dimensions and FE-Nets

3 Results

Table 3 shows the comparison of settlement influence factors *I* obtained by *ELPLA* with those obtained by *Bowles* (1977) for different loaded areas.

Table 3 Comparison of settlement influence factors *I* obtained by *ELPLA* with those obtained by *Bowles* (1977)

Settlement influence factor *I* [-]				
Shape of area	Center		Corner	
	Bowles (1977)	*ELPLA*	*Bowles* (1977)	*ELPLA*
Circle	1.00	1.00	0.64 (edge)	0.63 (edge)
Square	1.12	1.12	0.56	0.56
Rectangular	1.53	1.53	0.77	0.77

Table 3 shows that the results of settlement influence factors *I* obtained by *ELPLA* and those obtained by *Bowles* (1977) are in good agreement.

Example 4: Immediate settlement under a rectangular loaded area on layered subsoil

1 Description of the problem

To verify the mathematical model of *ELPLA* for computing the immediate (elastic) settlement under a rectangular loaded area on layered subsoil, the immediate settlement of saturated clay layers under a rectangular loaded area calculated by *Graig* (1978), Example 6.4, page 175, is compared with that obtained by *ELPLA*.

Janbu/ Bjerrum/ Kjaernsli (1956) presented a solution for the average settlement under an area carrying a uniform pressure q [kN/m^2] on the surface of a limited soil layer using dimensionless factors. Factors are determined for *Poisson's* ratio equal to ν_s = 0.5 [-]. The average vertical settlement s_a [m] is given by

$$s_a = my_0 \; my_1 \frac{qB}{E_s} \qquad (5)$$

where:

μ_0, μ_1 Coefficients for vertical displacement according to *Janbu/ Bjerrum/ Kjaernsli* (1956)
E_s undrained modulus of the soil [kN/m^2]
B lesser side of a rectangular area [m]
q Load intensity [kN/m^2]

Eq. 5 can be used to estimate the immediate (elastic) settlement of loaded areas on saturated clays; such settlement occurs under undrained conditions. The principle of superposition can be used in cases of a number of soil layers each having a different undrained modulus E_s.

A foundation 4 [m] × 2 [m], carrying a uniform pressure of q = 150 [kN/m^2], is located at a depth of d_f = 1.0 [m] in a layer of clay 5.0 [m] thick for which the undrained modulus of the layer E_s is 40 [MN/m^2]. The layer is underlain by a second clay layer 8.0 [m] thick for which the undrained modulus of the layer E_s is 75 [MN/m^2]. A hard stratum lies below the second layer. A plan of the foundation with dimensions and FE-Net as well as a cross section through the soil under the foundation are presented in Figure 4. It is required to determine the average immediate settlement under the foundation.

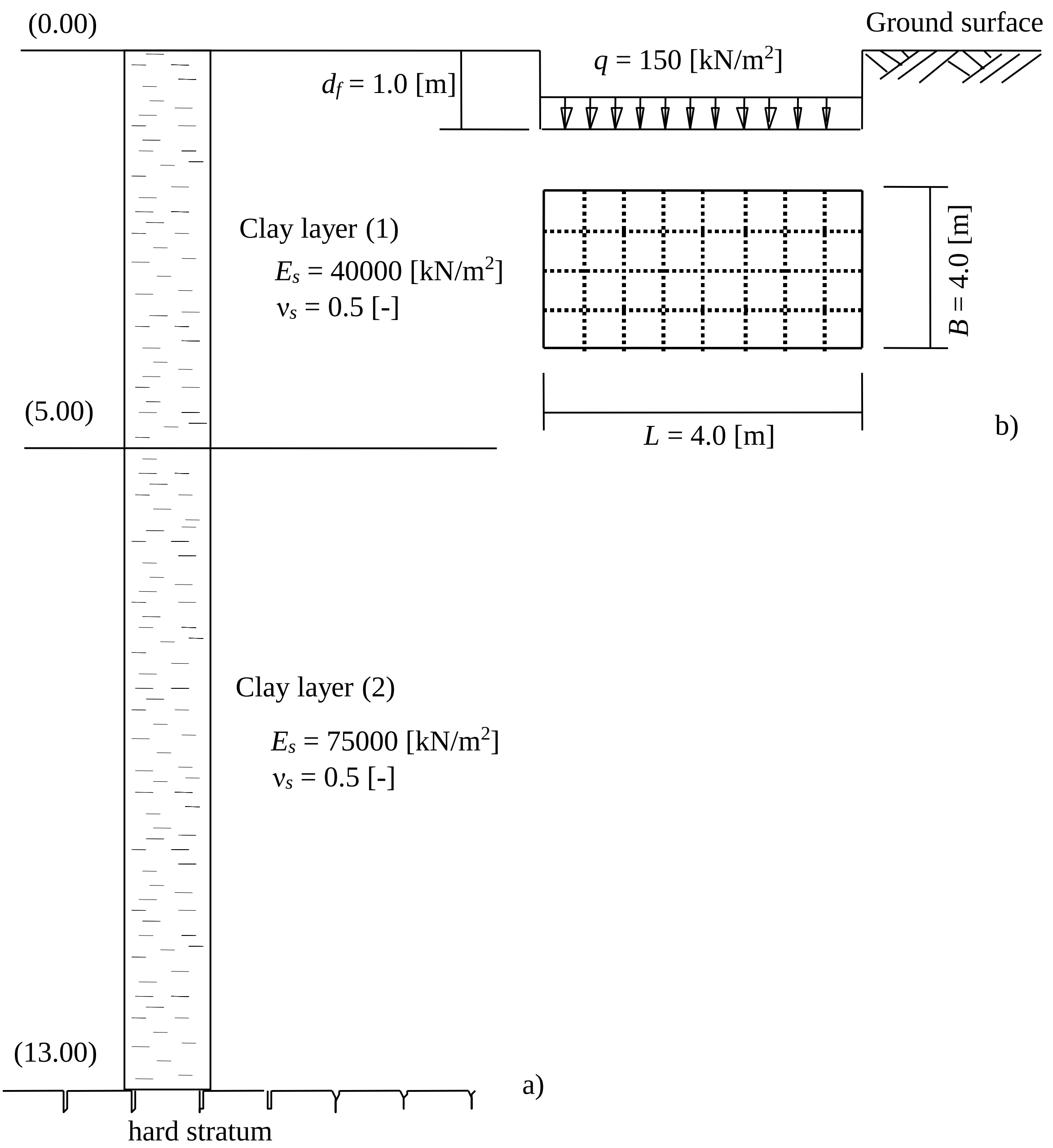

Figure 4 a) Cross section through the soil under the foundation

b) Plan of the foundation with dimensions and FE-Net

2 Hand calculation of the immediate settlement

According to *Graig* (1978), the average immediate settlement under the foundation can be obtained by hand calculation as follows:

Determination of the coefficient μ_0

$$\frac{d_f}{B} = \frac{1}{2} = 0.5[-] \text{ and } \frac{L}{B} = \frac{4}{2} = 2\ [-]$$

From charts of *Janbu/ Bjerrum/ Kjaernsli* (1956)

$$my_0 = 0.9 \text{ [-]}$$

a) Considering the upper clay layer, with E_s = 40 [MN/m^2] and thickness H = 4.0 [m]

$$\frac{H}{B} = \frac{4}{2} = 2 \text{ [-] and } \frac{L}{B} = \frac{4}{2} = 2 \text{ [-]}$$

then my_1 = 0.7 [-]

Hence from Eq. 5

$$s_{a1} = 0.9 \times 0.7 \times \frac{150 \times 2}{40000} = 0.0047 \text{ [m]} = 0.47 \text{ [cm]}$$

b) Considering the two layers combined, with E_s = 75 [MN/m^2] and thickness H = 12.0 [m]

$$\frac{H}{B} = \frac{12}{2} = 6 \text{ [-] and } \frac{L}{B} = \frac{4}{2} = 2 \text{ [-]}$$

then my_1 = 0.9 [-]

Hence from Eq. 5

$$s_{a2} = 0.9 \times 0.9 \times \frac{150 \times 2}{75000} = 0.0032 \text{ [m]} = 0.32 \text{ [cm]}$$

c) Considering the upper layer, with E_s = 75 [MN/m^2] and thickness H = 4.0 [m]

$$\frac{H}{B} = \frac{4}{2} = 2 \text{ [-] and } \frac{L}{B} = \frac{4}{2} = 2 \text{ [-]}$$

then my_1 = 0.7 [-]

Hence from Eq. 5

$$s_{a3} = 0.9 \times 0.7 \times \frac{150 \times 2}{75000} = 0.0025 \text{ [m]} = 0.25 \text{ [cm]}$$

Hence, using the principle of superposition, the average immediate settlement s_a of the foundation is given by

$$s_a = s_{a1} + s_{a2} - s_{a3} = 0.47 + 0.32 - 0.25 = 0.54 \text{ [cm]}$$

For rectangular flexible foundation the average settlement s_a is equal to 0.85. Then, the central immediate settlement s_c of the foundation is given by

$$s_c = \frac{1}{0.85} s_a = \frac{0.54}{0.85} = 0.64 \text{ [cm]}$$

Christian/ Carrier (1978) carried out a critical evaluation of the factors μ_0 and μ_1 of *Janbu/ Bjerrum/ Kjaernsli* (1956). The results are presented in a graphical form. The interpolated values of μ_0 and μ_1 from these graphs are given in Table 4. The average settlement s_c according to this table is s_c = 0.60 [cm].

Table 4 Factors μ_0 and μ_1 according to *Christian/ Carrier* (1978)

Variation of μ_0 with d_f/B

d_f/B	μ_0
0	1.0
2	0.9
4	0.88
6	0.875
8	0.87
10	0.865
12	0.863
14	0.860
16	0.856
18	0.854
20	0.850

Variation of μ_1 with L/B

H/B	Circle	L/B				
		1	2	5	10	∞
1	0.36	0.36	0.36	0.36	0.36	0.36
2	0.47	0.53	0.63	0.64	0.64	0.64
4	0.58	0.63	0.82	0.94	0.94	0.94
6	0.61	0.67	0.88	1.08	1.14	1.16
8	0.62	0.68	0.90	1.13	1.22	1.26
10	0.63	0.70	0.92	1.18	1.30	1.42
20	0.64	0.71	0.93	1.26	1.47	1.74
30	0.66	0.73	0.95	1.29	1.54	1.8
						4

3 Immediate settlement by *ELPLA*

The available method "Flexible foundation 9" in *ELPLA* is used to determine the immediate settlement under the center of the foundation. A net of equal square elements is chosen. Each element has a side of 0.5 [m] as shown in Figure 4b. The immediate settlement obtained by *ELPLA* under the center of the raft is s_c = 0.65 [cm] and nearly equal to that obtained by hand calculation.

Example 5: Immediate settlement under a circular tank on layered subsoil

1 Description of the problem

To verify the immediate settlement under a circular loaded area calculated by *ELPLA*, the immediate settlement at the center of a tank calculated by *Das* (1983), Example 6.2, page 354, is compared with that obtained by *ELPLA*.

A circular tank of 3.0 [m] diameter is considered as shown in Figure 5. The base of the tank is assumed to be flexible and having a uniform contact pressure of q = 100 [kN/m^2]. A sand layer 9.0 [m] thick is located under the tank. The modulus of elasticity of the sand is E_s = 21000 [kN/m^2] while *Poisson's* ratio of the sand is ν_s = 0.3 [-]. It is required to determine the immediate settlement at the center of the tank for two cases:

- Considering the underlying soil as one layer of 9.0 [m] thickness
- Dividing the underlying soil into three layers of equal thickness of 3.0 [m]

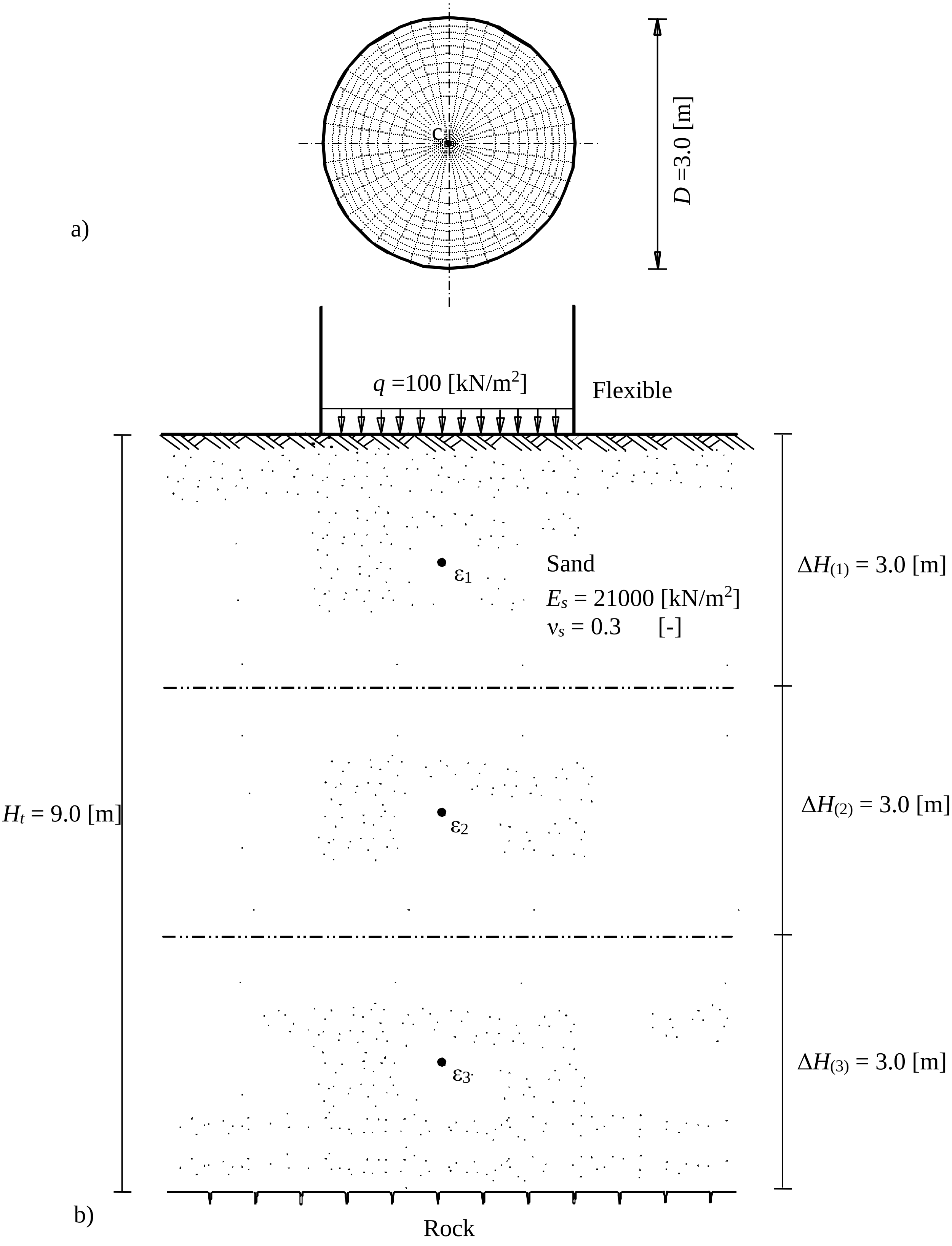

Figure 5 a) Plan of the tank with dimensions and FE-Net

b) Cross section through the soil under the tank

2 Hand calculation of the immediate settlement

According to *Das* (1983), the immediate settlement at the center of the tank can be obtained by hand calculation as follows:

a) Considering the underlying soil as one layer of 9.0 [m] thickness

The vertical deflection s_e [m] under the center of a circular loaded area at a depth z [m] from the surface can be obtained from

$$s_e = q \frac{1 + ny_s}{E_s} r \left[\frac{z}{r} I_1 + (1 - ny_s) I_2\right] \qquad (6)$$

where:

I_1, I_2	Coefficients for vertical deflection (which is a function of z/r and s/r) according to *Ahlvin/ Ulery* (1962) [-]
ν_s	*Poisson's* ratio of the soil [-]
E_s	Modulus of elasticity of the soil [kN/m^2]
r	Radius of the circular area [m]
q	Load intensity [kN/m^2]
s	Distance from the center of the circular area [m]

Settlement at the surface $s_{e\,(z=0)}$

At surface z/r = 0 and s/r = 0. Then, I_1 = 1 and I_2 = 2

$$s_{e(z=0)} = 100 \frac{1 + 0.3}{21000} 1.5 \left[0 + (1 - 0.3)2\right] = 0.013 \text{ [m]}$$

Settlement at depth z = 9.0 [m] from the surface $s_{e\,(z=9)}$

For z/r = 9/1.5 = 6 and s/r = 0. Then, I_1 = 0.01361 and I_2 = 0.16554

$$s_{e(z=9)} = 100 \frac{1 + 0.3}{21000} 1.5 \left[\frac{9}{1.5} 0.0136 + (1 - 0.3)0.16554\right] = 0.00183 \text{ [m]}$$

The immediate settlement s_e is given by

$$s_e = s_{e(z=0)} - s_{e(z=9)} = 0.0130 - 0.00183 = 0.01117 \text{ [m]}$$

b) Dividing the underlying soil into three layers of equal thickness of 3.0 [m]

Another general method for estimation of immediate settlement is to divide the underlying soil into *n* layers of finite thickness $\Delta H_{(i)}$. If the strain $\varepsilon_{z(i)}$ at the middle of each layer can be calculated, the total immediate settlement s_e [m] can be obtained as

$$s_e = \sum_{i=1}^{i=n} \Delta H_{(i)} \, \varepsilon_{z(1)} \qquad (7)$$

The strain ε_z at the middle of the layer is given by

$$\varepsilon_z = q \frac{1 + ny_s}{E_s} \left[\left(1 - 2ny_s \right) A' + B' \right] \qquad (8)$$

where:

A', B' Coefficients for vertical deflection (which is a function of *z/r* and *s/r*) according to *Ahlvin/ Ulery* (1962)

Layer (1)

For z/r = 1.5/1.5 = 1 and s/r = 0. Then, A' = 0.29289 and B' = 0.35355

Layer (2)

For z/r = 4.5/1.5 = 3 and s/r = 0. Then, A' = 0.05132 and B' = 0.09487

Layer (3)

For z/r = 7.5/1.5 = 5 and s/r = 0. Then, A' = 0.01942 and B' = 0.03772

The final stages in the calculation are listed in Table 5.

Table 5 Final stages in the calculation of immediate settlement s_e

Layer No.	Layer thickness $\Delta H_{(i)}$ [m]	Strain at the center of the layer $\varepsilon_{z(i)}$ [-]	Immediate settlement $s_{e(i)}$ [m]
1	3.0	0.00291	0.00873
2	3.0	0.00071	0.00213
3	3.0	0.00028	0.00084
Total immediate settlement $s_e = \sum$			0.0117

3 Immediate settlement by *ELPLA*

The tank rests on a layer of sand. However, in *ELPLA*, it will be sufficiently accurate to consider the sand layer as a whole but the immediate settlement is to be calculated twice. The first calculation by considering the underlying soil as one layer of 9.0 [m] thickness and the second calculation by dividing the underlying soil into three layers of equal thickness of 3.0 [m]. The contact pressure of the tank in this example is known where the tank base is considered to be flexible. Therefore, the available method "Flexible foundation 9" in *ELPLA* is used here to determine the immediate settlement of the sand layer. The immediate settlements obtained by *ELPLA* under the center of the tank in both cases of calculations are compared with those obtained by hand calculation in Table 6.

Table 6 Comparison of immediate settlements s_e [cm] obtained by *ELPLA* and *Das* (1983)

Calculation	s_e [cm]	
	Das (1983)	*ELPLA*
Considering the underlying soil as one layer	1.117	1.115
Dividing the underlying soil into three layers	1.170	1.115

Table 6 shows that results of the immediate settlements obtained by *ELPLA* and those obtained by *Das* (1983) for both cases are in good agreement.

Example 6: Consolidation settlement under a rectangular raft

1 Description of the problem

To verify the consolidation settlement calculated by *ELPLA*, the final consolidation settlement of a clay layer under a rectangular raft calculated by *Graig* (1978), Example 7.2, page 186, is compared with that obtained by *ELPLA*.

A building supported on a raft 45 [m] × 30 [m] is considered. The contact pressure is assumed to be uniformly distributed and equal to q = 125 [kN/m^2]. The soil profile is as shown in Figure 6. The coefficient of volume change for the clay is m_v = 0.35 [m^2/MN]. It is required to determine the final settlement under the center of the raft due to consolidation of the clay.

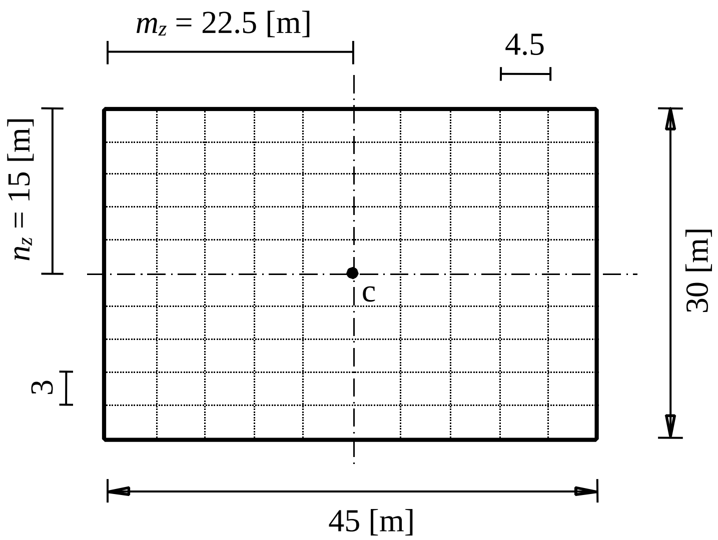

a)

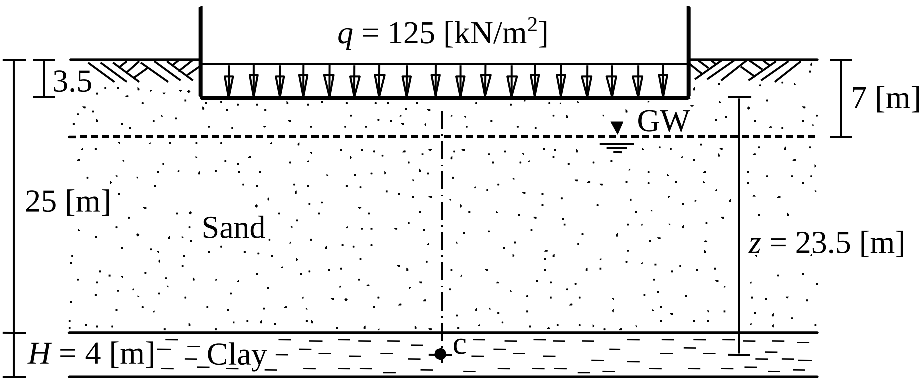

b)

Figure 6 a) Plan of the raft with dimensions and FE-Net

b) Cross section through the soil under the raft

2 Hand calculation of consolidation

According to *Graig* (1978), the consolidation of the clay layer can be obtained by hand calculation as follows:

The clay layer is thin relative to the dimensions of the raft. Therefore, it can be assumed that the consolidation is approximately one-dimensional. In this case, it will be sufficiently accurate to consider the clay layer as a whole. The consolidation settlement is to be calculated in terms of m_v. Therefore, only the effective stress increment at mid-depth of the layer is required. The increment is assumed constant over the depth of the layer. Also, $\Delta\sigma' = \Delta\sigma$ for one-dimensional consolidation and can be evaluated from *Fadum's* charts (1948), Figure 7.

The effective stress increment $\Delta\sigma'$ at mid-depth z = 23.5 [m] of the layer below the center of the raft is obtained as follows

$$\mathbf{m} = \frac{\mathbf{m_z}}{\mathbf{z}} = \frac{22.5}{23.5} = 0.96 \text{ [-]}$$

$$\mathbf{n} = \frac{\mathbf{n_z}}{\mathbf{z}} = \frac{15}{23.5} = 0.64 \text{ [-]}$$

From *Fadum's* charts (1948)

$$I_r = 0.14 \text{ [-]}$$

The effective stress $\Delta\sigma'$ is given by

$$\Delta\sigma' = 4\, I_r\, q = 4\times0.14\times125 = 70 \text{ [kN/m}^2\text{]}$$

The final consolidation settlement s_c is given by

$$s_c = \Delta\sigma'\, m_v\, H = 0.35\times70\times4 = 98 \text{ [mm]} = 9.8 \text{ [cm]}$$

3 Consolidation by *ELPLA*

The raft rests on two different soil layers. The first layer is sand of 21.5 [m] thickness, while the second layer is clay 4.0 [m] thick as shown in Figure 6. As it is required to determine the settlement due to the consolidation of the clay only, the settlement due to the sand can be eliminated by assuming very great value for modulus of compressibility of the sand E_{s1}. Consequently, the settlement due to the sand tends to zero. The settlement due to the sand becomes nearly equal to zero when for example $E_{s1} = 1 \times 10^{20}$ [kN/m²]. The modulus of compressibility of the clay E_{s2} is obtained from the modulus of volume change m_v as

$$\mathbf{E_{s2}} = \frac{\mathbf{1}}{\mathbf{m_v}} = \frac{1}{0.35} = 2.857 \text{ [MN/m}^2\text{]} = 2857 \text{ [kN/m}^2\text{]}$$

Because the settlement is considered in the vertical direction only, *Poisson's* ratio for the clay is assumed to be zero, $\nu_s = 0.0$ [-].

The contact pressure of the raft in this example is known. Also, the raft rigidity is not required. Therefore, the available method "Flexible foundation 9" in *ELPLA* may be used here to determine the consolidation of the clay. A coarse FE-Net may be chosen, where more details about the results are not required, only the settlement under the center of the raft due to consolidation of the clay. A net of equal elements is chosen. Each element has dimensions of 3 [m] × 4.5 [m] as shown in Figure 6a. The final consolidation settlement of the clay under the center of the raft obtained by the program *ELPLA* is s_c = 9.8 [cm] and quite equal to that obtained by hand calculation.

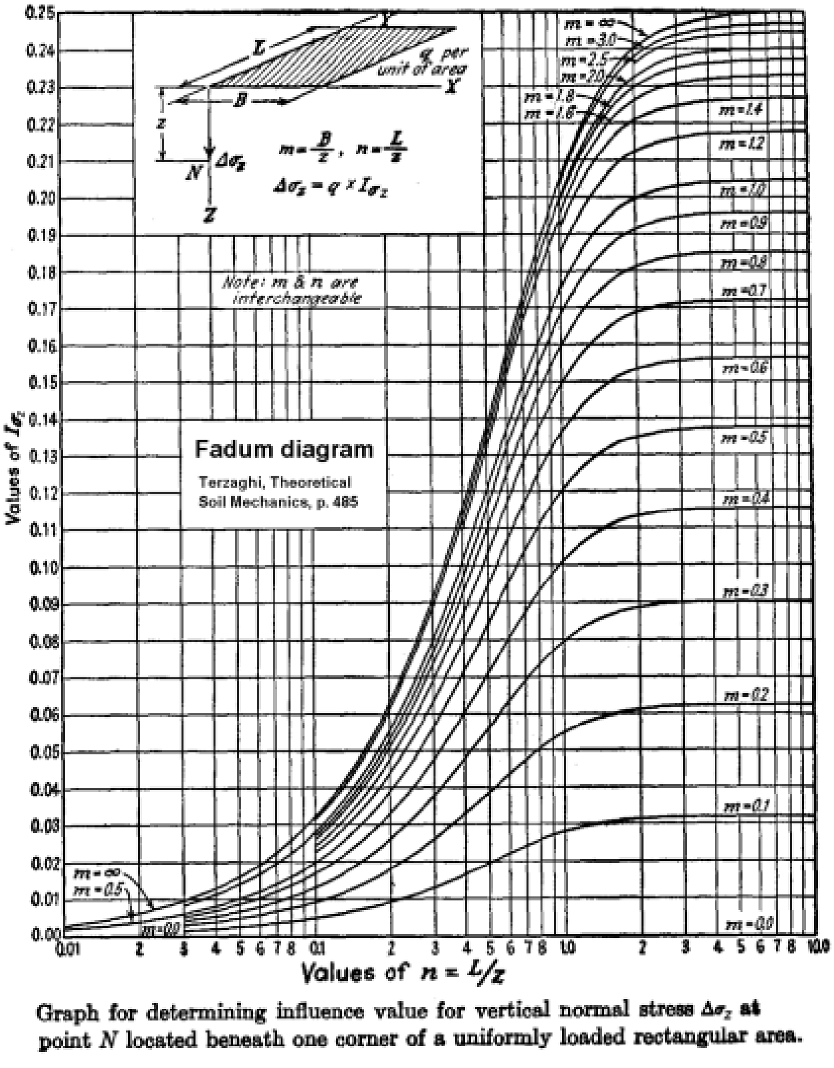

Figure 7 *Fadum* diagram after *Terzaghi* (1970)

Example 7: Consolidation settlement under a circular footing

1 Description of the problem

To verify the consolidation settlement calculated by *ELPLA*, the final consolidation settlement of a clay layer under a circular footing calculated by *Das* (1983), Example 6.3, page 371, is compared with that obtained by *ELPLA*.

A circular footing 2 [m] in diameter at a depth of 1.0 [m] below the ground surface is considered as shown in Figure 8. Water table is located at 1.5 [m] below the ground surface. The contact pressure under the footing is assumed to be uniformly distributed and equal to q = 150 [kN/m^2]. A normally consolidated clay layer 5 [m] thick is located at a depth of 2.0 [m] below the ground surface. The soil profile is shown in Figure 8, while the soil properties are shown in Table 7. It is required to determine the final settlement under the center of the footing due to consolidation of the clay.

Table 7 Soil properties

Layer No.	Type of Soil	Depth of the layer under the ground surface z [m]	Unit weight of the soil γ [kN/m^3]	Compression index C_c [-]	Void ratio e_o [-]
1	Sand	1.5	17.00	-	-
2	Sand	2.0	9.19	-	-
3	Clay	7.0	8.69	0.16	0.85

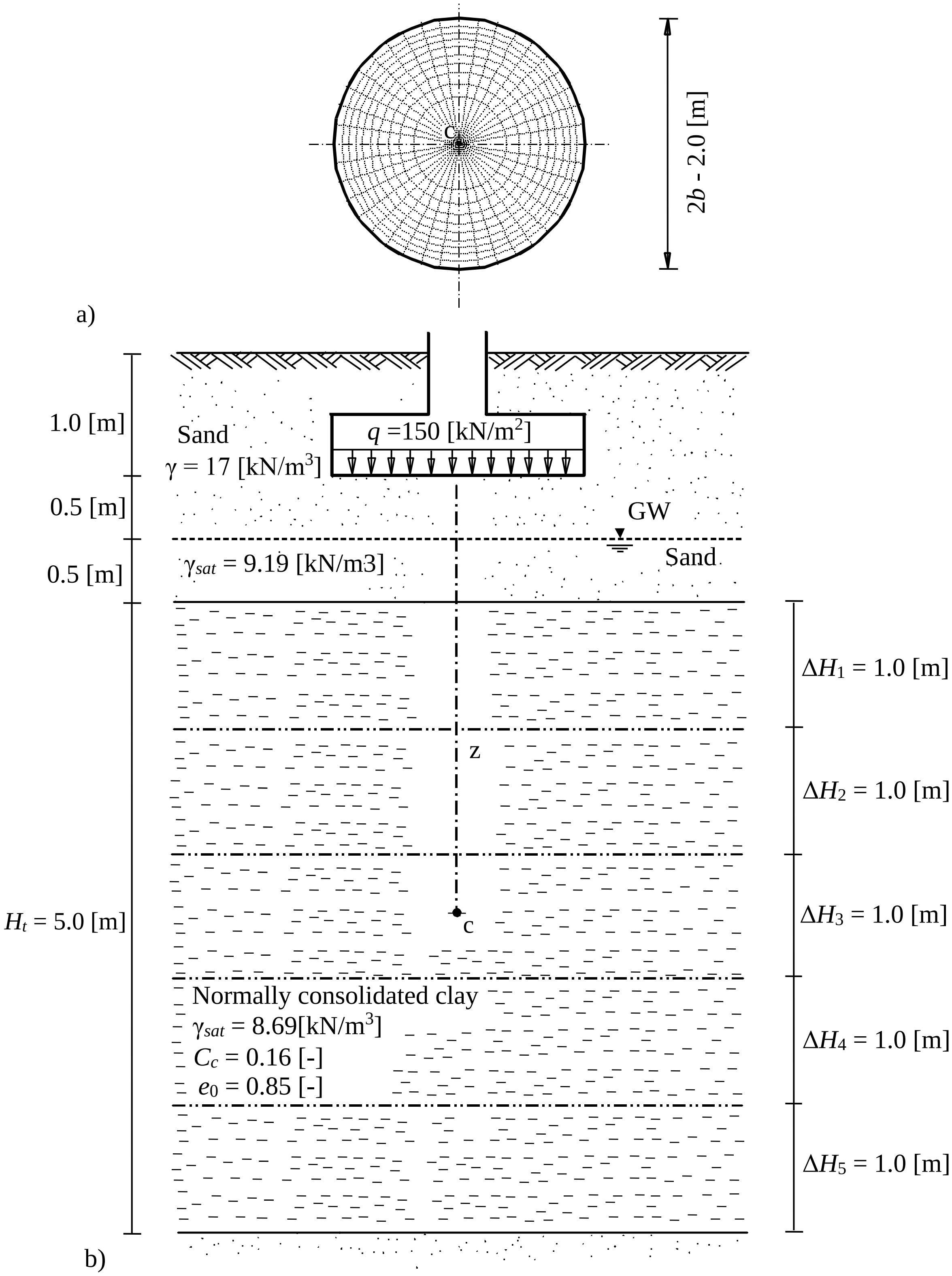

Figure 8 a) Plan of the footing with dimensions and FE-Net

b) Cross section through the soil under the footing

2 Hand calculation of consolidation

According to *Das* (1983), the consolidation of the clay layer can be obtained by hand calculation as follows:

The clay layer is thick relative to the dimensions of the footing. Therefore, the clay layer is divided into five layers each 1.0 [m] thick.

Calculation of the effective stress $\sigma'_{o(i)}$

The effective stress $\sigma'_{o(1)}$ at the middle of the first layer is

$$\sigma'o(1) = \gamma_1 z_1 + \gamma_2 z_2 + \gamma_3 \frac{\Delta H_1}{2}$$

$$\sigma'o(1) = 17 \times 1.5 + 9.19 \times 0.5 + 8.69 \times \frac{1}{2} = 34.44 \text{ [kN/m}^2\text{]}$$

The effective stress $\sigma'_{o(2)}$ at the middle of the second layer is

$$\sigma'o(2) = \sigma'o(1) + \gamma_3 \left(\frac{\Delta H_1}{2} + \frac{\Delta H_2}{2}\right)$$

$$\sigma'o(2) = 34.44 + 8.69 \left(\frac{1}{2} + \frac{1}{2}\right) = 43.13 \text{ [kN/m}^2\text{]}$$

Similarly

$$\sigma'_{o(3)} = 43.13 + 8.69 = 51.82 \text{ [kN/m}^2\text{]}$$

$$\sigma'_{o(4)} = 51.82 + 8.69 = 60.51 \text{ [kN/m}^2\text{]}$$

$$\sigma'_{o(5)} = 60.51 + 8.69 = 69.20 \text{ [kN/m}^2\text{]}$$

Calculation of the increase of effective stress $\Delta\sigma'_i$

For a circular loaded area of radius b and load q, the increase of effective stress $\Delta\sigma'_i$ below the center at depth z is given by (*Das* (1983))

$$\Delta\sigma'i = q\left(1 - \frac{1}{\left[\left(\frac{b}{z}\right)^2 + 1\right]^{3/2}}\right) \quad (9)$$

Hence

$$\Delta\sigma_1 = 150\left(1 - \frac{1}{\left[\left(\frac{1}{1.5}\right)^2 + 1\right]^{3/2}}\right) = 63.59\ [\mathrm{kN/m^2}]$$

$$\Delta\sigma_2 = 150\left(1 - \frac{1}{\left[\left(\frac{1}{2.5}\right)^2 + 1\right]^{3/2}}\right) = 29.93\ [\mathrm{kN/m^2}]$$

$$\Delta\sigma_3 = 150\left(1 - \frac{1}{\left[\left(\frac{1}{3.5}\right)^2 + 1\right]^{3/2}}\right) = 16.66\ [\mathrm{kN/m^2}]$$

$$\Delta\sigma_4 = 150\left(1 - \frac{1}{\left[\left(\frac{1}{4.5}\right)^2 + 1\right]^{3/2}}\right) = 10.46\ [\mathrm{kN/m^2}]$$

$$\Delta\sigma_5 = 150\left(1 - \frac{1}{\left[\left(\frac{1}{5.5}\right)^2 + 1\right]^{3/2}}\right) = 7.14\ [\mathrm{kN/m^2}]$$

Calculation of consolidation settlement s_c

The steps of the calculation of consolidation settlement s_c are given in Table 8 and Figure 8.

Table 8 Steps of calculation of consolidation settlement s_c

Layer No.	Layer thickness ΔH_i [m]	Effective stress $\sigma'_{o(i)}$ [kN/m^2]	Increase of effective stress $\Delta\sigma'_i$ [kN/m^2]	Decrease of void ratio $\Delta e_{(i)}$ [-]	Consolidation settlement $s_{c(i)}$ [m]
1	1.0	34.44	63.59	0.07270	0.0393
2	1.0	43.13	29.93	0.03660	0.0198
3	1.0	51.82	16.66	0.01940	0.0105
4	1.0	60.51	10.46	0.01110	0.0060
5	1.0	69.20	7.14	0.00682	0.0037
Total consolidation settlement Σ					0.0793

In Table 8 the decrease of void ratio $\Delta e_{(i)}$ and the consolidation settlement $s_{c(i)}$ are given by

$$\Delta e_{(i)} = C_c \log\left(\frac{\sigma''_{0(i)} + \Delta\sigma''_{(i)}}{\sigma''_{0(i)}}\right) \quad (10)$$

$$s_{c(i)} = \frac{\Delta e_{(i)}}{1 + e_0} \Delta H_i \quad (11)$$

The total consolidation settlement obtained by hand calculation is

$$s_c = 0.0793 \text{ [m]} = 7.93 \text{ [cm]}$$

3 Consolidation by *ELPLA*

Taking advantage of the symmetry in shape and load geometry about both x- and y-axes, the analysis was carried out by considering only a quarter of the footing. The footing rests on two different soil layers. The first layer is sand of 2.0 [m] thickness, while the second layer is clay 5.0 [m] thick as shown in Figure 8. As it is required to determine the settlement due to the consolidation of the clay only, the settlement due to the sand can be eliminated by assuming very great value for modulus of compressibility of the sand E_{s1}. Consequently, the settlement due to the sand tends to zero. The settlement due to the sand becomes nearly equal to zero when for example $E_{s1} = 1 \times 10^{20}$ [kN/m^2]. *ELPLA* can consider the clay layer as a whole and calculate the consolidation settlement directly in terms of Compression index C_c and Void ratio e_o. The contact pressure of the footing in this example is known. Also, the footing rigidity is not required. Therefore, the available method "Flexible foundation 9" in *ELPLA* may be used here to determine the consolidation of the clay. The effective stress σ'_o and the increase of effective stress $\Delta\sigma'$ at mid-depth of the clay layer calculated in Table 8 can be also obtained by *ELPLA* through the option "Determination of limit depth", where the limit depth calculation is required to know the stress on soil against the depth under the foundation. The effective stress σ'_o and increase of effective stress $\Delta\sigma'$ against depth obtained by *ELPLA* are plotted and compared with those obtained by hand calculation in Figure 8. The final consolidation settlement of the clay under the center of the footing obtained by the program *ELPLA* is s_c = 8.09 [cm] and nearly equal to that obtained by hand calculation.

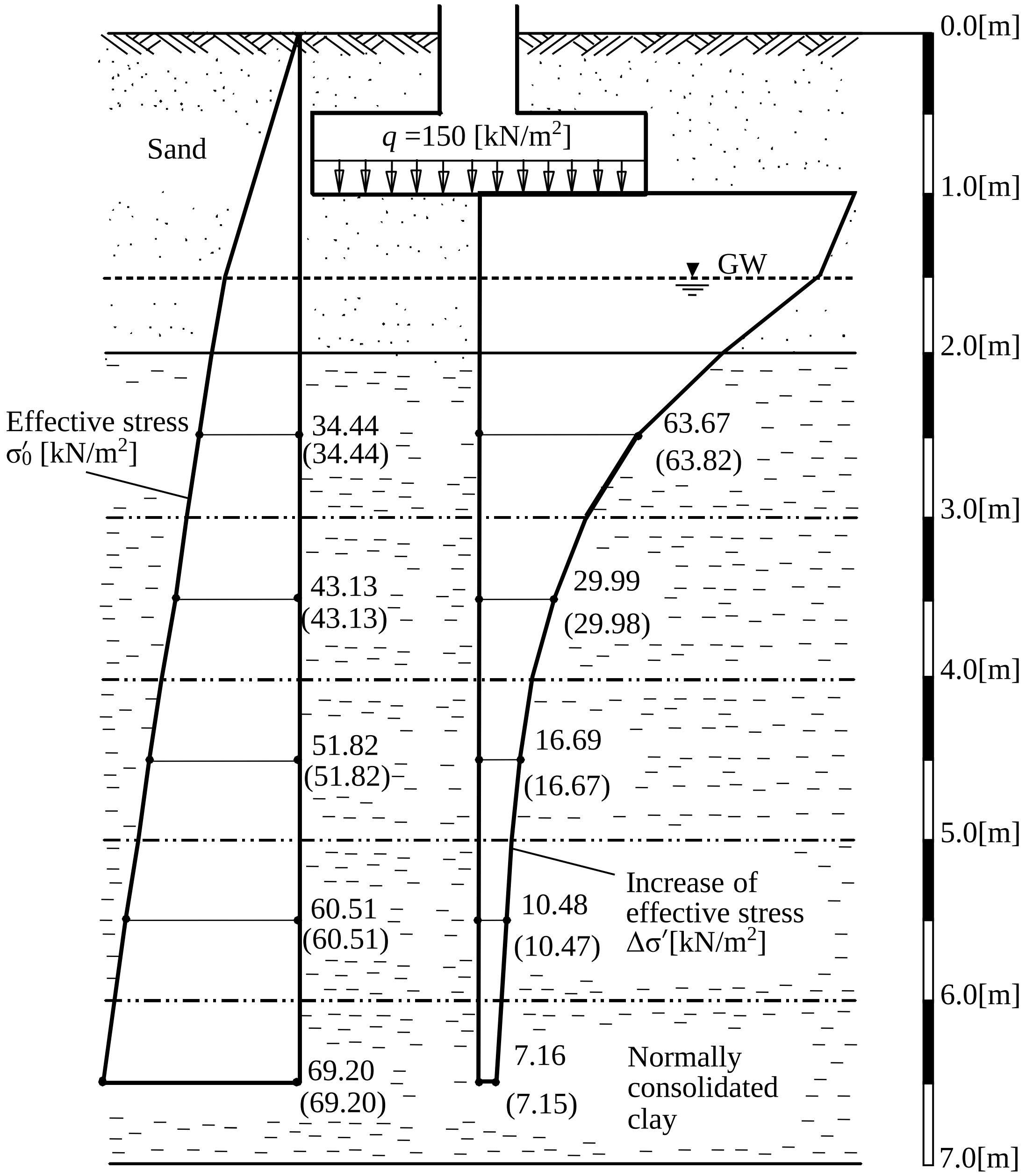

Figure 9 Effective stress σ'_o [kN/m^2] and increase of effective stress $\Delta\sigma'$ [kN/m^2]

(Results of $\Delta\sigma'$ without brackets obtained from *ELPLA*
while with brackets obtained by hand calculation)

Example 8: Rigid square raft on Isotropic elastic half-space medium

1 Description of the problem

To verify the mathematical model of *ELPLA* for rigid square raft, the results of a rigid square raft obtained by other analytical solutions from *Kany* (1974), *Fraser*/ *Wardle* (1976), *Chow* (1987), *Li*/ *Dempsey* (1988) and *Stark* (1990), Section 5.4, page 114, are compared with those obtained by *ELPLA*.

The vertical displacement *w* [m] of a rigid square raft on Isotropic elastic half-space medium may be evaluated by

$$w = \frac{pB\left(1 - ny_s^2\right)}{E_s} I \qquad (12)$$

where:

ν_s	*Poisson's* ratio of the soil [-]
E_s	*Young's* modulus of the soil [kN/m^2]
B	Raft side [m]
I	Displacement influence factor [-]
p	Load intensity on the raft [kN/m^2]

A square raft on Isotropic elastic half-space soil medium is chosen and subdivided to different nets. The nets range from 2 × 2 to 48 × 48 elements. Load on the raft, raft side and the elastic properties of the soil are chosen to make the first term from Eq. 13 equal to unit, hence:

Raft side	B	= 10	[m]
Uniform load on the raft	p	= 500	[kN/m^2]
Modulus of compressibility	E_s	= 5000	[kN/m^2]
Poisson's ratio of the soil	ν_s	= 0.0	[-]

2 Analysis of the raft

The available method "Rigid raft 8" in *ELPLA* is used here to determine the vertical displacement of the raft on Isotropic elastic half-space medium. Taking advantage of the symmetry in shape, soil and load geometry about both *x*- and *y*-axes, the analysis is carried out by considering only a quarter of the raft. Figure 10 shows a quarter of the raft with a net of total 16 × 16 elements.

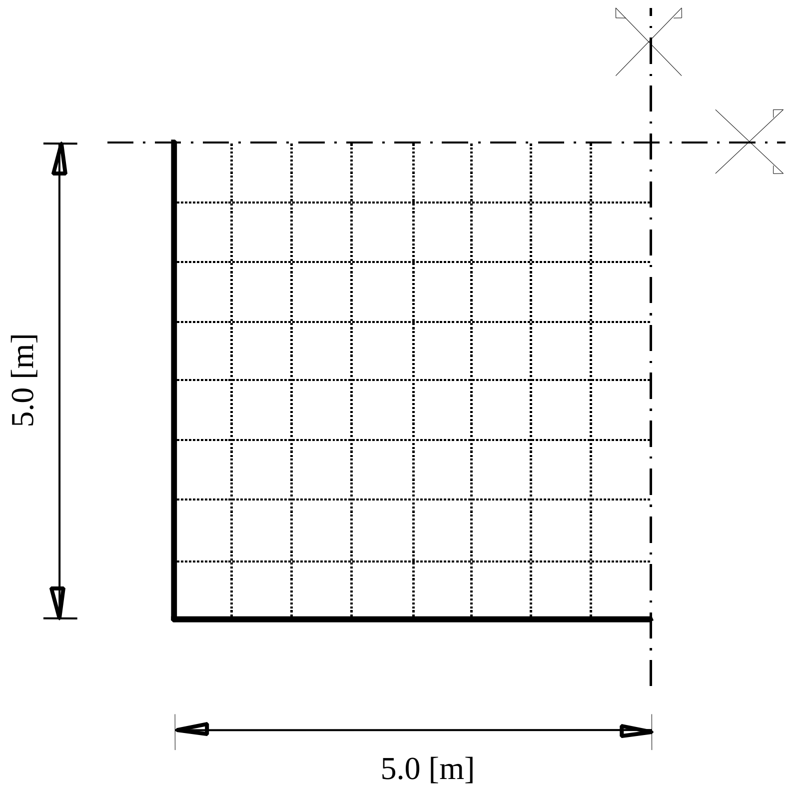

Figure 10 Quarter of rigid square raft with dimensions and FE-Net

3 Results

Table 9 shows the comparison of the displacement influence factor *I* obtained by *ELPLA* with those obtained by other published solutions from *Fraser/ Wardle* (1976), *Chow* (1987), *Li/ Dempsey* (1988) and *Stark* (1990) for a net of 16 × 16 elements. In addition, the displacement influence factor *I* is obtained by using *Kany's* charts (1974) through the conventional solution of a rigid raft.

Table 9 Comparison of displacement influence factor *I* obtained by *ELPLA* with those obtained by other authors for a net of 16 × 16 elements

Displacement influence factor *I* [-]					
Kany (1974)	*Fraser/ Wardle* (1976)	*Chow* (1987)	*Li/ Dempsey* (1988)	*Stark* (1990)	*ELPLA*
0.85	0.835	0.8675	0.8678	0.8581	0.8497

Table 10 shows the convergence of solution for the displacement influence factor *I* obtained by *ELPLA* with those obtained by *Stark* (1990) for different nets. Under the assumption of *Li*/ *Dempsey* (1988), the convergence of the solution occurs when the displacement influence factor I = 0.867783 while using *Kany's* charts (1974) gives I = 0.85 for the ratio z/B =100. *Fraser*/ *Wardle* (1976) give I = 0.87 based on an extrapolation technique, *Gorbunov-Possadov*/ *Serebrjanyi* (1961) give I = 0.88 and *Absi* (1970) gives I = 0.87. In general, the displacement influence factor *I* in this example ranges between I = 0.85 and I = 0.88. Table 10 shows that a net of 16 × 16 elements gives a good result for a rigid square raft in this example by *ELPLA*. The convergence of the solutions is in a good agreement with that of *Stark* (1990) for all chosen nets.

Table 10 Convergence of solution for displacement influence factor *I* obtained by *ELPLA* with those obtained by *Stark* (1990) for different nets

Net	Displacement influence factor *I* [-]	
	Stark (1990)	*ELPLA*
2 × 2	0.8501	0.7851
4 × 4	0.8477	0.8143
6 × 6	0.8498	0.8281
8 × 8	0.8525	0.8360
12 × 12	0.8559	0.8449
16 × 16	0.8581	0.8497
20 × 20	0.8597	0.8528
24 × 24	0.8601	0.8550
32 × 32	0.8626	0.8578
48 × 48	0.8647	0.8609

Example 9: Rigid circular raft on Isotropic elastic half-space medium

1 Description of the problem

To verify the mathematical model of *ELPLA* for rigid circular raft, results of a rigid circular raft obtained by other analytical solutions from *Borowicka* (1939) and *Stark* (1990), Section 5.2, page 106, are compared with those obtained by *ELPLA*.

According to *Borowicka* (1939), the vertical displacement w [m] of a rigid circular raft on Isotropic elastic half-space medium may be evaluated by

$$w = \frac{pr\pi\left(1 - ny_s^2\right)}{2E_s} \qquad (13)$$

where:

ν_s *Poisson's* ratio of the soil [-]
E_s *Young's* modulus of the soil [kN/m^2]
r Raft radius [m]
p Load intensity on the raft [kN/m^2]

While the contact pressure distribution q [kN/m^2] under the raft at a distance e [m] from the center may be evaluated by

$$q = \frac{pr}{2\sqrt{r^2 - e^2}} \qquad (14)$$

A circular raft on Isotropic elastic half-space soil medium is chosen and subdivided into 40 × 40 elements. Each element has a side of 0.25 [m]. Load on the raft, raft radius and the elastic properties of the soil are chosen as follows:

Raft radius	r	= 5	[m]
Uniform load on the raft	p	= 100	[kN/m^2]
Young's modulus of the soil	E_s	= 6000	[kN/m^2]
Poisson's ratio of the soil	ν_s	= 0.25	[-]

2 Analysis of the raft

The available method "Rigid raft 9" in *ELPLA* is used here to determine the vertical displacement of the raft on Isotropic elastic half-space medium. Taking advantage of the symmetry in shape, soil and load geometry about both x- and y-axes, the analysis is carried out by considering only a quarter of the raft. Figure 11 shows a quarter of the raft with FE-Net.

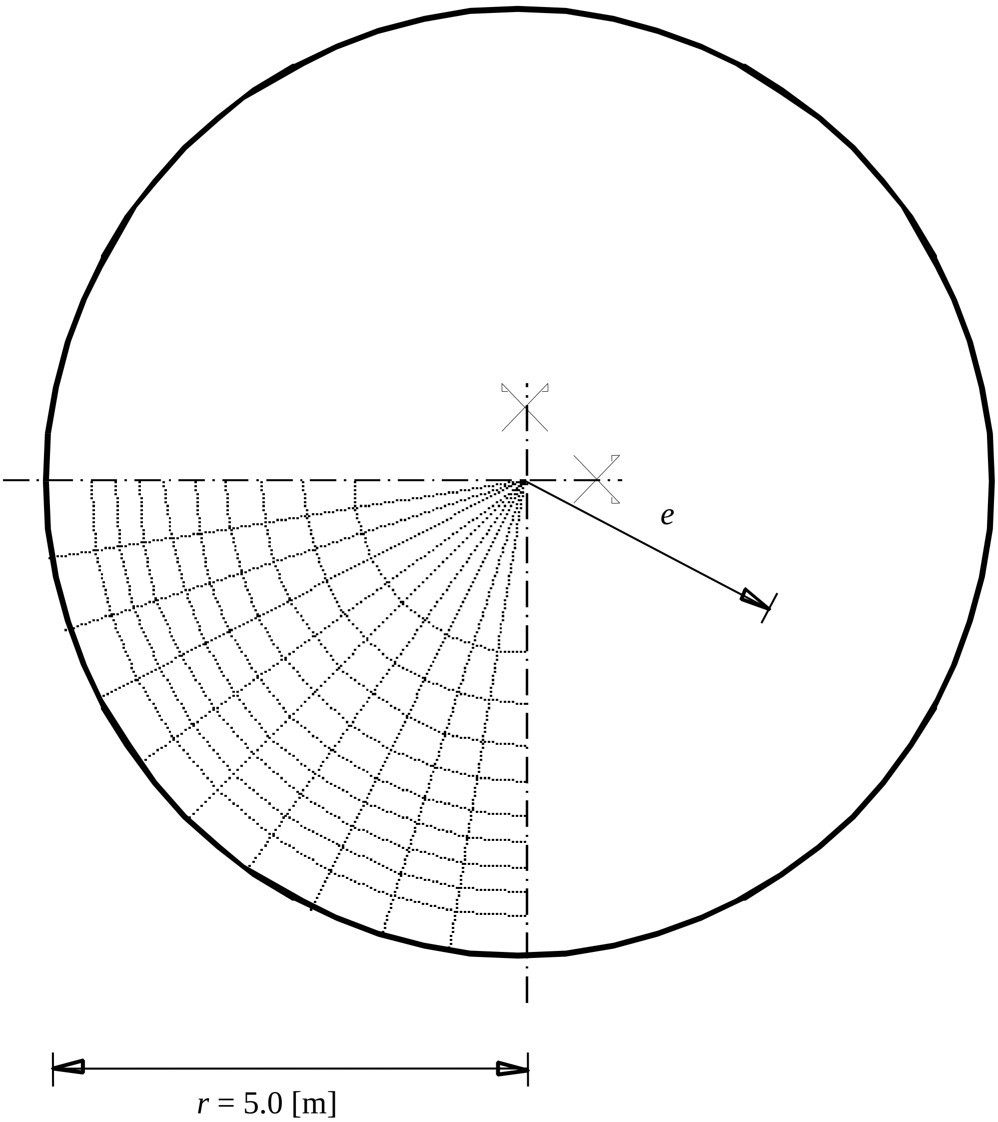

Figure 11 Quarter of rigid square raft with dimensions and FE-Net

3 Results

Figure 12 shows the comparison of the contact pressure ratio *q/p* [-] at the middle section of the raft obtained by *ELPLA* with those obtained by *Borowicka* (1939) and *Stark* (1990). Besides, Table 11 shows the comparison of the central displacement *w* obtained by *ELPLA* with those obtained by *Borowicka* (1939) and *Stark* (1990).

Table 11 Comparison of the central displacement *w* obtained by *ELPLA* with those obtained by *Borowicka* (1939) and *Stark* (1990)

	Borowicka (1939)	*Stark* (1990)	*ELPLA*
Central displacement *w* [cm]	12.272	12.195	12.164

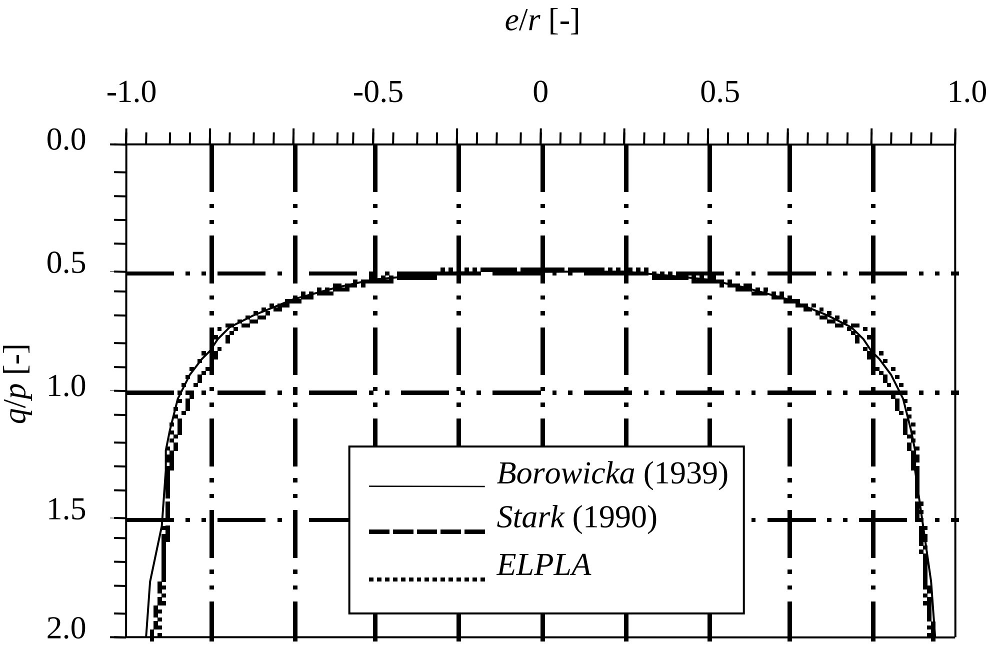

Figure 12 Contact pressure ratio *q/p* [-] under the middle of the circular rigid raft

It is obviously from Table 11 and Figure 12 that results of the circular rigid raft obtained by *ELPLA* are nearly equal to those obtained by *Borowicka* (1939) and *Stark* (1990).

Example 10: Rigid circular raft on Isotropic elastic half-space medium

1 Description of the problem

The definition of the characteristic point s_o according to *Graßhoff* (1955) can be used to verify the mathematical model of *ELPLA* for flexible foundation and rigid raft. The characteristic point of a uniformly loaded area on the surface is defined as the point of a flexible settlement s_o identical with the rigid displacement w_o. For a rectangular area, the characteristic point takes the coordinates $a_c = 0.87A$ and $b_c = 0.87B$, where A and B are the area sides.

Figure 13 shows a raft of dimensions 8 [m] × 12 [m] resting on three different soil layers of thicknesses 7 [m], 5 [m] and 6 [m], respectively.

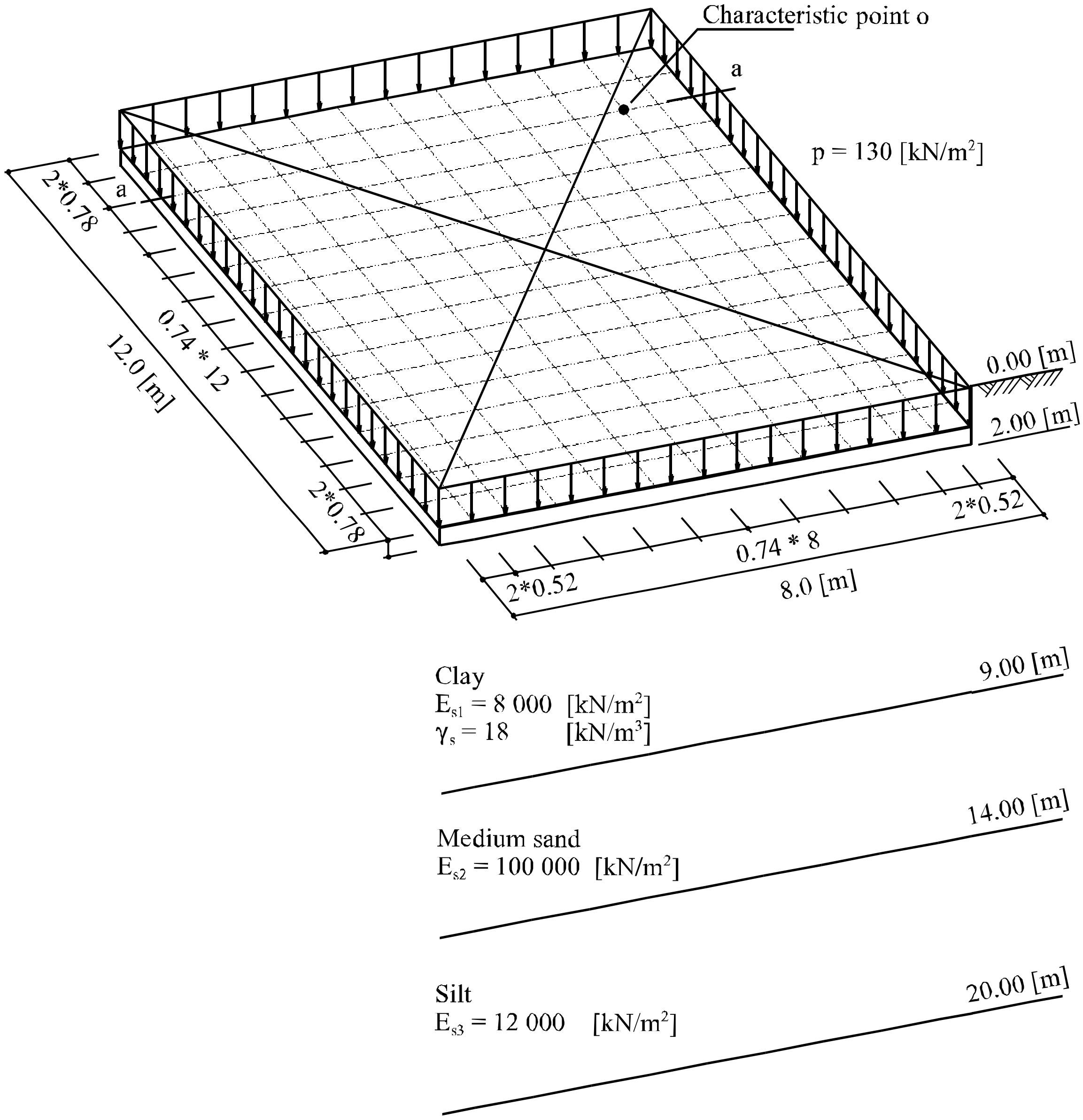

Figure 13 Raft dimensions, loads, FE-Net and subsoil

2 Soil properties

The raft rests on three different soil layers of clay, medium sand and silt overlying a rigid base as shown in Figure 13 and Table 12. *Poisson's* ratio is constant for all soil layers and is taken ν_s = 0.0 [-]. The foundation level of the raft is 2.0 [m] under the ground surface.

Table 12 Soil properties

Layer No.	Type of soil	Depth of layer underground surface z [m]	Modulus of compressibility E_s [kN/m^2]	Unit weight of the soil γ_s [kN/m^3]
1	Clay	9.0	8 000	18
2	Medium sand	14.0	100 000	-
3	Silt	20.0	12 000	-

3 Loading

The raft carries a uniform load of p = 130 [kN/m^2].

4 Analysis of the raft

The raft is divided into 12 × 16 elements as shown in Figure 13. First, the analysis is carried out for the flexible foundation using the method "Flexible foundation 9", where the contact stress is equal to the applied stress on the soil. Then, the analysis is carried out for the rigid raft using the method "Rigid raft 8", where for a raft without eccentricity such as the studied raft, all points on the raft will settle the same value w_o. The settlement s_o may be obtained by using *Kany's* charts (1974) for determining the settlement under the characteristic point of a rectangular loaded area. Table 13 compares the settlement at the characteristic point $s_o = w_o$ obtained by using *Kany's* charts with the settlements of flexible foundation and rigid raft obtained by *ELPLA*.

Table 13 Settlement $s_o = w_o$ [cm] obtained by using *Kany's* charts and *ELPLA*

	Kany (1974) $s_o = w_o$	*ELPLA* - Flexible raft s_o	*ELPLA* - Rigid raft w_o
Settlement [cm]	7.37	7.56	7.33
Difference [%]	0	2.58	0.54

Figure 14 shows the settlements at the section a-a through the characteristic point *o* for flexible foundation and rigid raft. It can be clearly observed that the settlement s_o at characteristic point *o* for flexible foundation is identical to the vertical displacement w_o of rigid raft according to the assumption of *Graßhoff* (1955).

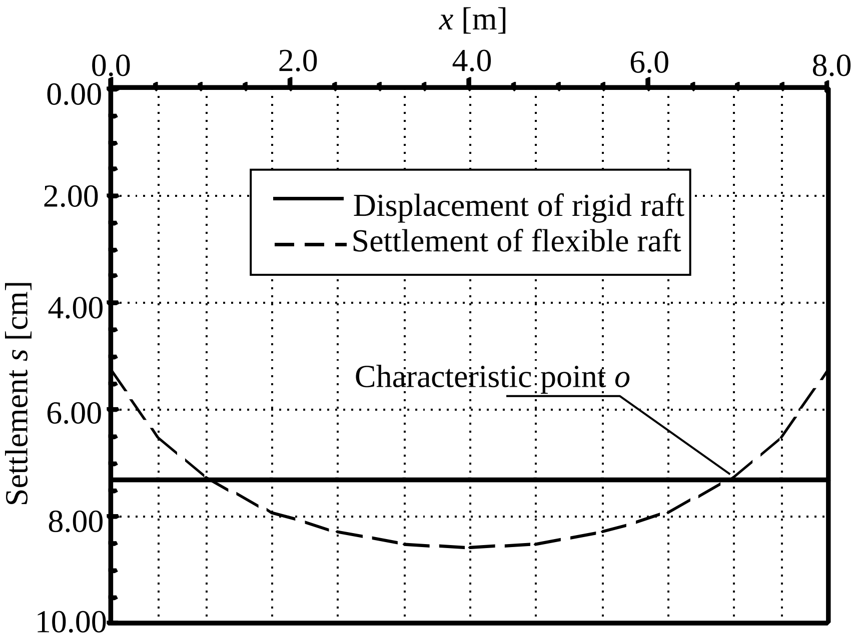

Figure 14 Settlement *s* [cm] at section a-a through the characteristic point *o*

Example 11: Verifying ultimate bearing capacity for a footing on layered subsoil

1 Description of the problem

To verify the ultimate bearing capacity calculated by *ELPLA*, the results of Example 2, page 9 in DIN 4017 for determining the ultimate bearing capacity of a footing on layered subsoil are compared with those obtained by *ELPLA*.

A rectangular footing of 4.0 [m] × 5.0 [m] on layered subsoil is considered. Footing dimensions and soil layers under the footing with soil constants are shown in Figure 15. It is required to determine the ultimate bearing capacity of the soil under the footing.

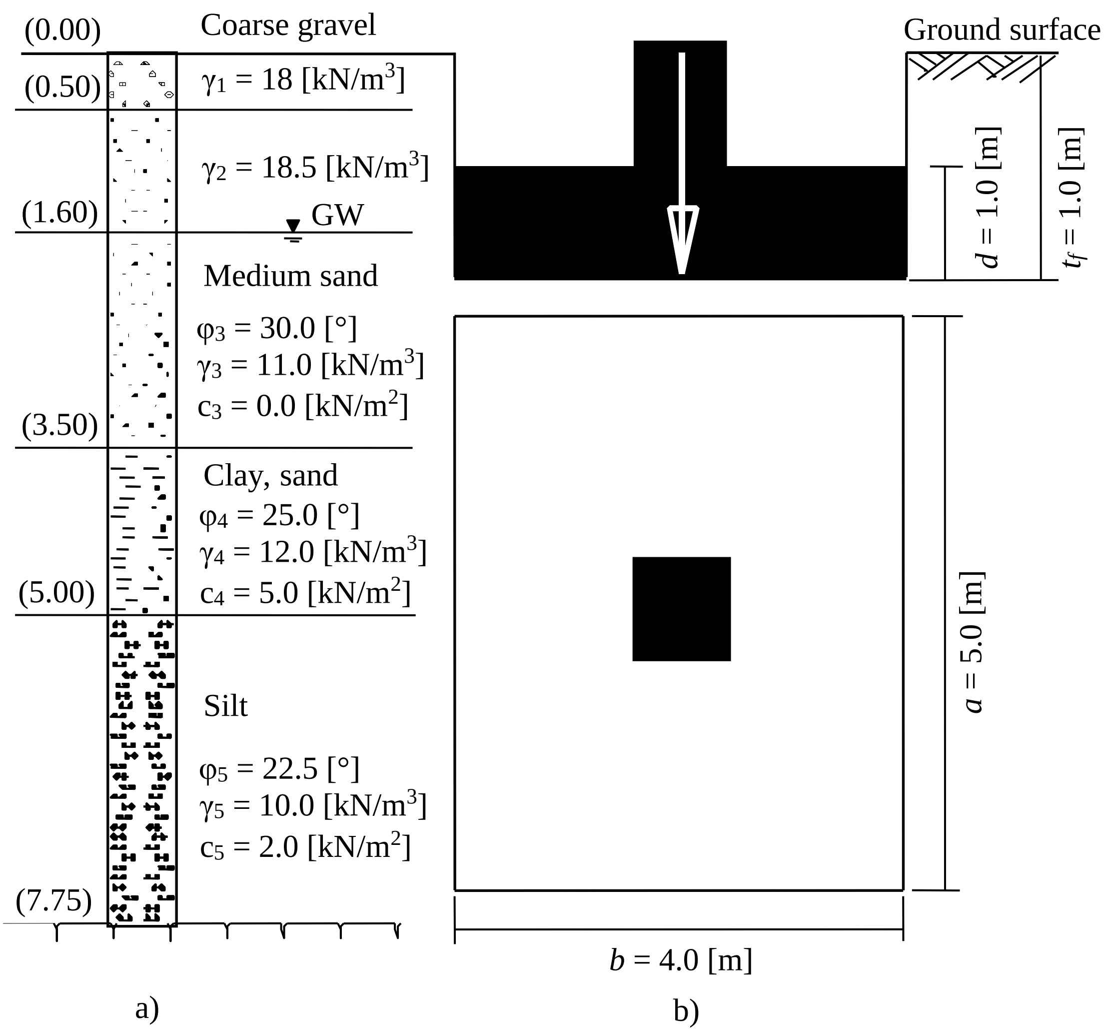

Figure 15 a) Cross section through the soil under the footing
b) Plan of the footing with dimensions

2 Hand calculation of ultimate bearing capacity

According to DIN 4017, the ultimate bearing capacity can be obtained by hand calculation as follows:

Iterative determination of the soil constant φ_m

According to DIN 4017, the mean values of the soil constants are only accepted, if the angle of internal friction for each individual layer φ_i does not exceed the average value of the internal friction $\varphi_{av.}$ by 5 [°].

The average value $\varphi_{av.}$ for the three layers is given by

$$\varphi_{av.} = \frac{30 + 25 + 22.5}{3} = 25.83 \text{ [°]}$$

The difference between each individual value φ_i and the average value φ_{av} is less than 5 [°]. The iteration begins with the angle of internal friction φ_{m0} of the first layer, which lies directly under the footing.

1st Iteration step

The first step is determining the failure shape of the soil under the footing for φ_{m0} = 30 [°]. The failure shape is described in Figure 16. The geometry of the failure shape can be described by the angles β, α, and ω, which are given by

$$\beta = 45 - \frac{\varphi_{m0}}{2} = 45 - \frac{30}{2} = 30 \text{ [°]}$$

$$\alpha = \square = 45 + \frac{\varphi_{m0}}{2} = 45 + \frac{30}{2} = 60 \text{ [°]}$$

Therefore

$$\omega = 90 \text{ [°]}$$

The triangular side r_0 is given by

$$r_0 = \frac{b}{\sin\left(90 - \varphi_{m0}\right)} \sin \square = \frac{4}{\sin\left(90 - 30\right)} \sin 60 = 4 \text{ [m]}$$

The triangular side r_1 is given by

$$r_1 = r_0 e^{(\mathrm{arc}\,\omega \, \tan \varphi_{m0})} = 4e^{\left(\frac{90\pi}{180} \tan 30\right)} = 9.91 \text{ [m]}$$

The length of the slide shape l is given by

$$l = 2r_1 \cos\beta = 2 \times 9.91 \cos 30 = 17.16 \text{ [m]}$$

The depth of the slide shape $max\,T_s$ under the footing is given by

$$\max T_s = r_0 \cos\varphi_0\, e^{(\mathrm{arc}\,\omega\,\tan\varphi_{m0})} = 4 \cos 30\, e^{\left(\frac{60\pi}{180}\tan 30\right)} = 6.34 \text{ [m]}$$

The depth of failure shape z under the ground surface is given by

$$z = maxT_s + t_f = 6.34 + 2 = 8.34 \text{ [m]}$$

β

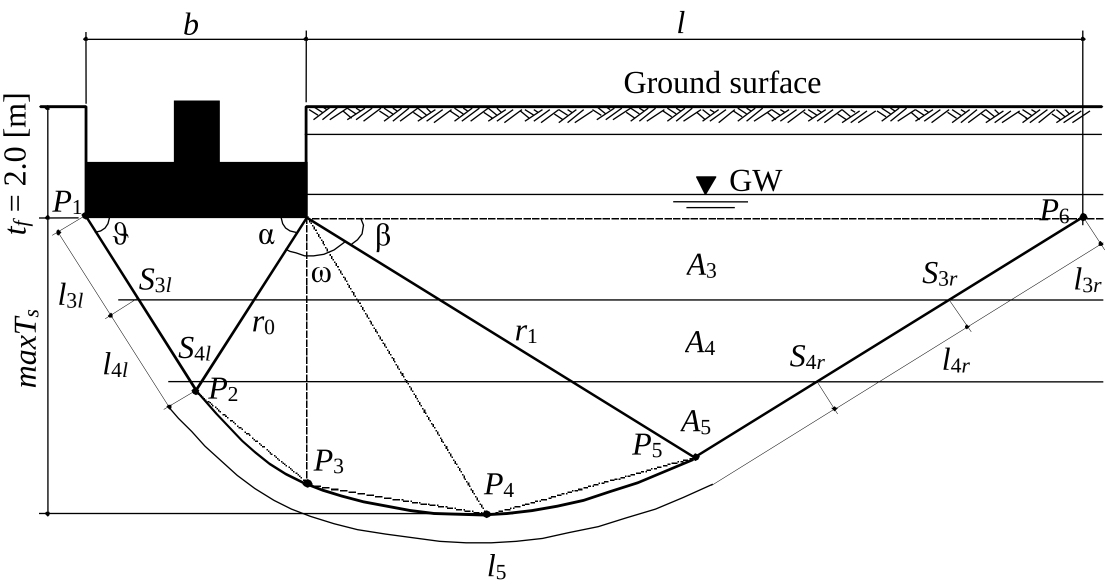

Figure 16 Ultimate bearing capacity for multi-layers system

To simplify the analytical calculation, the slip line is approximated by a polygon. Accordingly, by dividing the angle ω of the logarithmic spiral into three sub angles, the polygon P_1 to P_6 can be drawn. Then, the layer boundaries with the polygonal sequence are determined. The intersection points can be determined also graphically, when the bottom failure shape is considered and hence the intersection points are taken from the drawing. Considering a Cartesian coordinate system in which the origin coordinate is point P_1, the following intersection points are given

S_{3l} (0.87, 1.50), S_{3r} (18.56, 1.50), S_{4l} (1.73, 3.00), S_{4r} (15.96, 3.00)

Due to intersection of polygon points with soil layers, the following proportional lengths are determined

$$l_3 = l_{3l} + l_{3r} = 1.73 + 3 = 4.73 \text{ [m]}$$

$$l_4 = l_{4l} + l_{4r} = 4.73 \text{ [m]}$$

$$l_5 = 16.12 \text{ [m]}$$

$$\text{total length } l_{tot.} = 25.58 \text{ [m]}$$

From these proportional lengths, the main value of the angle of the internal friction for the first iteration can be determined as follows

$$\tan \varphi_{m1} = \frac{l_3 \tan \varphi_3 + l_4 \tan \varphi_4 + l_5 \tan \varphi_5}{l_3 + l_4 + l_5}$$

$$\tan \varphi_{m1} = \frac{4.73 \tan 30 + 4.73 \tan 25 + 16.12 \tan 22.5}{25.58}$$

or

$$\varphi_{m1} = 24.42 \text{ [°]}$$

The deviation Δ_i of the output value φ_{m1} from the input value φ_{m0} is

$$\Delta_i = \frac{\varphi_{m0} - \varphi_{m1}}{\varphi_{m0}} \times 100 = \frac{30 - 24.42}{30} \times 100 = 18.60 \text{ [\%]}$$

The deviation Δ_i is greater than 3 [%]. Therefore, a further iteration is necessary. The new angle of internal friction for the 2nd iteration step is given by

$$\varphi_{m1} = \frac{\varphi_{m0} + \varphi_{m1}}{2} = \frac{30 + 24.42}{2} = 27.21 \text{ [°]}$$

2^{nd} Iteration step

The failure shape for φ_{m1} = 27.21 [°] is determined. Then, the calculation is carried out analog to the first iteration step. The calculated proportional lengths are

$$l_3 = 4.64 \text{ [m]}$$

$$l_4 = 4.64 \text{ [m]}$$

$$l_5 = 13.49 \text{ [m]}$$

The main angle of the internal friction is given by

$$\tan \varphi_{m2} = \frac{4.64 \tan 30 + 4.64 \tan 25 + 13.49 \tan 22.5}{22.77}$$

$$\varphi_{m2} = 24.61 \text{ [°]}$$

The deviation Δ_i = 9.55 [%] is still greater than 3 [%]. Therefore, a further iteration step is to be carried out with

$$\varphi_{m2} = \frac{\varphi_{m1} + \varphi_{m2}}{2} = \frac{24.61 + 27.21}{2} = 25.91 \text{ [°]}$$

3^{rd} Iteration step

The results of the 3^{rd} iteration step give

$$\varphi_{m3} = 24.70 \text{ [°]}$$

The deviation Δ_i = 4.66 [%] is still greater than 3 [%]. Therefore, a further iteration step is to be carried out with

$$\varphi_{m3} = \frac{\varphi_{m2} + \varphi_{m3}}{2} = \frac{24.70 + 25.91}{2} = 25.31 \text{ [°]}$$

4^{th} Iteration step

The results of the 4^{th} iteration step give φ_{m4} = 24.74 [°]. The deviation Δ_i = 2.22 [%] is less than 3 [%]. Therefore, the iteration process will stop here. The mean value of the angle of internal friction is given by

$$\varphi_{m4} = \frac{\varphi_{m3} + \varphi_{m4}}{2} = \frac{24.70 + 25.31}{2} = 25 \text{ [°]}$$

Determination of the soil constant c_m

In this step the geometry of the failure shape for φ_m = 25.00 [°] can be determined. Then, the proportional lengths are

$$l_3 = 4.57 \text{ [m]}$$

$$l_4 = 4.57 \text{ [m]}$$

$$l_5 = 15.62 \text{ [m]}$$

The mean cohesion c_m is given from proportional lengths by

$$c_m = \frac{l_3\, c_3 + l_4\, c_4 + l_5\, c_5}{l_3 + l_4 + l_5}$$

$$c_m = \frac{4.57 \times 0 + 4.57 \times 5 + 15.62 \times 2}{24.76} = 2.19 \text{ [kN/m}^2\text{]}$$

Determination of the soil constant γ_m

a) Mean unit weigh of the soil γ_m under the foundation level

Due to intersection of polygon points with soil layers the following proportional areas A_3, A_4 and A_5 can be determined

$$A_3 = 23.13 \text{ [m}^2\text{]}$$

$$A_4 = 18.17 \text{ [m}^2\text{]}$$

$$A_5 = 15.62 \text{ [m}^2\text{]}$$

$$\text{total area } A_{tot.} = 56.92 \text{ [m}^2\text{]}$$

The mean unit weight of the soil under the foundation level γ_m is given from proportional areas by

$$\gamma_m = \frac{A_3\, \gamma_3 + A_4\, \gamma_4 + A_5\, \gamma_5}{A_3 + A_4 + A_5}$$

$$\gamma_m = \frac{23.13 \times 11 + 18.17 \times 12 + 15.62 \times 10}{56.92} = 11.05 \text{ [kN/m}^3\text{]}$$

b) Mean unit weigh of the soil γ'_m above the foundation level

The mean unit weight of the soil above the foundation level γ'_m is given from proportional areas above the foundation level by

$$\gamma'_m = \frac{0.5 \times 18 + 1.1 \times 18.5 + 0.4 \times 11}{2} = 16.88 \text{ [kN/m}^3\text{]}$$

Now, from the above calculated mean soil constants φ_m, c_m, γ_m and γ'_m, the bearing capacity factors can be determined for homogenous subsoil. Formulae used to determine the bearing capacity factors are described in DIN 4017 Part 1. From these formulae, the bearing capacity factors for φ_m = 25.00 [°] are

$$N_d = 10.7$$

$$N_c = 20.8$$

$$N_b = 4.5$$

while the shape factors for φ_m = 25.00 [°] and a = 4.0 [m], b = 5.0 [m] are

$$ny_d = 1.34$$

$$ny_c = 1.37$$

$$ny_b = 0.76$$

The ultimate bearing capacity of the soil q_{ult} can be determined according to DIN 4017 from

$$q_{ult} = c\, N_c\, ny_c + \gamma_1\, t_f\, N_d\, ny_d + \gamma_2\, B\, N_b\, ny_b$$

$$q_{ult} = 2.19 \times 20.8 \times 1.37 + 16.88 \times 2 \times 10.7 \times 1.34 + 11.05 \times 4 \times 4.5 \times 0.76$$

$$q_{ult} = 698 \text{ [kN/m}^2\text{]}$$

3 Ultimate bearing capacity by *ELPLA*

To determine the ultimate bearing capacity by *ELPLA*, one of the available calculation methods 2 to 8 used to carry out the nonlinear analysis of foundations may be used. Here the nonlinear analysis of foundation requires to know the ultimate bearing capacity of the soil. The ultimate bearing capacity obtained by *ELPLA* is q_{ult} = 701 [kN/m^2] and nearly equal to that obtained by hand calculation according to DIN 4017.

Example 12: Verifying simple assumption model for irregular raft

1 Description of the problem

To verify the simple assumption model of *ELPLA*, the contact pressure distribution of an irregular foundation obtained by *Bowles* (1977), Example 9-6, page 265, is compared with that obtained by *ELPLA*.

A square foundation that has 10 [m] side is chosen. The foundation is subjected to a column load of 540 [kN] at the center. It is required to determine the distribution of the contact pressure when the corner is notched as shown in Figure 17. The notch has the following properties:

Area	A =	4.5	[m^2]
Center of gravity from *o* in x-direction	x' =	3.5	[m]
Center of gravity from *o* in y-direction	y' =	4.25	[m]

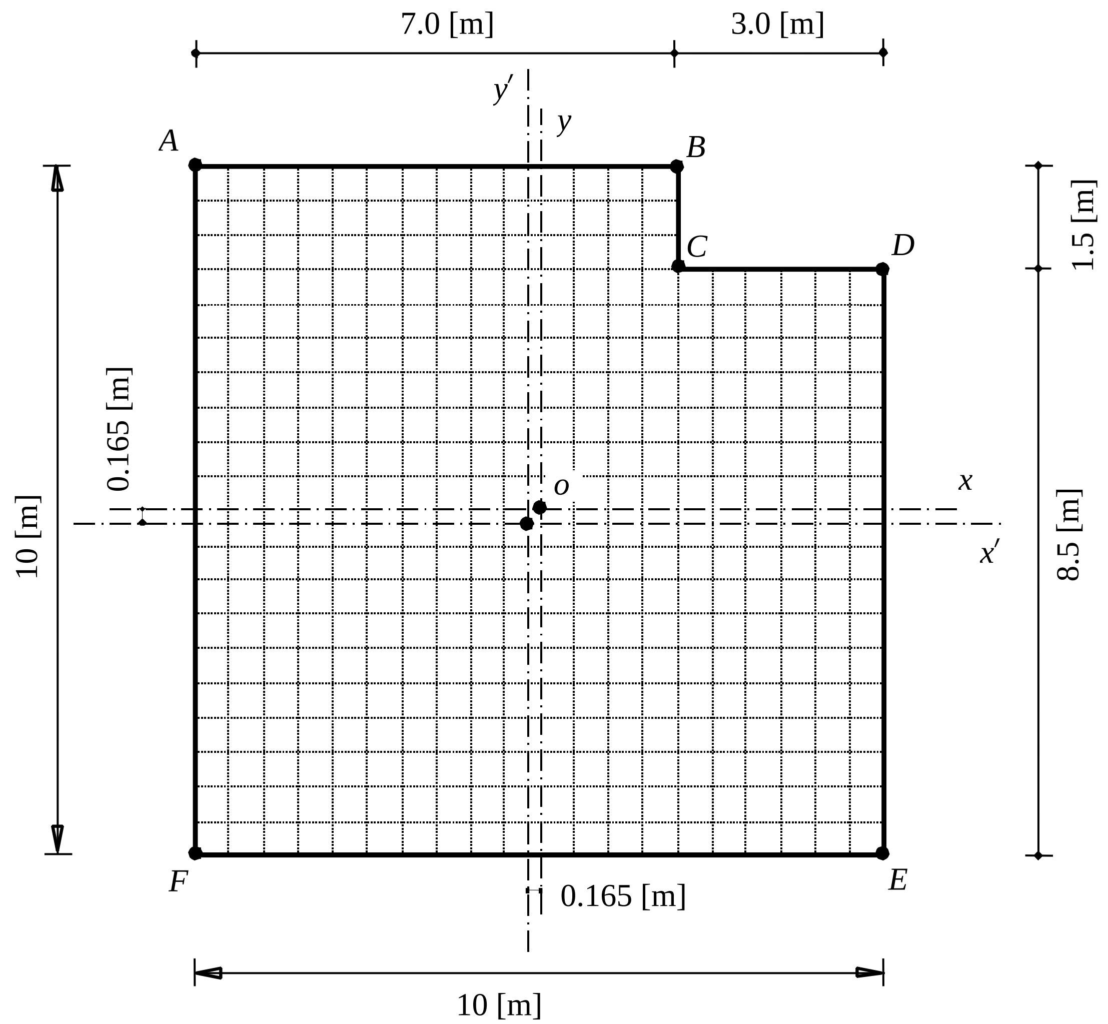

Figure 17 Foundation dimensions and FE-Net

The simple assumption model assumes a linear distribution of contact pressure on the base of the foundation. In the general case of a foundation with an arbitrary unsymmetrical shape and loading, based on *Navier´s* solution, the contact pressure q_i [kN/m²] at any point (x_i, y_i) [m] from the geometry centroid on the bottom of the foundation is given by:

$$q_i = \frac{N}{A_f} + \frac{M_y I_x - M_x I_{xy}}{I_x I_y - I_{xy}^2} x_i + \frac{M_x I_y - M_y I_{xy}}{I_x I_y - I_{xy}^2} y_i \qquad (15)$$

where:

N	Sum of all vertical applied loads on the foundation [kN]
A_f	Foundation area [m^2]
M_x	Moment due to N about the x-axis [kN.m]
M_y	Moment due to N about the y-axis [kN.m]
I_x	Moment of inertia of the foundation about the x-axis [m^4]
I_y	Moment of inertia of the foundation about the y-axis [m^4]
I_{xy}	Product of inertia [m^4]

2 Hand calculation of contact pressure

According to *Bowles* (1977), the contact pressure distribution under the foundation can be obtained by hand calculation as follows:

Step 1: Find new *x*-, *y*-axis

$$\bar{x} = \frac{-15.75}{95.5} = -0.165 \text{ [m]}$$

$$\bar{x} = \frac{-19.13}{95.5} = -0.20 \text{ [m]}$$

which gives the location of new axes x' and y' as shown in Figure 17

Step 2: Compute new properties $I_{x'}$, $I_{y'}$ and $I_{xy'}$

Determining properties of foundation parts are listed in Table 14.

Table 14 Properties of foundation parts

Part	Area A [m^2]	x [m]	Y [m]	Ax^2 [m]	Ay^2 [m]	I_{ox} [m^4]	I_{oy} [m^4]
Uncut	100	-0.165	-0.20	2.72	4.00	833.3	833.3
Notch	-4.5	3.66	4.45	-60.3	-89.1	-0.84	-3.38
Total	95.5						

$$I_x = I_{ox} - I_{ox\,notch} + A_y^2$$

$$I_x = 833.3 - 0.84 + 4.0 - 89.0 = 747.5 \text{ [m}^4\text{]}$$

$$I_y = I_{oy} - I_{oy\,notch} + A_x^2$$

$$I_y = 833.3 - 3.38 + 2.73 - 60.5 = 772.15 \text{ [m}^4\text{]}$$

$$I_{xy} = I_{oxy} + A_{\overline{xy}}$$

Step 3: Compute moments

$$M_y = 540 \times 0.165 = 89.1 \text{ [kN.m]}$$

$$M_x = 540 \times 0.2 = 108 \text{ [kN.m]}$$

Step 4: Compute contact pressure at selected locations

The contact pressure q_i at any point (x_i, y_i) from the geometry centroid on the bottom of the foundation is obtained from

$$q_i = \frac{N}{A_f} + \frac{M_y I_x - M_x I_{xy}}{I_x I_y - I_{xy}^2} x_i + \frac{M_x I_y - M_y I_{xy}}{I_x I_y - I_{xy}^2} y_i$$

$$q_i = \frac{540}{95.5} + \frac{(89.1)(747.5) - (108)(-70)}{(747.5)(772.15) - (-70)^2} x_i + \frac{(108)(772.15) - (89.1)(-70)}{(747.5)(772.15) - (-70)^2} y_i$$

$$q_i = 5.65 + 0.13 x_i + 0.157 y_i$$

3 Contact pressure by *ELPLA*

The available method "Linear Contact pressure 1" in *ELPLA* is used to determine the contact pressure distribution under the foundation. A net of equal square elements is chosen. Each element has a side of 0.5 [m] as shown in Figure 17. The contact pressures at the foundation corners obtained by *ELPLA* are compared with those obtained by *Bowles* (1977) in Table 15. It is obviously from this table that contact pressures obtained by *ELPLA* are equal to those obtained by hand calculation.

Table 15 Contact pressures at foundation corners

Point	*Bowles* (1977)						*ELPLA*
	x_i [m]	y_i [m]	N/A_f [kN/m^2]	0.13 x_i [kN/m^2]	0.157 y_i [kN/m^2]	q [kN/m^2]	q [kN/m^2]
A	-4.84	5.20	5.65	-0.63	0.82	5.84	5.84
B	2.16	5.20	5.65	0.28	0.82	6.75	6.75
C	2.16	3.70	5.65	0.28	0.58	6.51	6.52
D	5.16	3.70	5.65	0.67	0.58	6.90	6.90
E	5.16	-4.80	5.65	0.67	-0.75	5.57	5.57
F	-4.84	-4.80	5.65	-0.63	-0.75	4.27	4.28

Example 13: Verifying main modulus of subgrade reaction k_{sm}

1 Description of the problem

It is known that the modulus of subgrade reaction k_s is not a soil constant but is a function of the contact pressure and settlement. It depends on foundation loads, foundation size and stratification of the subsoil. The main modulus of subgrade reaction k_{sm} for a rectangular foundation on layered subsoil can be obtained from dividing the average contact pressure q_o over the settlement s_o under the characteristic point on the foundation, which has been defined by *Graßhoff* (1955). Clearly, this procedure is valid only for rectangular foundations on a layered subsoil model. Determining the main modulus of subgrade reaction k_{sm} for irregular foundation on an irregular subsoil model using another analysis is also possible by *ELPLA*.

In this example, settlement calculations at the characteristic point on the raft, using *Steinbrener's* formula (1934) for determining the settlement under the corner of a rectangular loaded area with the principle of superposition, are used to verify *ELPLA* analysis for determining the main modulus of subgrade reaction k_{sm}.

Consider the square raft in Figure 18, with area of $A_f = 8 \times 12$ [m^2] and thickness of $d = 0.6$ [m].

2 Soil properties

The soil under the raft consists of three layers as shown in Figure 18 and Table 16. *Poisson's* ratio is $\nu_s = 0.0$ [-] for the three layers. The foundation level of the raft is $d_f = 2.0$ [m].

Table 16 Soil properties

Layer No.	Type of soil	Depth of layer z [m]	Modulus of compressibility E_s [kN/m^2]	Unit weight of the soil γ_s [kN/m^3]
1	Clay	9.0	8 000	18
2	Medium sand	14.0	100 000	-
3	Silt	20.0	12 000	-

3 Loads

The raft carries 12 column loads, each is $P = 1040$ [kN].

4 Raft material

The raft material (concrete) has the following properties:

Young's modulus	E_b	$= 2.0 \times 10^7$	[kN/m²]
Poisson's ratio	ν_b	$= 0.25$	[-]
Unit weight	γ_b	$= 0.0$	[kN/m³]

Unit weight of the raft material is chosen $\gamma_b = 0.0$ [kN/m³] to neglect the self-weight of the raft.

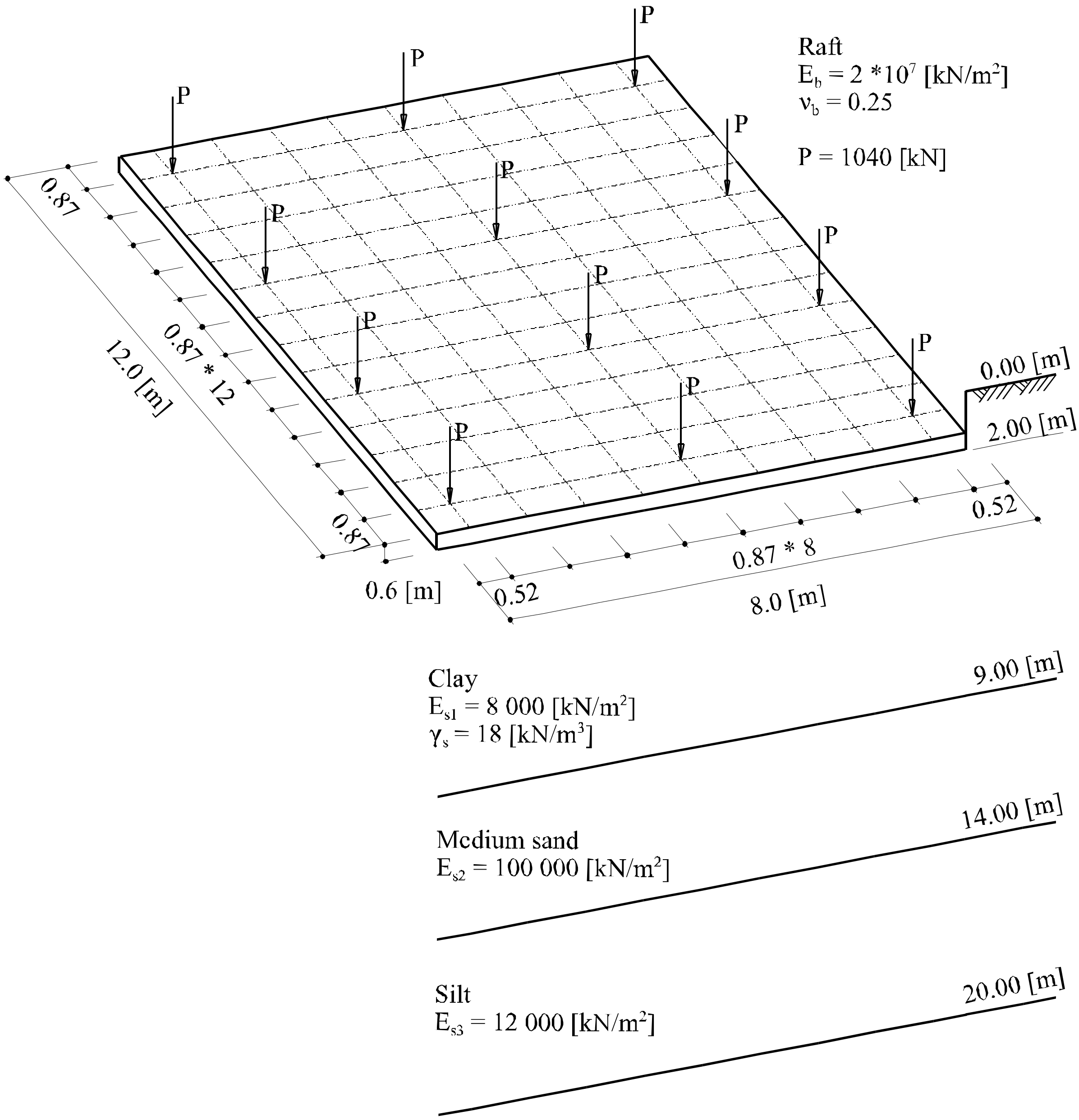

Figure 18 Raft dimensions, loads, FE-Net and subsoil

5 Settlement calculations

The average contact pressure q_o is given by

$$q_o = \Sigma P/A_f = 12\times1040 / (8 \times 12) = 130 \text{ [kN/ m}^2\text{]}.$$

The raft settlement is obtained at the characteristic point *o* by hand calculation. This point *o* takes the coordinates $a_c = 0.87\ A$ and $b_c = 0.87\ B$ as shown in Figure 19. The raft is divided into four rectangular areas I, II, III and IV as shown in Figure 19. The settlement of point *o* is then the sum of settlements of areas I, II, III and IV.

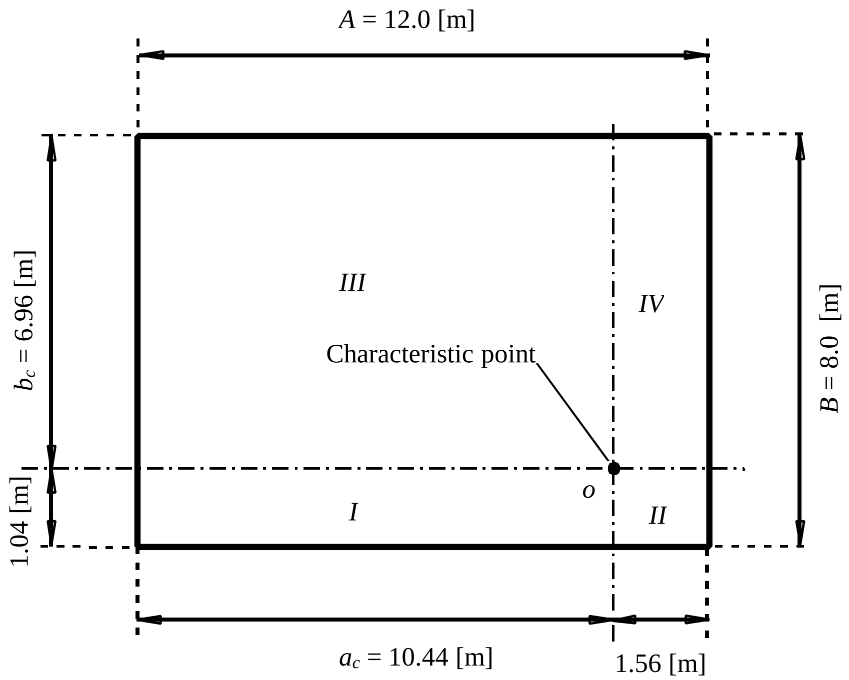

Figure 19 Characteristic point o of the settlement on the raft

According to *Steinbrenner* (1934) the settlement *s* of a point lying at a depth *z* under the corner of a rectangular loaded area $a \times b$ and intensity *q* is given by

$$s = \frac{q(1-\nu_s^2)}{2\pi E_s}\left(b.\ln\frac{(c-a)(m+a)}{(c+a)(m-a)} + a.\ln\frac{(c-b)(m+b)}{(c+b)(m-b)}\right) + \frac{q(1-\nu_s-2\nu_s^2)}{2\pi E_s}\left(z\tan^{-1}\frac{a.b}{z.c}\right) \quad (16)$$

The above equation can be rewritten as:

$$s = \frac{q(1-\nu_s^2)}{2\pi E_s}\left(B_n + A_n + D_n\right) = \frac{q(1-\nu_s^2)}{2\pi E_s} C_n = \frac{q}{E_s} f \quad (17)$$

Where $m = \sqrt{(a^2+b^2)}$ and $c = \sqrt{(a^2+b^2+z^2)}$

The settlement calculations of the 1st soil layer are carried out in Table 17.

Table 17 Settlement calculations of the 1st soil layer (z_1 = 7 [m])

Area	a [m]	b [m]	m [m]	c [m]	B_n	A_n	D_n	C_n
I	6.96	1.56	7.133	9.994	4.183	0.904	1.078	6.165
II	1.04	1.56	1.875	7.247	1.500	2.030	0.224	3.754
III	6.96	10.44	12.547	14.368	2.013	3.803	4.380	10.196
IV	1.04	10.44	10.492	12.613	0.351	3.788	0.857	4.996
ΣC_n								25.111

The settlement coefficient f_1 for the 1st layer is given by:

$$f_1 = \Sigma C_n / 2\pi = 25.111/ (2\pi) = 3.997$$

The settlement s_1 for the 1st soil layer is given by:

$$s_1 = q_o\, f_1 / E_{s1} = 130 \times 3.997/ 8000 = 0.06494 \text{ [m]}$$

In similar manner, the settlement coefficient f_2 for a soil layer until depth z =12 [m] is

$$f_2 = 5.2$$

The settlement s_2 for the 2nd soil layer is given by:

$$s_2 = q_o\, (f_2 - f_1)/ E_{s2} = 130\ (5.2 - 3.997)/ 100000 = 0.00156 \text{ [m]}$$

The settlement coefficient f_3 for a soil layer until depth z = 18 [m] is

$$f_3 = 6.038$$

The settlement s_3 for the 3rd soil layer is given by:

$$s_3 = q_o\, (f_2 - f_3)/ E_{s3} = 130\ (6.038 - 5.2)/ 12000 = 0.00908 \text{ [m]}$$

The total settlement s_o for all layers is given by:

$$s_o = s_1 + s_2 + s_3 = 0.06494 + 0.00156 + 0.00908 = 0.07558 \text{ [cm]}$$

The main modulus of subgrade reaction k_{sm} is given by:

$$k_{sm} = q_o / s_o = 130/ 0.07558 = 1720 \text{ [kN/m}^3\text{]}$$

6 Comparison of results

Table 18 compares the values of modulus of subgrade reaction obtained by using *Steinbrenner's* formula (1934) with that of *ELPLA*. It shows that the main modulus k_{sm} computed by using *Steinbrenner's* formula and that by *ELPLA* are nearly the same.

Table 18 Main modulus of subgrade reaction k_{sm} computed by using *Steinbrenner's* formula and *ELPLA*

Item	Hand calculation	*ELPLA*	Difference [%]
Main modulus k_{sm} [kN/m^3]	1720	1727	0.41

Example 14: Verifying beam foundation on elastic springs

1 Description of the problem

To verify the mathematical model of *ELPLA* for analyzing beam foundations, the results of beam foundation on elastic springs obtained by *Rombach* (2000), Section 2.4.2, page 34, are compared with those obtained by *ELPLA*.

Geometry and load of the foundation are the same as those of *Rombach* (2000) as shown in Figure 20. A strip foundation of thickness d = 0.60 [m] and length L = 5.0 [m] is considered. The analysis is carried out for 1.0 [m] width stripe. The beam cross section yields Moment of Inertia I = 0.018 [m^4] and Torsion modulus J = 0.045077 [m^4]. The beam is subjected to a wall load of P = 1000 [kN/m] at the center.

The parameters of beam material (Concrete C30/70) are *Young's* modulus $E_b = 3.2 \times 10^7$ [kN/m^2] and Shear modulus $G_b = 1.3 \times 10^7$ [kN/m^2]. Modulus of subgrade reaction of the soil is k_s = 50000 [kN/ m^3].

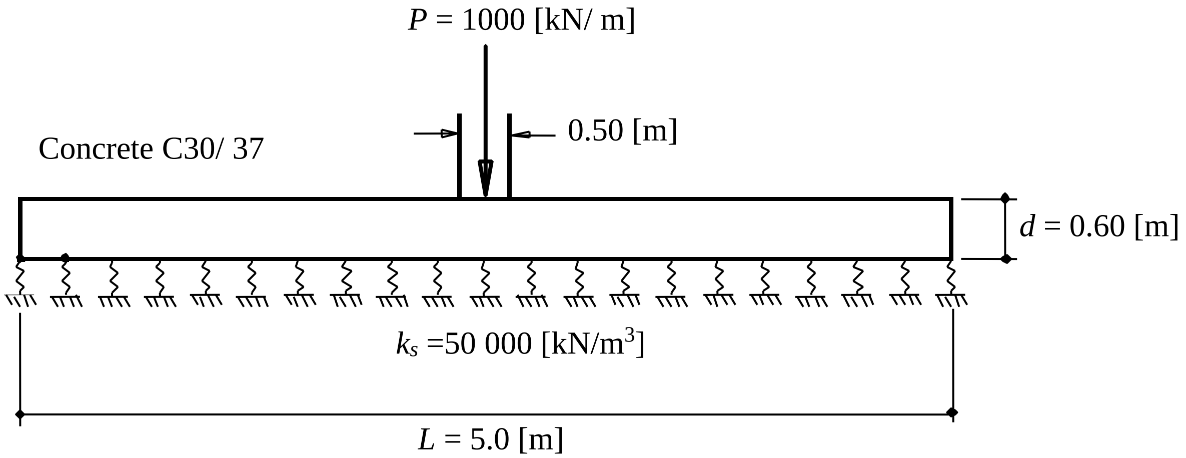

Figure 20 Beam on elastic springs, dimensions and load

2 Analysis and results

In *ELPLA* either ribbed rafts or only beams can be analyzed using plate elements together with beam elements. In which the grid elements are placed in regions close to plate element boundaries. In case of analyzing only beam foundation one can eliminate the plate element by assuming its rigidity to be zero (E_b = 0). Therefore, in this example the entire foundation is subdivided into rectangular elements, in which the width of the element is chosen to be equal to the width of the beam strip B = 1.0 [m]. Each element has area of 0.25 × 1.0 [m^2]. Accordingly, the beam elements represent the beam on the net as shown in Figure 21. The corresponding spring constant for nodes under beam elements is k_s = 50000 [kN/m^3] while for nodes under plate elements is k_s = 0.

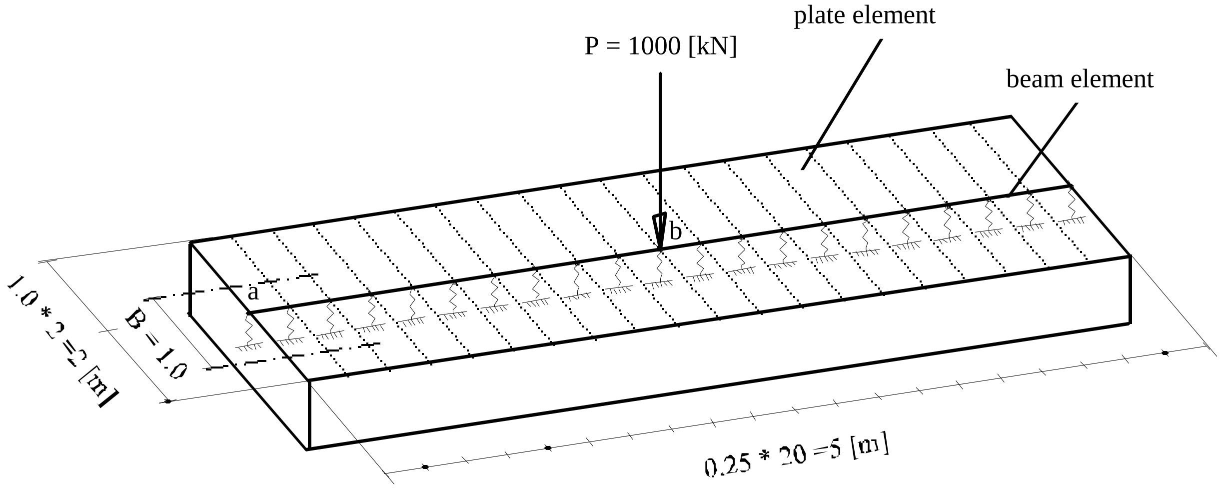

Figure 21 FE-Net of the foundation

3 Results

Table 19 shows the comparison of the results at two selected points *a* and *b* on the beam obtained by *ELPLA* with those obtained by *Rombach* (2000). From this table it can be seen that the results of both analyses are in good agreement.

Table 19 Comparison of the results at two selected points *a* and *b* on the beam obtained by *ELPLA* with those obtained by *Rombach* (2000)

Point	Settlement *s* [cm]		Moment M_b [kN.m]		Shear force Q_s [kN]	
	Rombach (2000)	*ELPLA*	*Rombach* (2000)	*ELPLA*	*Rombach* (2000)	*ELPLA*
a	0.31	0.31	-	-	-	-
b	0.47	0.46	520	582	471	471

Example 15: Verifying grid foundation on elastic springs

1 Description of the problem

To verify the mathematical model of *ELPLA* for analyzing grid foundations, the results of grid foundation on elastic springs obtained by *Szilard* (1986), Example 4.4.5, page 350, are compared with those obtained by *ELPLA*.

Geometry and loads of the foundation are the same as those of *Szilard* (1986) as shown in Figure 22. The grid has rectangular cross section of 2.5 [m] width and 0.5 [m] depth, yields Moment of Inertia I = 0.026 [m^4] and Torsion modulus J = 0.091 [m^4].

The parameters of grid material are *Young's* modulus $E_b = 3 \times 10^7$ [kN/m^2] and Shear modulus $G_b = 1 \times 10^7$ [kN/m^2]. Modulus of subgrade reaction of the soil is k_s = 40 000 [kN/m^3].

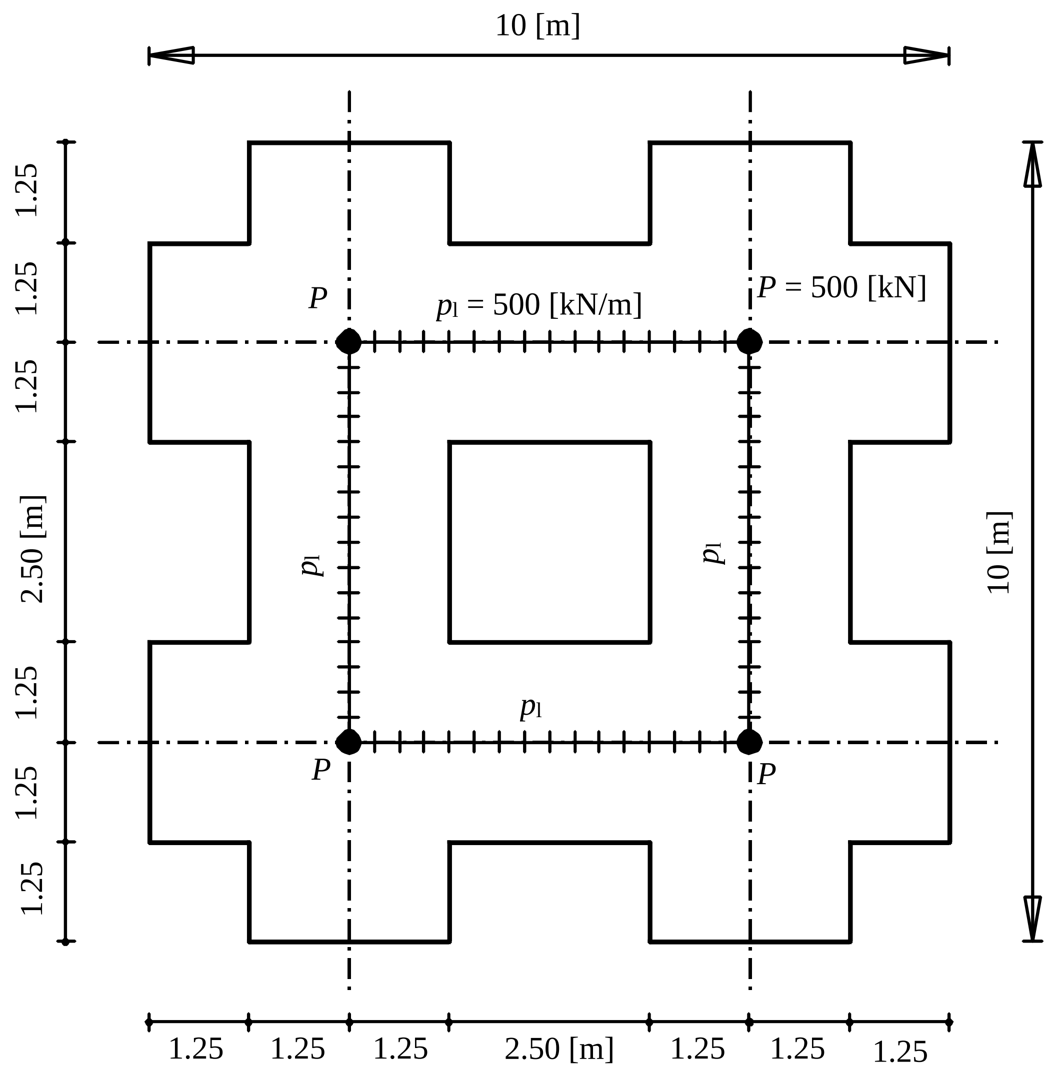

Figure 22 Grid foundation: geometry and loads

2 Analysis and results

In *ELPLA* either ribbed rafts or only girds can be analyzed using plate elements together with grid elements. In which the grid elements are placed in regions close to plate element boundaries. In case of analyzing only grid foundation one can eliminate the plate element by assuming its rigidity to be zero (E_b = 0). Therefore, in this example the entire foundation is subdivided into square elements, each has area of 0.417 × 0.417 [m^2]. Accordingly, the grid elements represent the grid on the net as shown in Figure 23. The corresponding spring constant for nodes under grid elements is k_s = 40000 × 2.5/0.417 = 240000 [kN/ m^3] while for nodes under plate elements is k_s = 0.

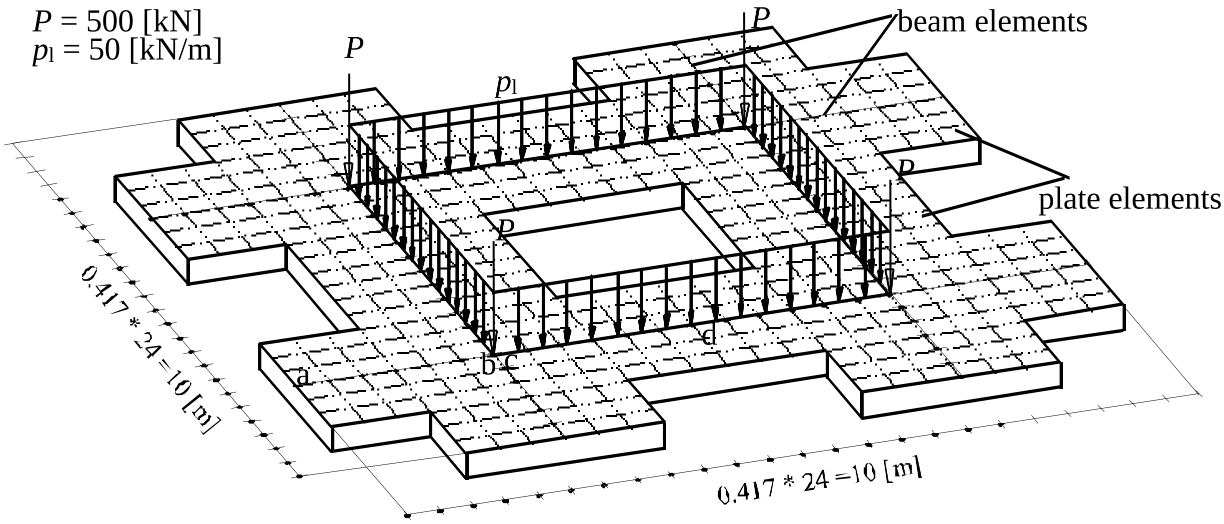

Figure 23 FE-Net of the foundation

3 Results

Table 20 shows the comparison of the results at four selected points *a*, *b*, *c* and *d* on the grid obtained by *ELPLA* with those obtained by *Szilard* (1986). Although the mathematical model used to determine the stiffness matrix of the soil by *Szilard* (1986) is different from that of *ELPLA*, the comparison is good.

Table 20 Comparison of the results at four selected points *a*, *b*, *c* and *d* on the grid obtained by *ELPLA* with those obtained by *Szilard* (1986)

Point	Settlement *s* [cm]		Moment M_b [kN.m]		Shear force Q_s [kN]	
	Szilard (1986)	*ELPLA*	*Szilard* (1986)	*ELPLA*	*Szilard* (1986)	*ELPLA*
a	0.02	0.02	0	0	0	5
b	0.09	0.09	153	151	148	130
c	0.09	0.09	125	149	-103	-112
d	0.10	0.10	-6	-7	0	-11

Example 16: Verifying elastic raft on Isotropic elastic half-space soil medium

1 Description of the problem

To verify the mathematical model of *ELPLA* for elastic raft, the results of an elastic raft at different relative stiffness obtained by other analytical solutions from *Stark/ Majer* (1988) and *Borowicka* (1939) are compared with those obtained by *ELPLA*.

A rectangular raft with sides 12 [m] and 6 [m], that rests on an isotropic elastic half-space soil medium is chosen and subdivided into 12 × 12 elements as shown in Figure 24. The elastic properties of the raft and the soil are E_s = 10 000 [kN/m^2], E_b = 2.6 × 10^7 [kN/m^2], ν_s = 0 [-] and ν_b = 0.15 [-]. The raft carries a uniform load of 100 [kN/m^2].

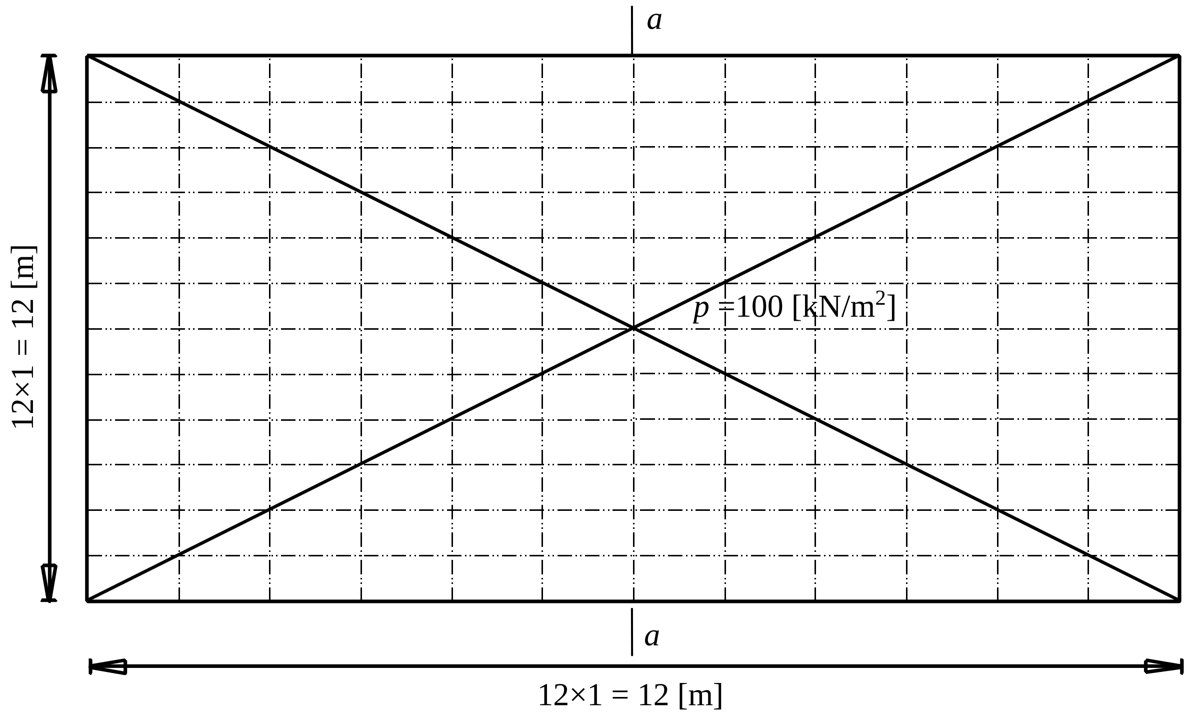

Figure 24 Raft geometry, loading and FE-Net

2 Results

Figure 24 to Figure 27 show the comparison of the results at the middle section a-a of the raft obtained by *ELPLA* with those obtained by *Stark/ Majer* (1988) and *Borowicka* (1939) for several relative stiffnesses k_B which are defined in Eq. 18 according to *Borowicka* (1939).

The relative stiffness of the soil-raft system, k_B [-], is defined by

$$k_B = \frac{1}{6}\left(\frac{1 - n\nu_s^2}{1 - n\nu_b^2}\right)\left(\frac{E_b}{E_s}\right)\left(\frac{d}{b}\right)^3 \qquad (18)$$

where:

ν_b and ν_s	*Poisson's* ratios for raft material and soil, respectively [-]
E_b and E_s	*Young's* modulus of raft material and soil, respectively [kN/m^2]
b	Half-width for the strip raft or radius for the circular raft [m]
d	Thickness of the raft [m]

In which, $k_B = 0.0$ indicates a perfectly flexible raft, and $k_B = \infty$ means a perfectly rigid raft. Eq. 18 was evaluated for $k_B = \pi/30$, $\pi/10$ and $\pi/3$.

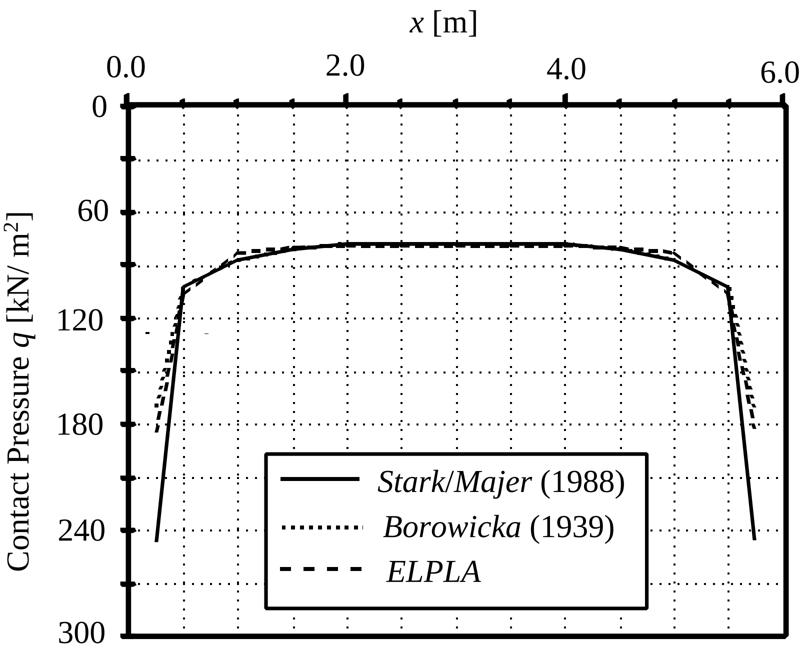

Figure 25 Contact pressure distribution q [kN/m^2] at section a-a, $k_B = \pi/30$, d = 18.5 [cm]

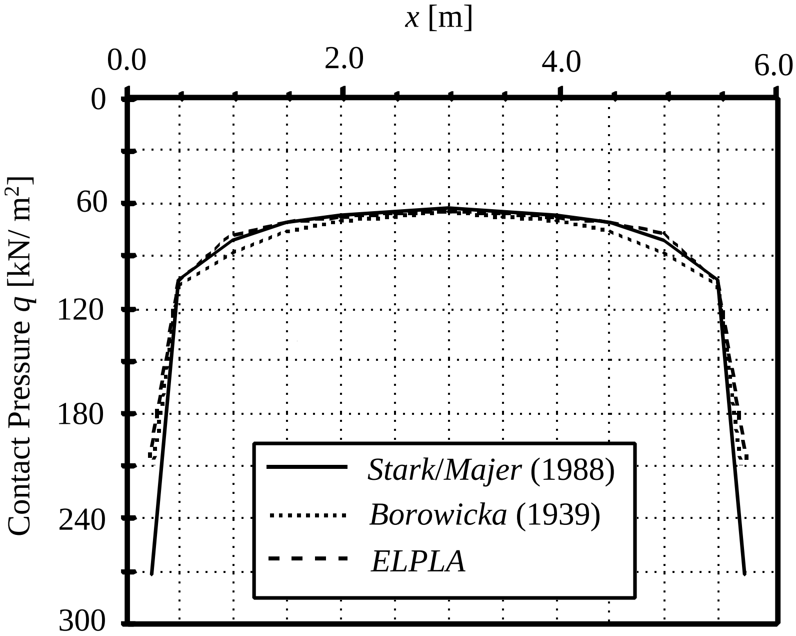

Figure 26 Contact pressure distribution q [kN/m^2] at section a-a, $k_B = \pi/10$, d = 26.7 [cm]

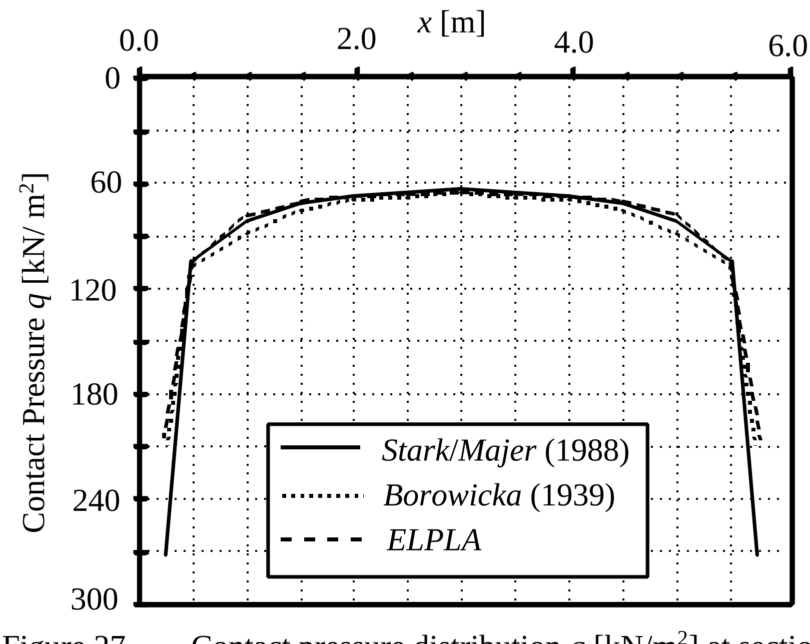

Figure 27 Contact pressure distribution q [kN/m^2] at section a-a, $k_B = \pi/3$, d = 40 [cm]

It is obviously from Figure 25 to Figure 27 that the results of elastic raft obtained by *ELPLA* are nearly equal to those obtained by *Stark/ Majer* (1988) and *Borowicka* (1939).

Example 17: Verifying *Winkler's* model and Isotropic elastic half-space soil medium

1 Description of the problem

A simple example was carried out to verify *Winkler's* model and Isotropic elastic half-space soil medium, by comparing *ELPLA* results with those of *Mikhaiel* (1978), Example 34, page 189, and *Henedy* (1987), Section 3.6, page 66, or *Bazaraa* (1997).

A square raft of 0.4 [m] thickness and 10 [m] side was chosen and subdivided into 64 square elements, each has dimensions of 1.25 [m] × 1.25 [m]. The raft carries four column loads, each 500 [kN] as shown in Figure 28.

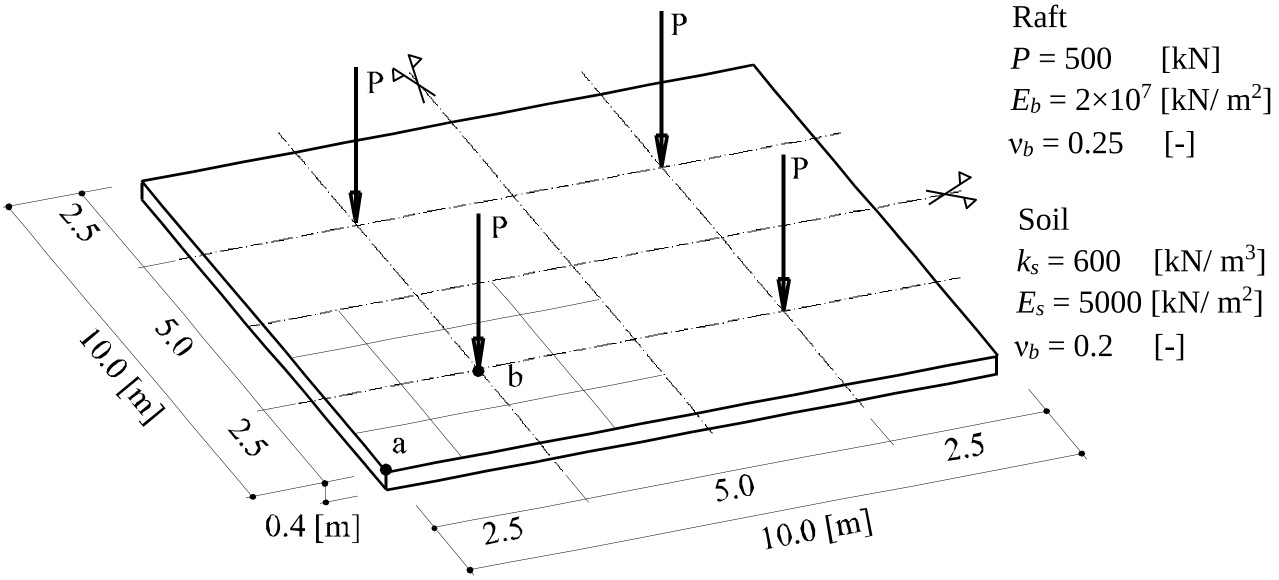

Figure 28 Raft dimensions, FE-Net and loads

The raft material has the following parameters:

Young's modulus	E_b	$= 2 \times 10^7$	[kN/m^2]
Poisson's ratio	ν_b	= 0.25	[-]
Unit weight	γ_b	= 0	[kN/m^3]

2 Results

Taking advantage of the symmetry in shape, soil and load geometry about both *x*- and *y*-axes, the analysis is carried out by considering only a quarter of the raft.

a) *Winkler's* model

The raft rests on *Winkler's* springs having modulus of subgrade reaction of k_s = 600 [kN/m^3]. Table 21 compares the results obtained by *ELPLA* with those of *Mikhaiel* (1978) and *Bazaraa* (1997) at the selected points *a* and *b*.

Table 21 Comparative examination of the results of *Mikhaiel* (1978), *Bazaraa* (1997) and *ELPLA* (*Winkler's* model)

Settlement *s* [cm]	*Mikhaiel* (1978)	*Bazaraa* (1997)	*ELPLA*
under the column (point *b*)	3.401	3.411	3.412
at the corner (point *a*)	3.143	3.070	3.069

b) Isotropic elastic half-space soil medium

The same problem shown in Figure 28 was examined for the case where Isotropic elastic half-space medium represents the soil. The soil has modulus of elasticity E_s = 5000 [kN/m^2] and *Poisson's* ratio ν_s = 0.2 [-]. The obtained results for Isotropic elastic half-space soil medium according to *Mikhaiel* (1978), *Bazaraa* (1997) and *ELPLA* at the selected points *a* and *b* are shown in Table 22.

Table 22 Comparative examination of the results of *Mikhaiel* (1978), *Bazaraa* (1997) and *ELPLA* (Isotropic elastic half-space soil medium)

Settlement *s* [cm]	*Mikhaiel* (1978)	*Bazaraa* (1997)	*ELPLA*
under the column (point *b*)	3.421	3.440	3.458
at the corner (point *a*)	2.834	2.709	2.746

It is obviously from Table 21 and Table 22 that the results of *Winkler's* model and Isotropic elastic half-space soil medium obtained by *ELPLA* are nearly equal to those obtained by *Mikhaiel* (1978) and *Bazaraa* (1997).

Example 18: Verifying simply supported slab

1 Description of the problem

To examine the accuracy of the calculation of Finite elements-method and the convergence characteristics of the stiffness matrix, the maximum values of deflection *w*, moments m_x, m_y and m_{xy} of a simply supported rectangular slab are obtained at different nets of finite elements. The slab carries a uniform distributed load of p = 100 [kN/m^2] as shown in Figure 29. *Young's* modulus of the slab material is $E_b = 1.2 \times 10^7$ [kN/m^2] and *Poisson's* ratio is ν_b= 0 [-]. The slab thickness is d = 0.1 [m].

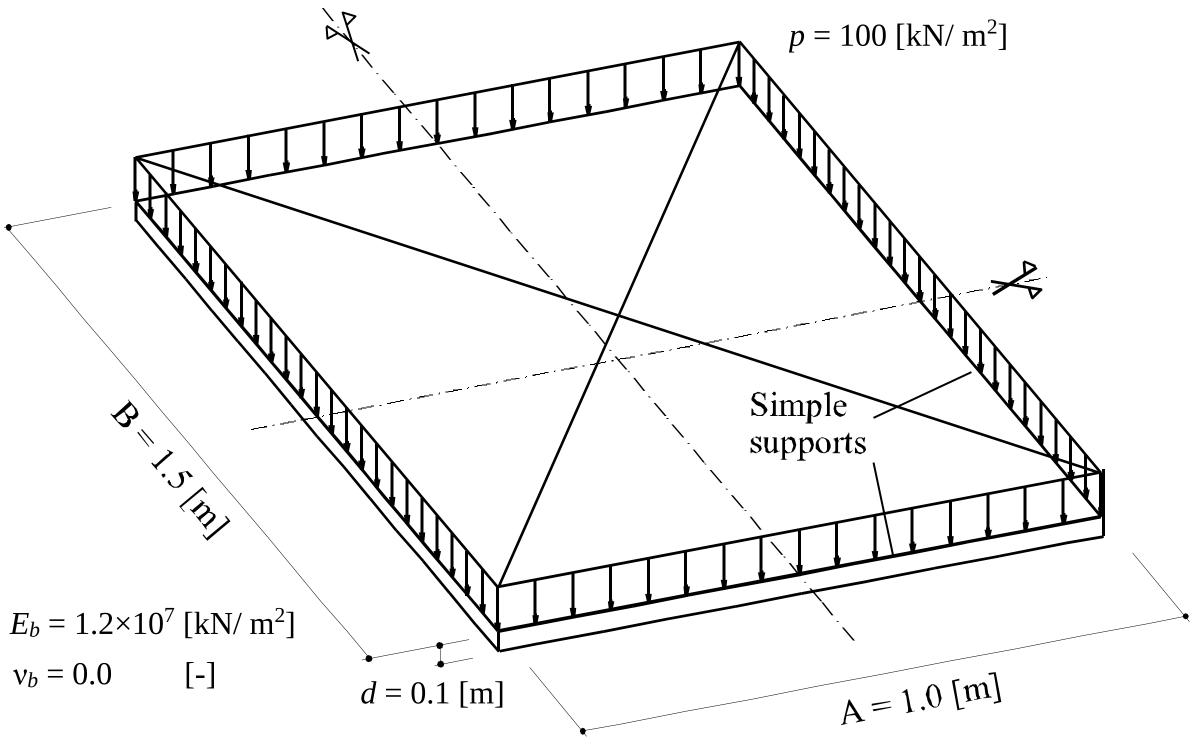

Figure 29 Simply supported rectangular slab

2 Analysis and results

Because of the symmetry it is sufficient to analyze only one quarter slab. The finite element nets of the slab are shown in Figure 30. Results of *ELPLA* are compared by the exact solution using the known charts from *Czerny* (1955) and Finite elements-solution from *Falter* (1992) in Table 23 to Table 26. From the tables, it can be noticed that results of deflection and moments obtained by *ELPLA* are the same as those of *Falter* (1992), Example 14.2, page 378, which are calculated using Finite elements-method. A sufficient accuracy for the results may be considered at slab mesh of 4 elements according to *Czerny's* charts.

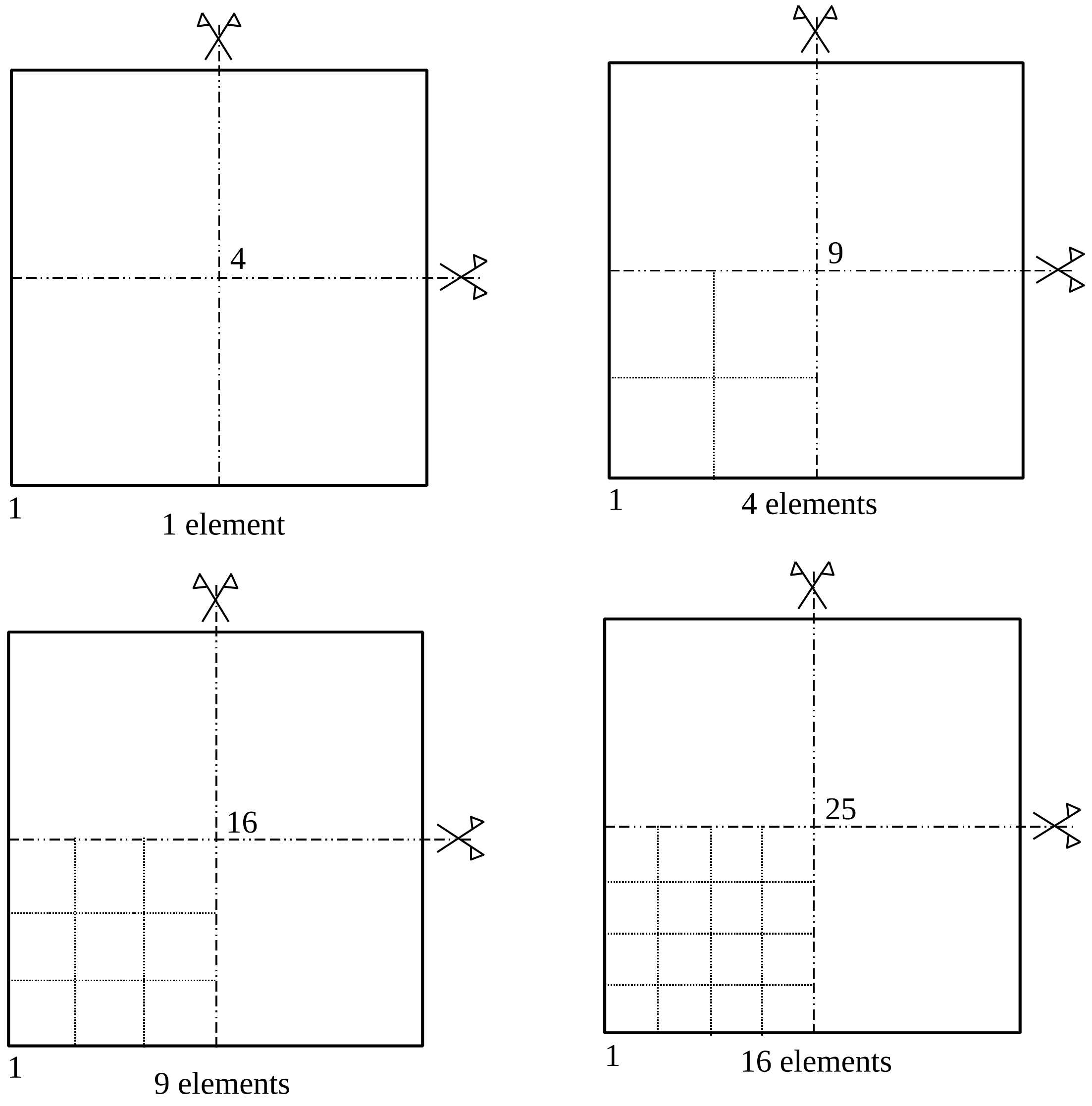

Figure 30 FE-Nets of the slab

Table 23 Deflection *w* [cm] computed by *Czerny's* charts (1955), *Falter* (1992) and *ELPLA*

No. of elements	Node No.	Deflection *w* [cm]		
		Czerny (1955)	*Falter* (1992)	*ELPLA*
1	4	0.077	0.094	0.094
4	9		0.082	0.082
9	16		0.079	0.079
16	25		0.078	0.078

Table 24 Moment m_x [kN.m/m] computed by *Czerny's* charts (1955), *Falter* (1992) and *ELPLA*

No. of elements	Node No.	Moment m_x [kN.m/m]		
		Czerny (1955)	*Falter* (1992)	*ELPLA*
1	4	7.30	10.29	10.29
4	9		7.99	7.99
9	16		7.58	7.59
16	25		7.45	7.45

Table 25 Moment m_y [kN.m/m] computed by *Czerny's* charts (1955), *Falter* (1992) and *ELPLA*

No. of elements	Node No.	Moment m_x [kN.m/m]		
		Czerny (1955)	*Falter* (1992)	*ELPLA*
1	4	2.88	3.36	3.36
4	6		3.42	3.29
9	12		2.98	2.98
16	20		2.89	2.89

Table 26 Moment m_{xy} [kN.m/m] computed by using *Czerny's* chart, *Falter* (1992) and *ELPLA*

No. of elements	Node No.	Moment m_x [kN.m/m]		
		Czerny (1955)	*Falter* (1992)	*ELPLA*
1	1	6.13	6.57	6.57
4	1		6.35	6.35
9	1		6.26	6.26
16	1		6.22	6.22

Example 19: Evaluation of iteration methods

1 Description of the problem

One of the difficulties to apply the Continuum model to practical problems is the long computation time. Therefore, a comparison for time and accuracy required for analysis of the raft by the Continuum model is carried out by the following calculation methods shown in Table 27.

Table 27 Calculation methods

Method No.	Method
4	Modification of modulus of subgrade reaction by iteration after *Ahrens/ Winselmann* (1984) (*Winkler's* model/ Continuum model)
6	Modulus of compressibility method for elastic raft on layered soil medium after *El Gendy* (1998) (Solving system of linear equations by iteration) (Layered soil medium - Continuum model)
7	Modulus of compressibility method for elastic raft on layered soil medium (Solving system of linear equations by elimination) (Layered soil medium - Continuum model)

To evaluate the iterative procedures used in *ELPLA*, consider the raft shown in Figure 31. The raft has a dimension of 10 [m] × 20 [m] and 0.6 [m] thickness.

2 Soil properties

The raft rests on two different soil layers of thickness 5 [m] and 10 [m], respectively. The modulus of compressibility of the first soil layer is E_{s1} = 20 000 [kN/ m^2], while for the second layer is E_{s2} = 100 000 [kN/ m^2]. *Poisson's* ratio for the soil is ν_s = 0.0 [-].

3 Raft material

The raft material was supposed to have the following parameters:

Young's modulus	E_b	= 2.6 × 10^7	[kN/m^2]
Poisson's ratio	ν_b	= 0.15	[-]
Unit weight	γ_b	= 0.0	[kN/m^3]

Unit weight of concrete is chosen γ_b = 0.0 to neglect the self weight of the raft.

4 Loads

The raft carries 15 column loads as shown in Figure 31. Each of the three inner columns carries a load of P_3 = 1850 [kN], each of the edge columns carries a load of P_2 = 1200 [kN] and each of the corners columns a load of P_1 = 750 [kN].

5 Analysis of the raft

The raft is divided into 1056 elements yielding to 1125 nodal points for the raft and the soil as shown in Figure 31. Because of the symmetry in shape and load geometry about *x*- and *y*-axes, only one quarter of the raft is considered. Taking advantage of the symmetry in shape, soil and load geometry about both *x*- and *y*-axes, the analysis is carried out by considering only a quarter of the raft. The quarter of the raft has 299 nodes, each node has three unknowns (w, θ_x, θ_y). This gives 897 equations by applying the method 7.

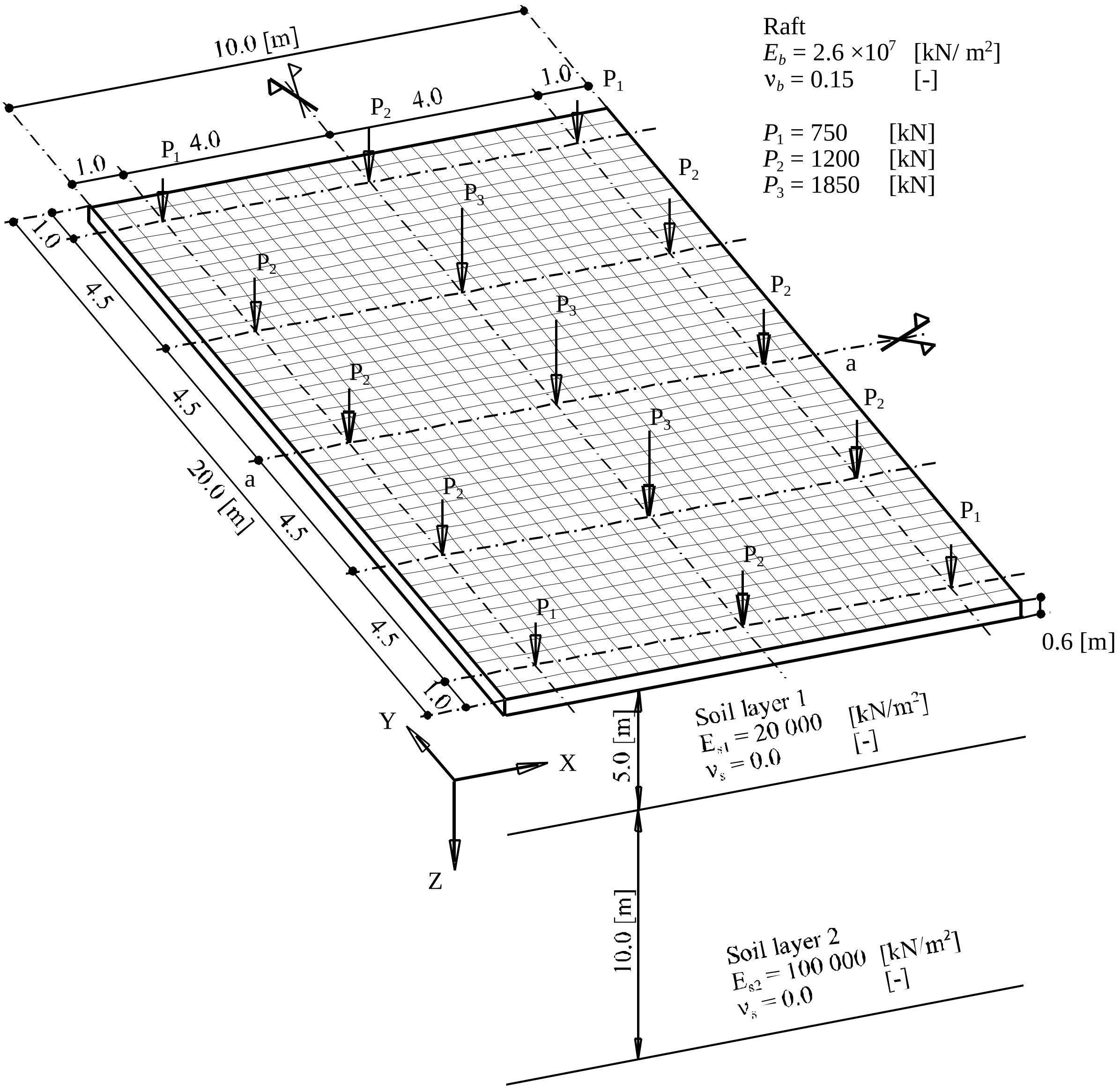

Figure 31 Raft dimensions, loads, FE-Net and subsoil

6 Evaluation of the iteration method 6

To judge the iteration method 6, the settlements *s*, contact pressures *q* and moments m_x at the middle section a-a of the raft against iterative cycles are plotted in Figure 32 to Figure 34. It can be concluded that the results of the computation can be obtained after only two iterative cycles. It can be shown also the first iterative cycle gives good results with maximum settlement error of 2.9 [%].

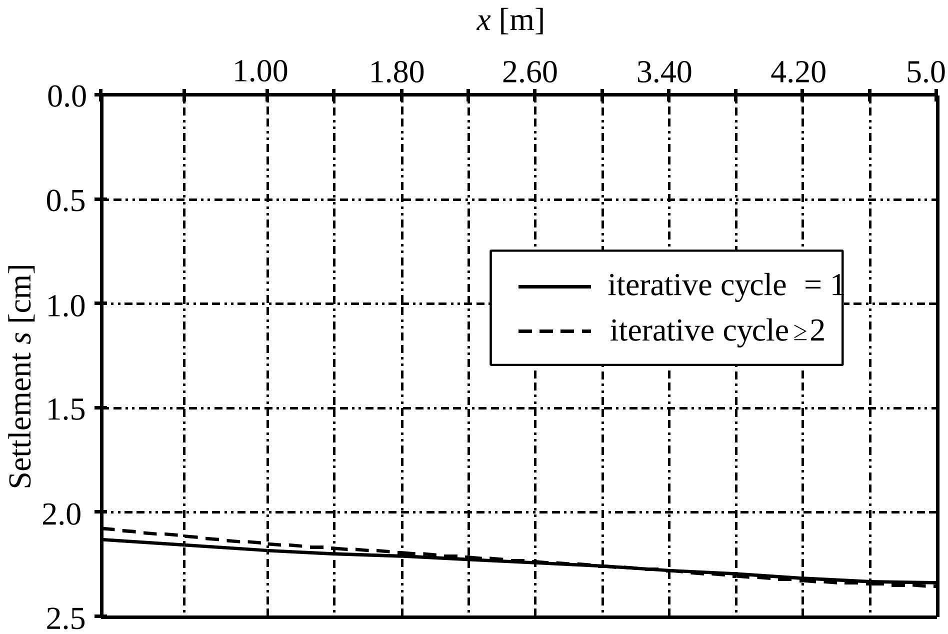

Figure 32 Settlements *s* [cm] at the middle section a-a for many iterative cycles

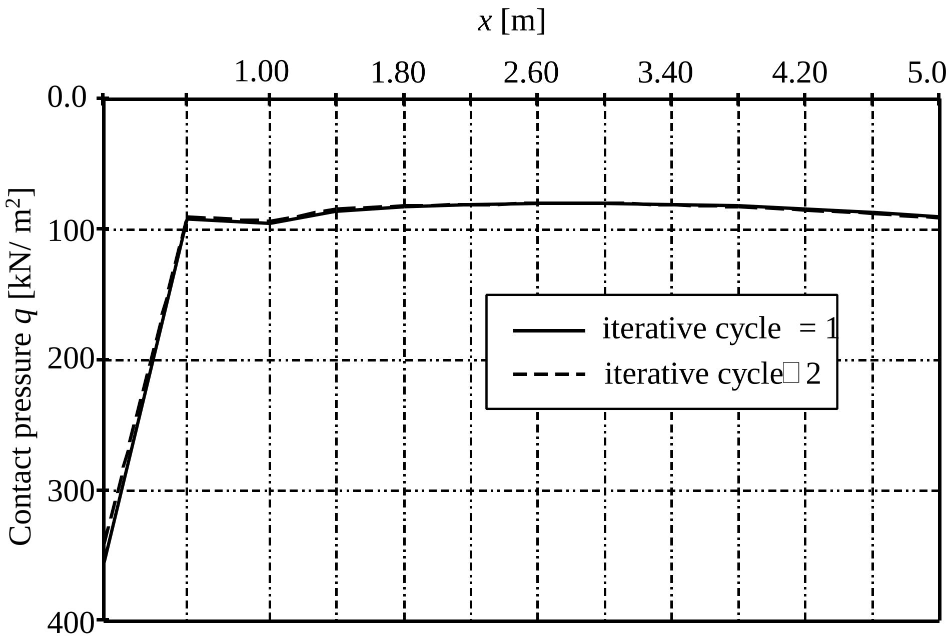

Figure 33 Contact pressures *q* [kN/m^2] at the middle section a-a for many iterative cycles

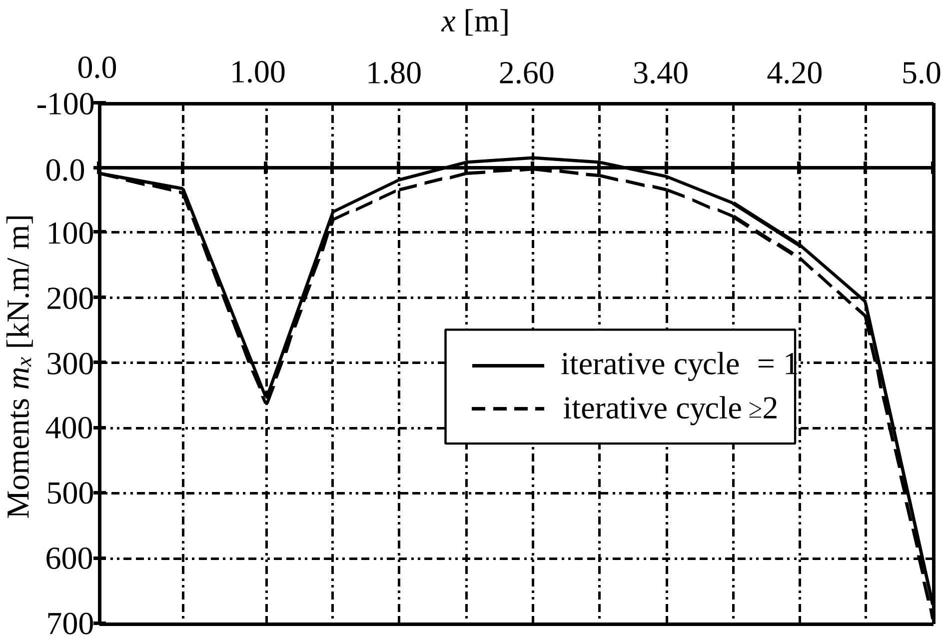

Figure 34 Moments m_x [kN.m/m] at the middle section a-a for many iterative cycles

7 Comparison between iteration method 4 and 6

To show the speed of convergence of the iteration method 4 with that of iteration method 6, a comparison between the two methods has been carried out. The maximum difference between the settlement calculated from iterative cycle *i* and that of the previous cycle *i*-1 is considered as an accuracy number for both methods 4 and 6. The accuracy of computation was plotted against the iterative cycle number in Figure 35 for the two iteration methods. This figure shows that the iteration method 6 converges more rapidly than method 4, which takes four iteration cycles while the iteration method 4 required 65 cycles to reach the same accuracy number.

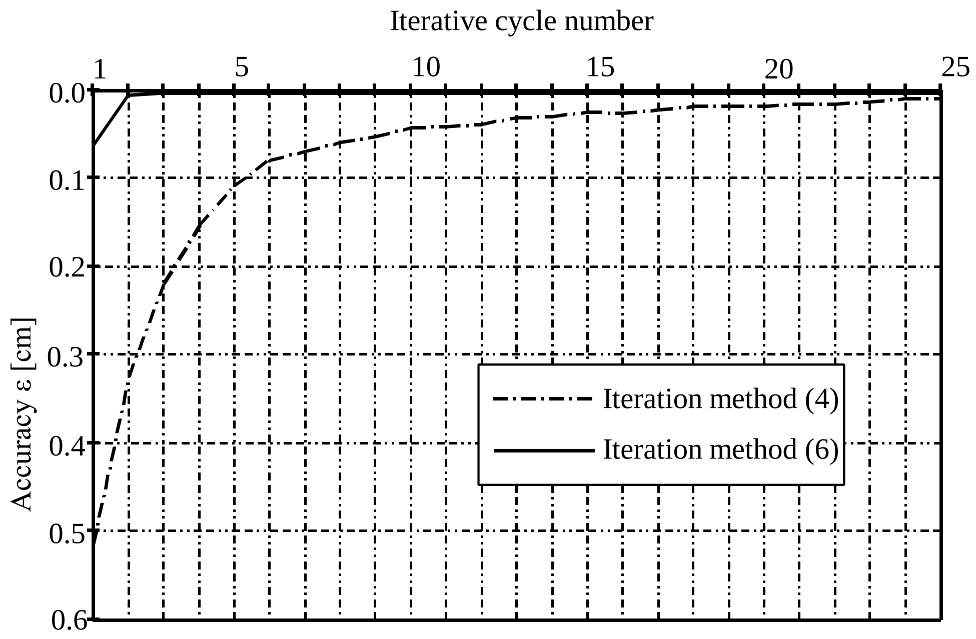

Figure 35 Accuracy against the iterative cycle number for the two iteration methods 4 and 6

8 Computation time required for solution of system equations

Table 28 compares the computation time required for the iteration processing by applying methods 4 and 6. In addition the computation time required for elimination processing by applying method 7. The analysis was carried out for the quarter raft (897 equations) using Pentium 100 computer. The accuracy was $\varepsilon = 0.0016$ [cm] for both two iteration methods.

Table 28 Computation time required for analysis of the raft (Computer Pentium 100)

Calculation method		Method 4	Method 6	Method 7
Number of iteration cycles		65	4	-
Center settlement [cm]		2.31	2.31	2.31
CPU Time [Min] required for	Assembling of soil stiffness matrix	-	1.05	1.05
	Assembling of plate stiffness matrix	-	-	0.04
	Iteration process	6.90	0.99	-
	Equation solving	-	-	11.30
	Total time	6.90	2.04	12.39

It can be seen from Table 28 that the iteration methods 4 and 6 give rapid results after a few steps of iteration process, especially by the method 6.

The settlement value, which is obtained at the center of the raft by iteration methods 4 and 6, coincides with that of the method 7, where the systems of equations are solved by elimination process.

The computation times used in Pentium 100 computer for the cases involving quarter of the raft are 6.9, 2.04 and 12.39 [Min.] for the three calculation methods 4, 6 and 7, respectively. Therefore, it can be concluded that for a symmetrically loaded raft, taking advantage of symmetry is always desirable and consider only a part of the raft rather than the entire raft to reduce the computation time.

Example 20: Examination of influence of overburden pressure

1 Description of the problem

One of the advantages of *ELPLA* is that the bilinear relation of deformation for the modulus of compressibility can be taken into consideration. Therefore, an example was carried out by the Modulus of compressibility method 7 to show the influence of overburden pressure on the settlements, contact pressures and moments.

A square raft that has the dimension of 18 × 18 [m^2] under an elevated water tank is chosen as shown in Figure 36.

For comparison, *ELPLA* was used to study the influence of overburden pressure (q_v, W_v) on the values of settlements, contact pressures and moments for the following three different assumptions:

- Without taking into consideration the influence of overburden pressure, where the modulus of compressibility for reloading W_s of the soil is taken to be equal to that of loading E_s

- The modulus of compressibility for reloading W_s of the soil is very great ($W_s = 9 \times 10^8$ [kN/m^2]), where the settlement due to the reloading of the soil is nearly zero

- The modulus of compressibility for reloading W_s = 12447 [kN/m^2] is three times as the modulus of compressibility for loading E_s = 4149 [kN/m^2], where the bilinear relation of deformation for the modulus of compressibility is taken into consideration

2 Raft material and thickness

The raft material and thickness are supposed to have the following parameters:

Young's modulus	E_b	$= 2 \times 10^7$	[kN/m^2]
Poisson's ratio	ν_b	= 0.25	[-]
Unit weight	γ_b	= 25	[kN/m^3]
Raft thickness	d	= 0.75	[m]

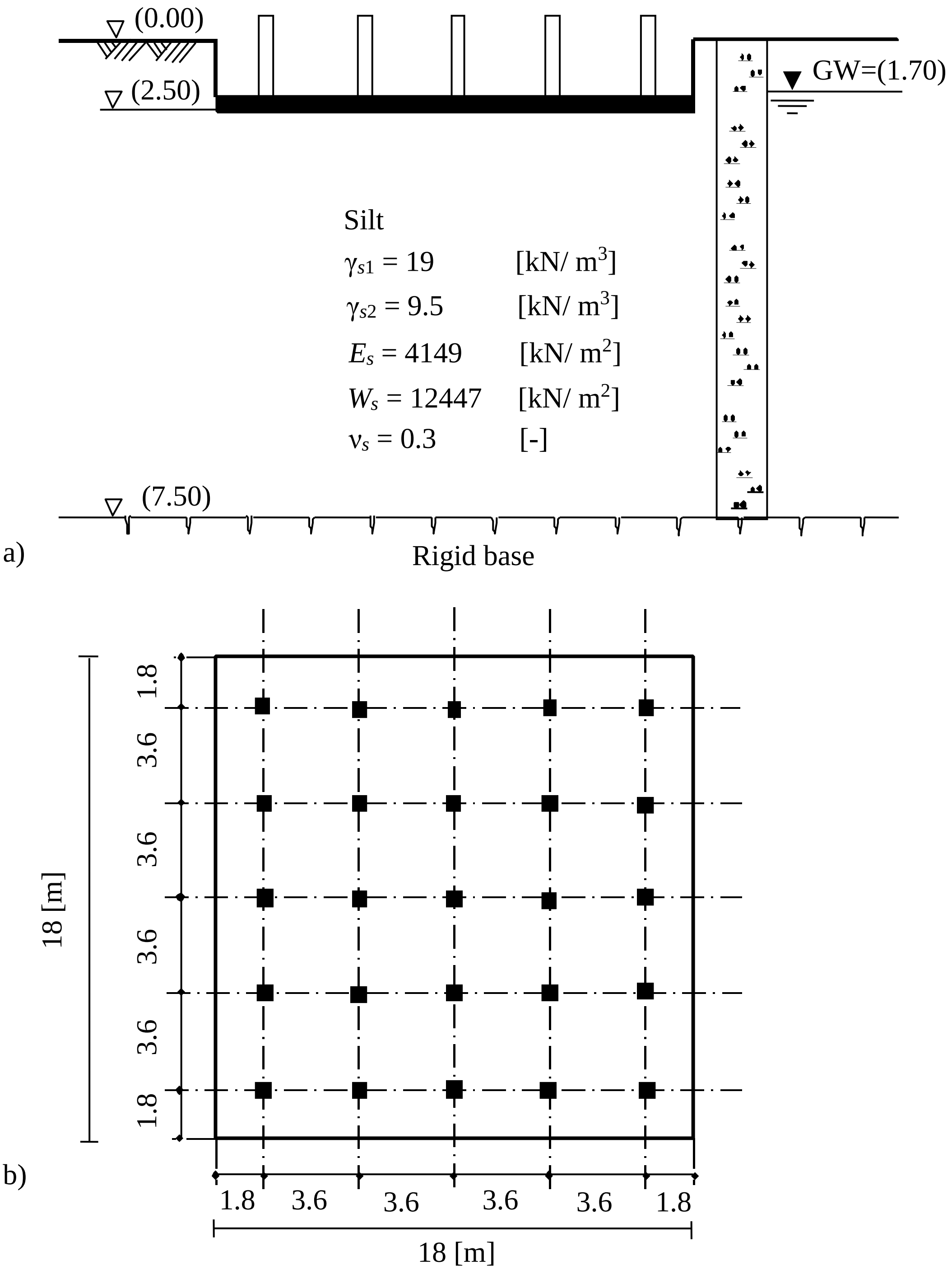

Figure 36 a) Section elevation in soil and raft

b) Dimensions [m] and columns (Each column load is 1685 [kN])

3 Soil properties

The subsoil under the raft is 5 [m] layer of silt resting on rigid base of rock. The layer parameters and the moduli of compressibility E_s (for loading) and W_s (for reloading) are given in the soil profile, Figure 36a. The level of water table under the ground surface is GW = 1.7 [m]. The level of foundation is d_f = 2.5 [m].

The silt has the following parameters:

Unit weight above the water table	γ_{s1}	= 19	[kN/m^3]
Unit weight under the water table	γ_{s2}	= 9.5	[kN/m^3]
Modulus of compressibility for loading	E_s	= 4149	[kN/m^2]
Modulus of compressibility for reloading	W_s	= 12447	[kN/m^2]
Poisson's ratio	ν_s	= 0.3	[-]

4 Loads

The raft transmits equal loads for all 25 columns, each of 1685 [kN]. The loads give average contact pressure on soil q_{av} = 130 [kN/m^2]. Columns are equally spaced, 3.6 [m] apart, in each direction as shown in Figure 36b.

5 Analysis of the raft

Taking advantage of the symmetry in shape and load geometry about *x*- and *y*-axes, the analysis was carried out by considering only a quarter of the raft, Figure 37. A net of equal square elements is chosen. Each element has a side of 1.8 [m]. There is a total of only 36 nodal points, each with three unknown displacements, so the total number of equations is reduced to 108.

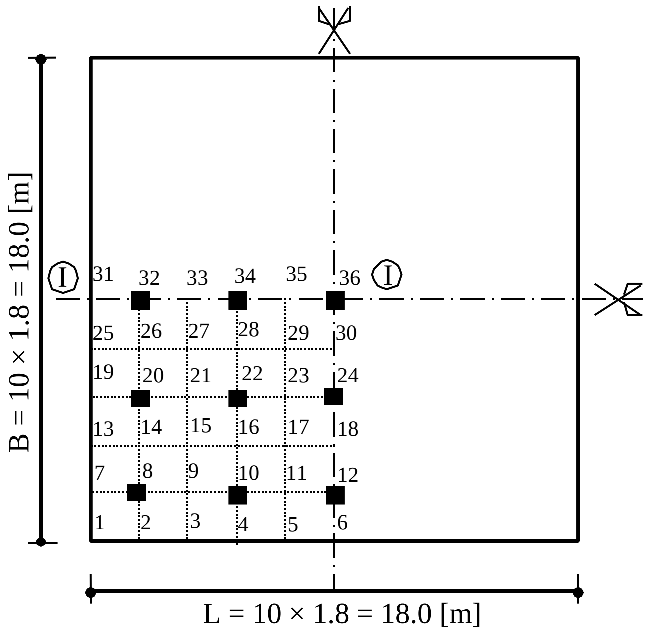

Figure 37 FE-Net of the raft with node numbering

6 Results and evaluation

Figure 38 to Figure 40 show the expected settlement s, contact pressure distribution q and moment m_x at the middle section I-I of the raft for the three cases of analysis. The results of the analysis with and without taking into consideration the influence of overburden pressure show that the settlement has great difference while the contact pressure and moment have practically no difference. On the other hand a great difference is remarkable for the settlements (Figure 38).

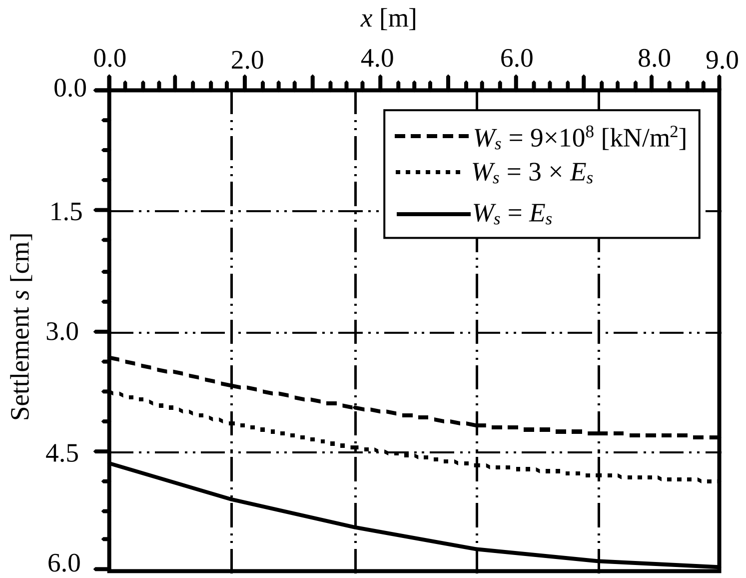

Figure 38 Settlement s [cm] at the middle section of the raft

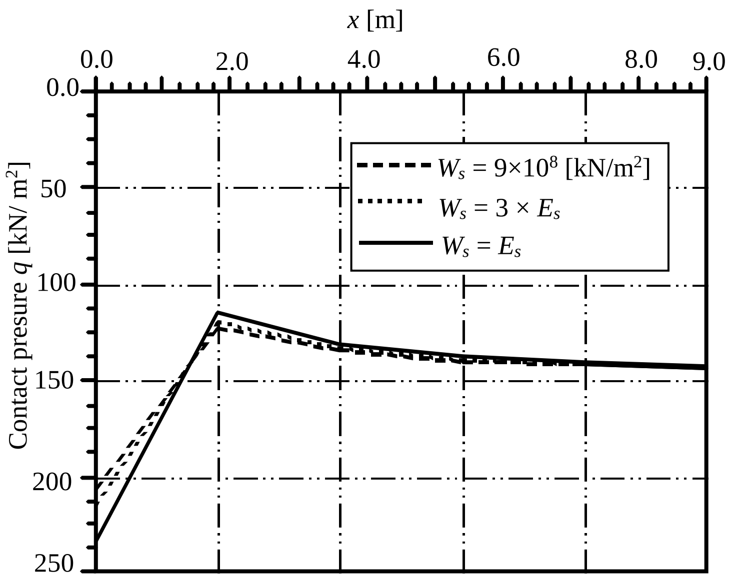

Figure 39 Contact pressure q [kN/m^2] at the middle section of the raft

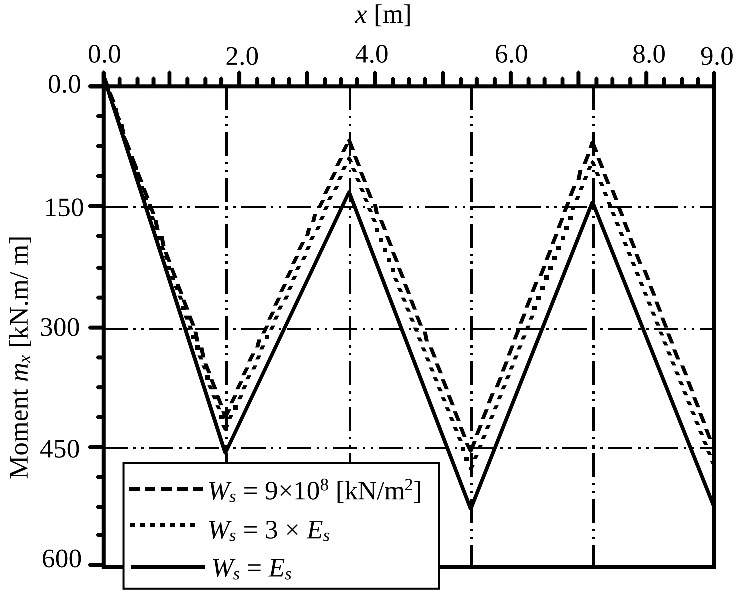

Figure 40 Moment m_x [kN.m/m] at the middle section of the raft

Example 21: Examination of influence of load geometry

1 Description of the problem

A simple example was carried out to show the influence of load geometry on the values of settlements and internal forces for the different subsoil models. To carry out the comparison between the different soil models, three different soil models are used to analyze the raft. The three mathematical models Simple assumption, *Winkler's* and Continuum models are represented by five calculation methods as shown in Table 29.

Table 29 Calculation methods and soil models

Method No.	Calculation method	Soil model
1	Linear contact pressure method	Simple assumption model
2	Modulus of subgrade reaction method	*Winkler's* model
5	Isotropic elastic half-space	Continuum model
7	Modulus of compressibility method	Continuum model
8	Rigid slab	Continuum model

A square raft with the dimensions of 10 × 10 [m^2] is chosen and subdivided into 144 square elements. Each element has dimensions of 0.833 × 0.833 [m^2] yielding to 13 × 13 nodal points for the raft and the soil as shown in Figure 41a.

2 Soil properties

The raft rests on a homogeneous soil layer of thickness 10 [m] equal to the raft length, overlying a rigid base as shown in Figure 41b. The raft thickness is d = 0.4 [m].

The soil material is supposed to have the following parameters:

Modulus of compressibility	E_s	= 10 000	[kN/m^2]
Poisson's ratio	ν_s	= 0.2	[-]
Unit weight	γ_s	= 18	[kN/m^3]

3 Raft material

The raft material is supposed to have the following parameters:

Young's modulus	E_b	= 2 × 10^7	[kN/m^2]
Poisson's ratio	ν_b	= 0.25	[-]
Unit weight	γ_b	= 0.0	[kN/m^3]

Unit weight of the raft is chosen γ_b = 0.0 to neglect the self-weight of the raft.

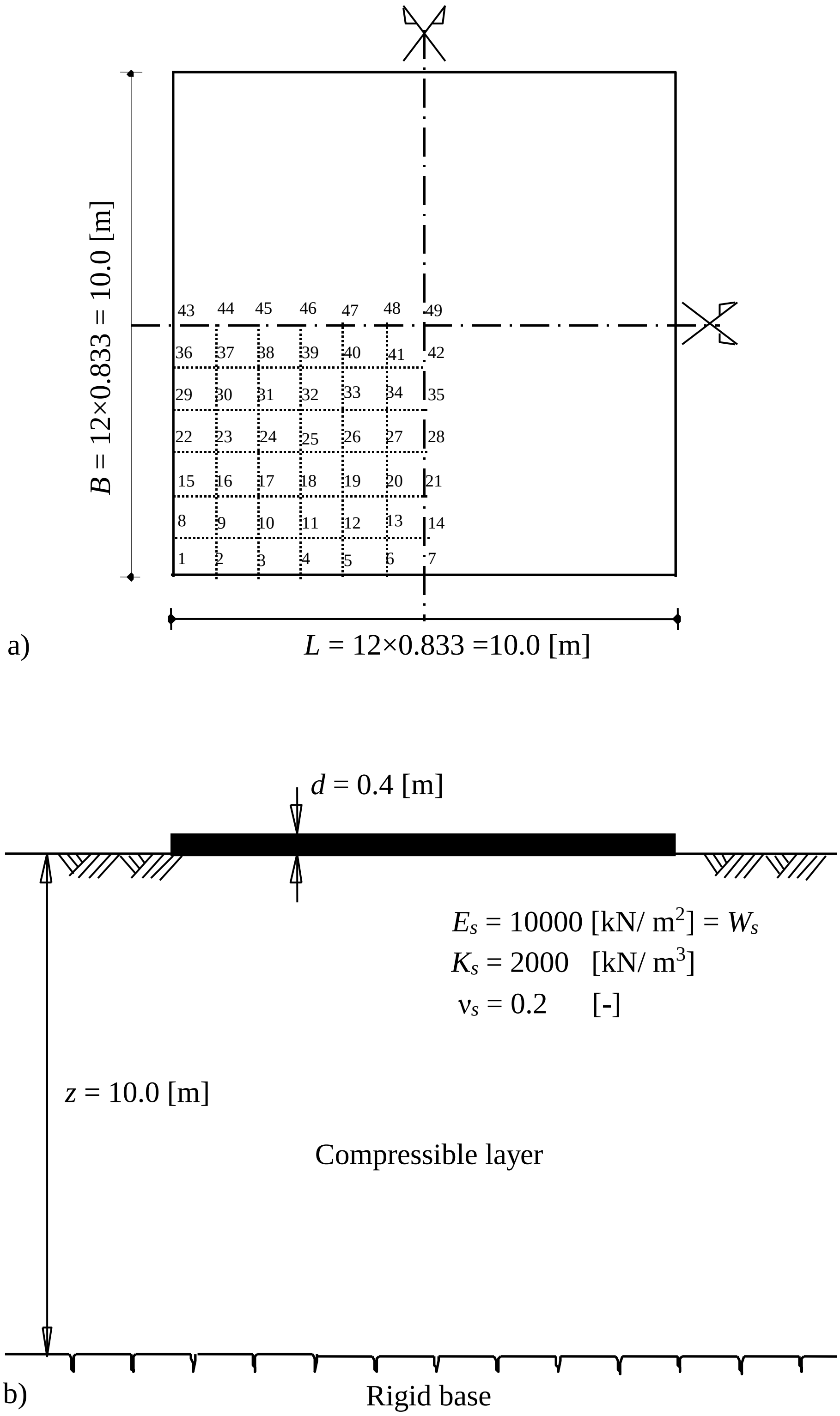

Figure 41 a) Slab numbering and dimensions
b) Soil cross section

4 Loads

To illustrate the raft behavior under various load arrangements, four different types of external load geometry are chosen such that each type gives 2000 [kN] total applied load and average contact pressure 20 [kN/m^2]. In addition, all loading cases are supposed to be symmetrical about the raft axes as shown in Figure 42.

The four load geometries are:

(a): A uniform load of intensity 20 [kN/m^2] on the entire raft
(b): Four inner loads, each 500 [kN]
(c): A concentrated central load 2000 [kN]
(d): Four corner loads, each 500 [kN]

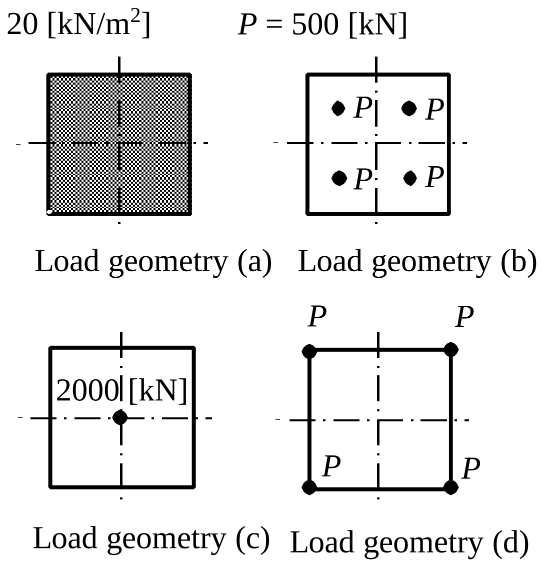

Figure 42 Arrangement of loads in the load cases (a) to (d)

5 Analysis of the raft

Taking advantage of the symmetry in shape and load geometry about both *x*- and *y*-axes, the analysis was carried out by considering only a quarter of the raft (Figure 41a). There is a total of only 49 nodal points; each node has three unknown displacements. Therefore, the total number of equations is reduced to 147.

5.1 Examination sections

For evaluation and comparison of the mathematical models, the numerical results for the four load geometries (a) to (d) were presented at three selected sections of the raft as follows:

Section I-I: at the edge of the raft (nodes 1 - 7)
Section II-II: at the quarter of the raft (nodes 22 - 28)
Section III-III : at the middle of the raft (nodes 43 - 49)

5.2 Mathematical models

The analysis was carried out by the modulus of Compressibility method 7 first and then the same raft with the same load geometries was analyzed using Simple assumption model 1, *Winkler's* model 2, Isotropic elastic half-space model 5 and Rigid slab 8.

5.3 Modulus of subgrade reaction

To make a comparison between *Winkler's* model and Continuum model the modulus of subgrade reaction was taken here so as to give nearly the same value for the average settlement, which was calculated by the Continuum model 7. This value for the modulus of subgrade reaction which is assumed to be constant at all foundation nodes is k_s = 2000 [kN/ m^3].

6 Results

6.1 Figures

The results of this example are plotted in Figure 43 to Figure 52 as follows:

- Figure 43 to Figure 45 show the settlements *s* (or deformation) at the middle of the raft (section III-III) for the four load geometries (a) to (d)

- Figure 46 to Figure 48 show the contact pressures *q* at edge of the raft (section I-I) for the four load geometries (a) to (d)

- Figure 49 to Figure 52 show the moments m_x in the three critical sections I, II and III of the raft for the four load geometries (a) to (d). From the assumption of the rigid slab, moments cannot be calculated. Therefore, moments in these figures are plotted only for methods 1, 2, 5 and 7

6.2 Tables

Furthermore, the results of this example are tabulated. Table 30 to Table 31 show the maximum values of the settlements s_{max} and the contact pressures q_{max} at the critical nodes by application of the different subsoil models for the four types of load geometries. The results of five calculation methods are given in these tables in order to observe the difference clearly.

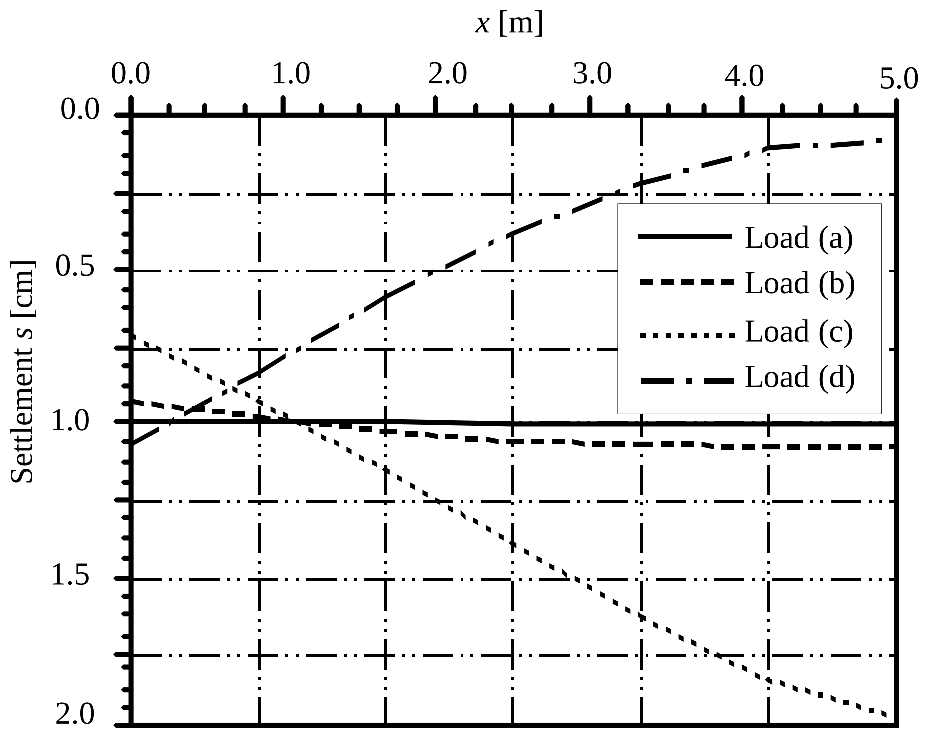

Figure 43 Settlement *s* [cm] at the middle section of the raft (method 2)

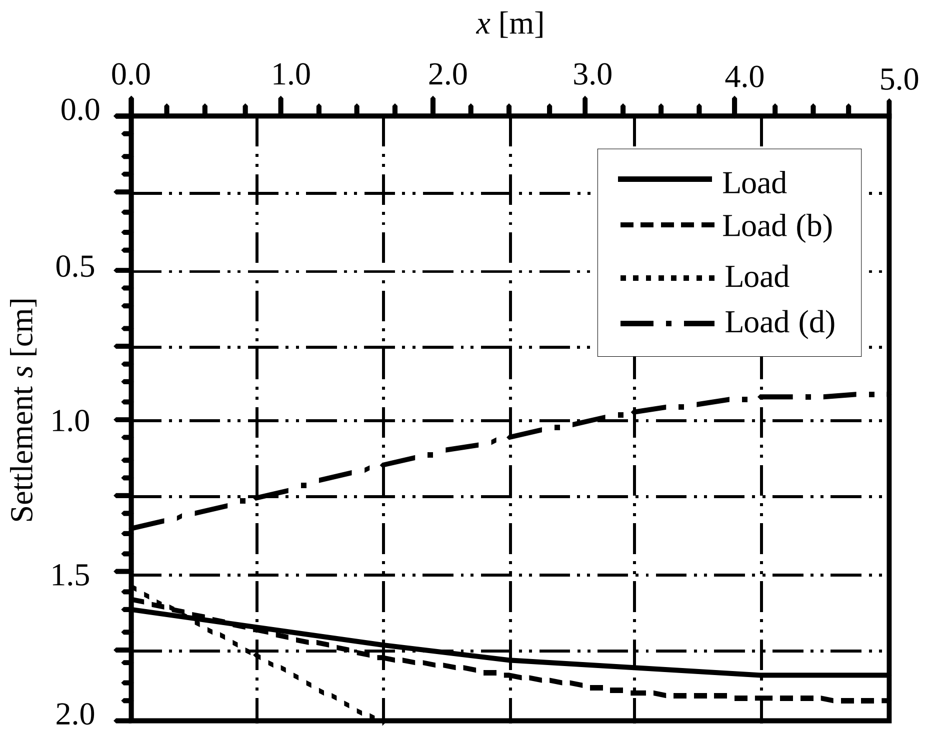

Figure 44 Settlement *s* [cm] at the middle section of the raft (method 5)

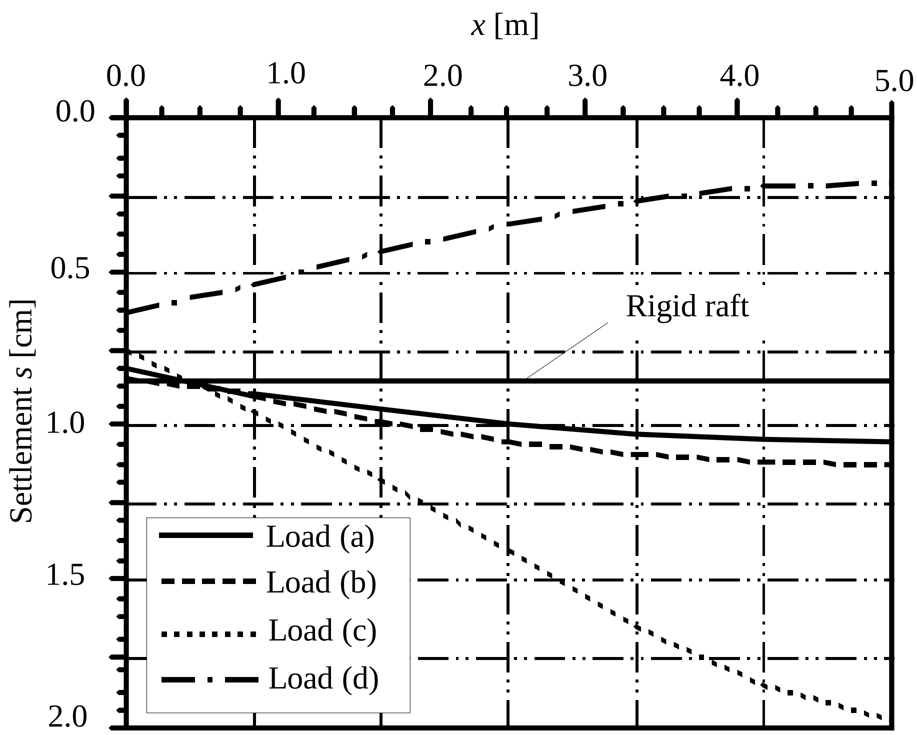

Figure 45 Settlement s [cm] at the middle section of the raft (methods 7 and 8)

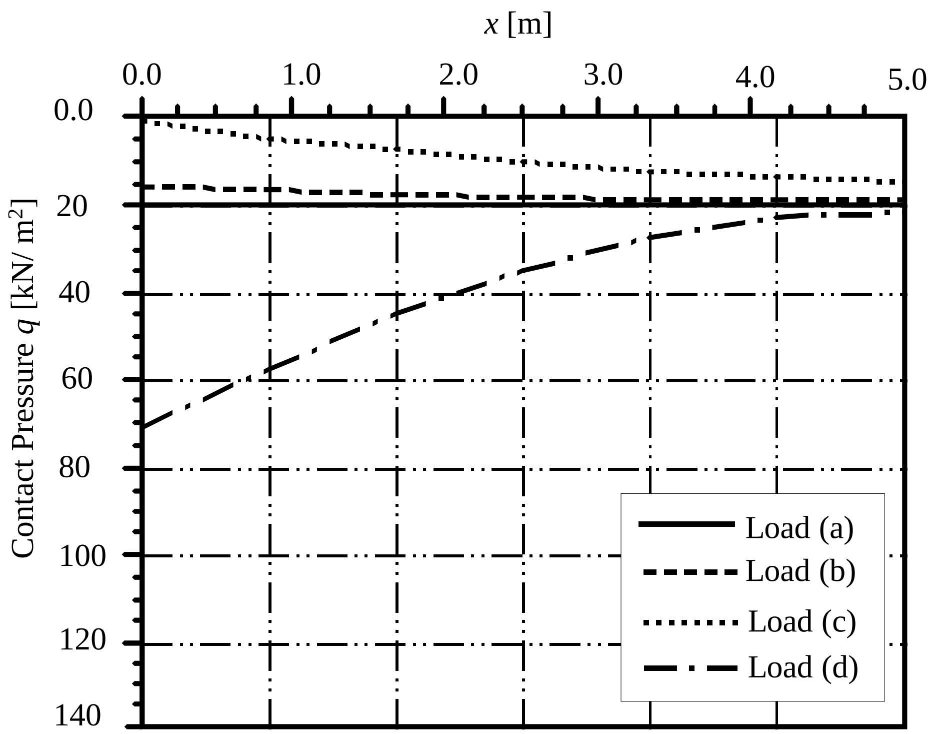

Figure 46 Contact pressure q [kN/m^2] at the raft edge (method 2)

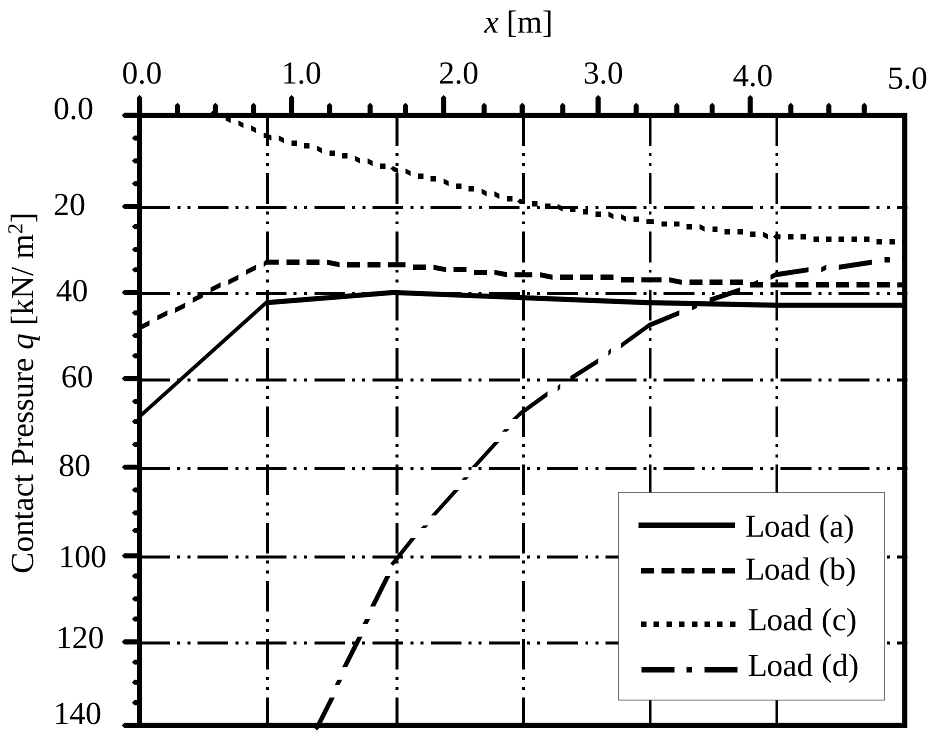

Figure 47 Contact pressure q [kN/m^2] at the raft edge (method 5)

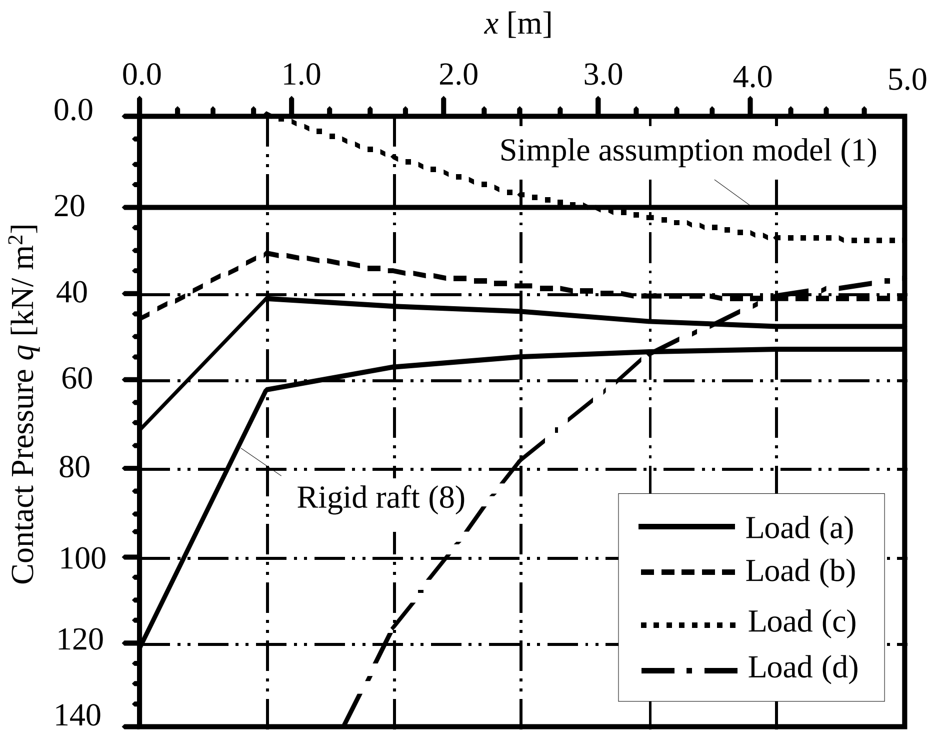

Figure 48 Contact pressure q [kN/m^2] at the raft edge (methods 1, 7 and 8)

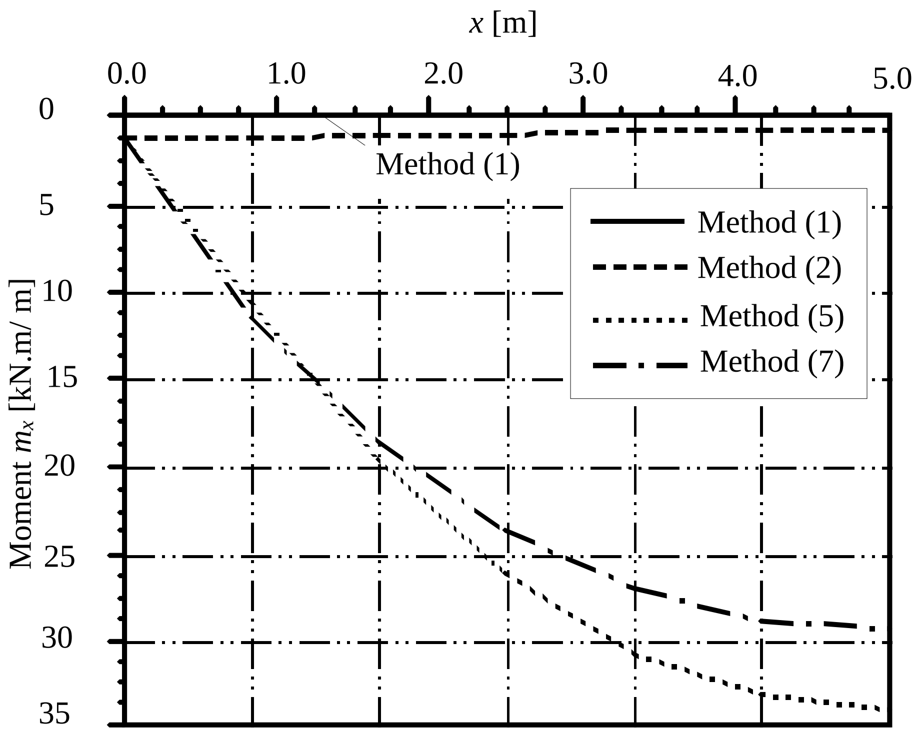

Figure 49 Moment m_x [kN.m/ m] at section III-III by application of different soil models, load geometry (a)

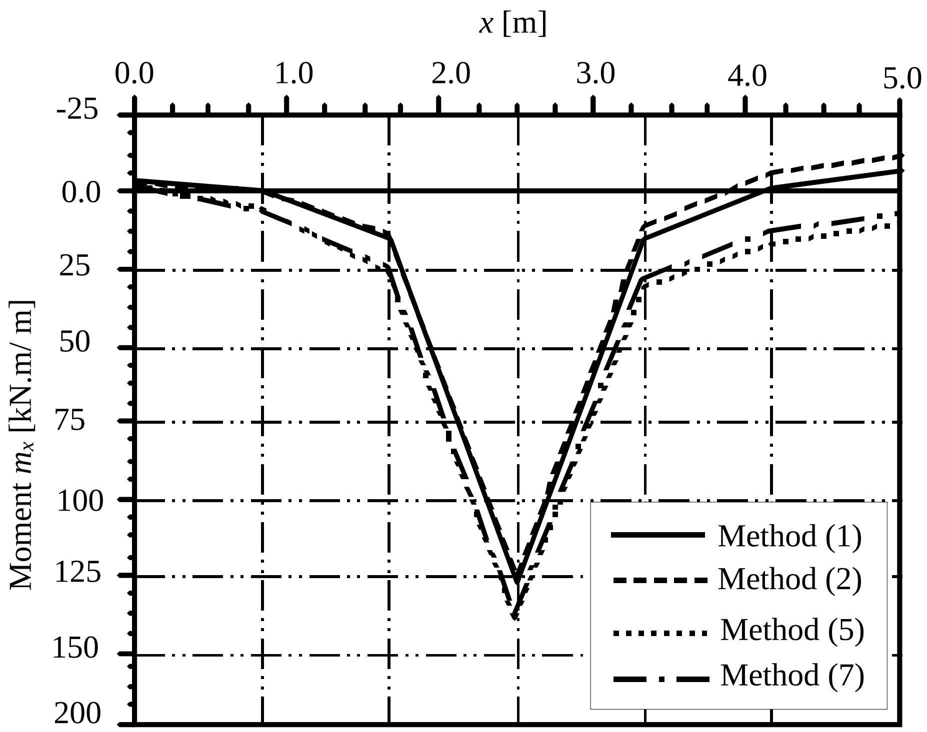

Figure 50 Moment m_x [kN.m/m] at section II-II by application of different soil models, load geometry (b)

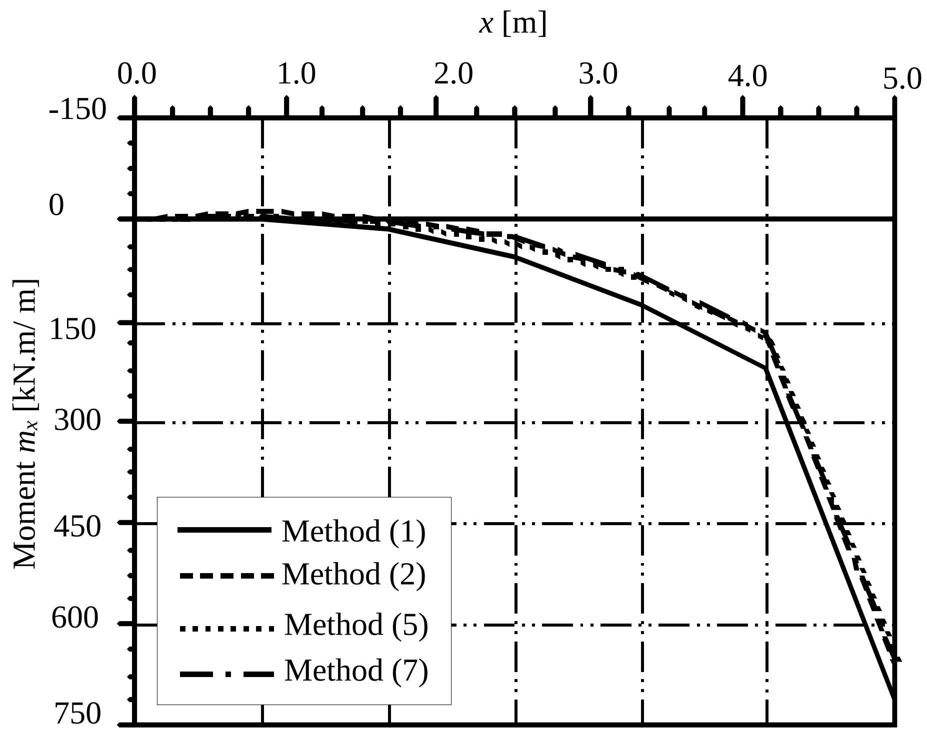

Figure 51 Moment m_x [kN.m/m] at section III-III by application of different soil models, load geometry (c)

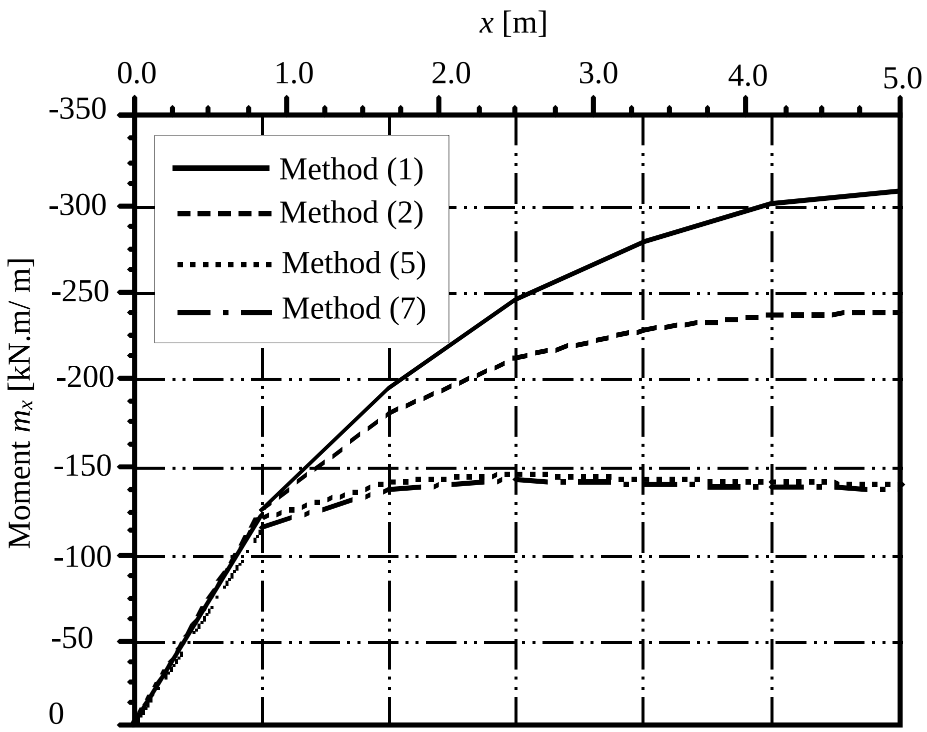

Figure 52 Moment m_x [kN.m/m] at section I-I by application of different soil models, load geometry (d)

Table 30 Maximum settlement *s* [cm] at critical nodes by applying calculation methods 2, 5, 7 and 8

Calculation method	Load geometry			
	(a)	(b)	(c)	(d)
Method 2	1.00 Center	1.08 center	1.96 center	3.57 corner
Method 5	1.86 Center	1.94 center	2.83 center	2.97 corner
Method 7	1.06 Center	1.12 center	1.97 center	2.20 corner
Method 8	0.85 all nodes	0.85 all nodes	0.85 all nodes	0.85 all nodes

Table 31 Maximum contact pressures *q* [kN/m^2] at critical nodes by applying calculation methods 1, 2, 5, 7 and 8

Calculation method	Load geometry			
	(a)	(b)	(c)	(d)
Method 1	20 all nodes	20 all nodes	20 all nodes	20 all nodes
Method 2	≈20 all nodes	22 center	39 center	71 corner
Method 5	68 corner	48 corner	51 center	360 corner
Method 7	71 corner	46 corner	58 center	442 corner
Method 8	121 corner	121 corner	121 corner	121 corner

7 Evaluation of the results

Settlement *s*

- Because the Simple assumption model (method 1) has no interaction between the soil and the raft, the soil settlement cannot be calculated

- For the elastic raft (methods 2, 5 and 7), the settlement distribution is concentrated near the external loads

- The Rigid raft (method 8) under the four types of external loads has a uniform settlement of s = 0.85 [cm] on the entire raft

- It is clear that the maximum differential settlement is due to load geometry (c) and the minimum is due to load geometry (a) for methods 2, 5 and 7, while for method 8 (Rigid raft) the settlement is uniform

- Isotropic elastic half-space (method 5) shows a higher settlement than that of method 7 due to the assumption of infinite thickness of the compressible soil layer by method 5

- The little difference between the results of both method 5 and that of method 7 is due to the compressible soil layer of this example is relatively thick ($z = L$)

Contact pressure *q*

- The Rigid raft (method 8) shows that the contact pressure is the same for the four types of external loads

- By load geometry (a), the Continuum model (methods 5, 7 and 8) shows that the distribution of the contact pressure is very different from that resulting of Simple assumption model (method 1) and *Winkler's* model (method 2)

- By load geometry (a), the distribution of the contact pressure by Simple assumption model (method 1) and *Winkler's* model (method 2) are nearly in agreement and equal to the applied load intensity 20 [kN/m^2] on the entire raft

- The Simple assumption model (method 1) for the four types of external loads has a uniform contact pressure of 20 [kN/m^2] on the entire raft

- For the methods 2, 5, 7 and 8, which have interaction between the soil and the raft, the values of contact pressure are different from a section to another

- For the elastic raft (methods 2, 5 and 7), the contact pressure is concentrated near the external loads

- For the elastic raft (methods 2, 5 and 7), the contact pressure near the load is higher for methods 5 and 7 than that for method 2

- The Continuum model (methods 5, 7 and 8) would predict contact pressure of infinite magnitude beneath the edges of the raft. Especially, if the raft is small or is loaded heavily at the middle

Moment *m*

- Applying methods 1 and 2 for analyzing load geometry (a) - uniform load on the raft -, gives also a uniform contact pressure. Therefore, there are no moments or shear forces on the raft. Thus, indicating the behavior of the raft by applying method 1 is similar to that of method 2 by this type of loading

- The high moment at the center of the raft by Continuum model (methods 5 and 7) is due to the high ordinates of the contact pressure distribution at the edge of the raft

- Figure 50 and Figure 51 show little difference between the results of moment by method 2 and that of methods 5 and 7 in case of load geometry (b) and (c), in spite of the contact pressure distribution is not the same for the three methods

- For load geometry (d), the maximum negative moment is small for higher values of contact pressure at the raft edges and high for smaller values of contact pressure at the raft edges. Therefore, the maximum negative moment for method 1 is higher than that of methods 2, 5 and 7

- It is clear that the maximum moment is due to load geometry (c) and the minimum is due to load geometry (a) for methods 1, 2, 5 and 7, while for method 8 (Rigid raft) the moment cannot be calculated

It can be concluded from the above comparisons that to be on the safe side, it is recommended to use the type of soil model for analysis of the raft according to the suitable case of study as shown in Table 32.

Table 32 Recommended soil model according to the suitable case

Case	Designing soil model
Uniform load on the entire raft	Continuum model (methods 5 or 7)
Edge loads	*Winkler's* model (method 2)
Small foundation	Simple assumption model (method 1) or *Winkler's* model (method 2)
Thin compressible soil layer over rigid base	*Winkler's* model (method 2)
Heavily loaded raft at the middle	Simple assumption model (method 1) or *Winkler's* model (method 2)
Influence of external foundation	Continuum model (methods 5,7 and 8)
Subsoil of different soil material	Continuum model (methods 7 or 8)
Influence of temperature change	Continuum model (methods 5 and 7) or *Winkler's* model (method 2)
Influence of the superstructure	Continuum model (methods 5 and 7) or *Winkler's* model (method 2)
Influence of tunneling or additional settlement	Continuum model (methods 5,7 and 8) or *Winkler's* model (2)
Very weak soil or a thick raft	Continuum model (method 8)
Infinite thickness of soil layer	Continuum model (method 5)

Example 22: Settlement calculation under flexible foundation of an ore heap

1 Description of the problem

In many cases, it is required to determine the settlement under an embankment, a metal plate foundation of a liquid tank, loads on small isolated plates or a raft of thin thickness. In these cases, the foundation will be assumed as flexible foundation.

Figure 53 shows an ore heap on thin concrete pavement slabs. The pavement slabs are connected with each other by movable joints. Consequently, the pavement slabs are considered as completely flexible foundation. The unit weight of the ore material is γ = 30 [kN/m^3].

The foundation base under the ore heap has the dimensions of 13 × 13 [m^2], while the top area of the ore heap has the dimensions of 9 × 9 [m^2]. The height of the ore heap is 4.0 [m] (Figure 53a). It is required to determine the expected settlement due to the ore heap.

2 Soil properties

The pavement slabs rest on two different soil layers of sand and clay as shown in Figure 53b. The modulus of compressibility of the sand is E_{s1} = 60 000 [kN/m^2], while for the clay is E_{s2} = 6000 [kN/m^2]. *Poisson's* ratio of the soil is taken to be ν_s = 0.2 [-].

3 Loads

In the analysis, the pressure on the foundation is estimated as a uniform pressure at the foundation middle and four areas of irregular distributed pressures near the foundation sides as shown in Figure 54. The middle pressure is $p = \gamma\, h$ = 30 × 4.0 = 120 [kN/m^2].

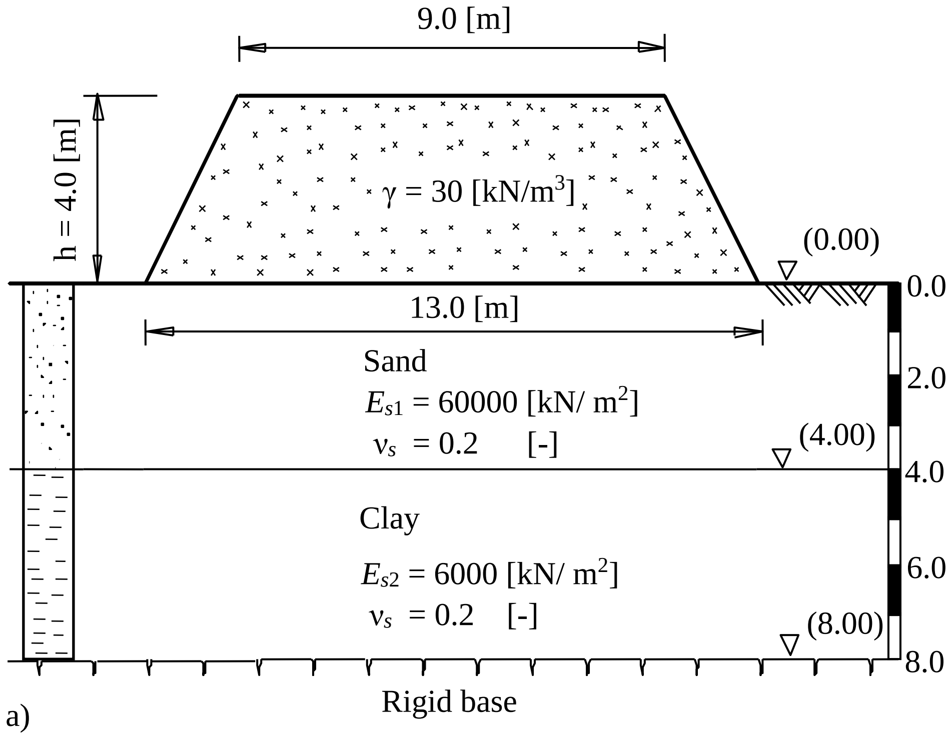

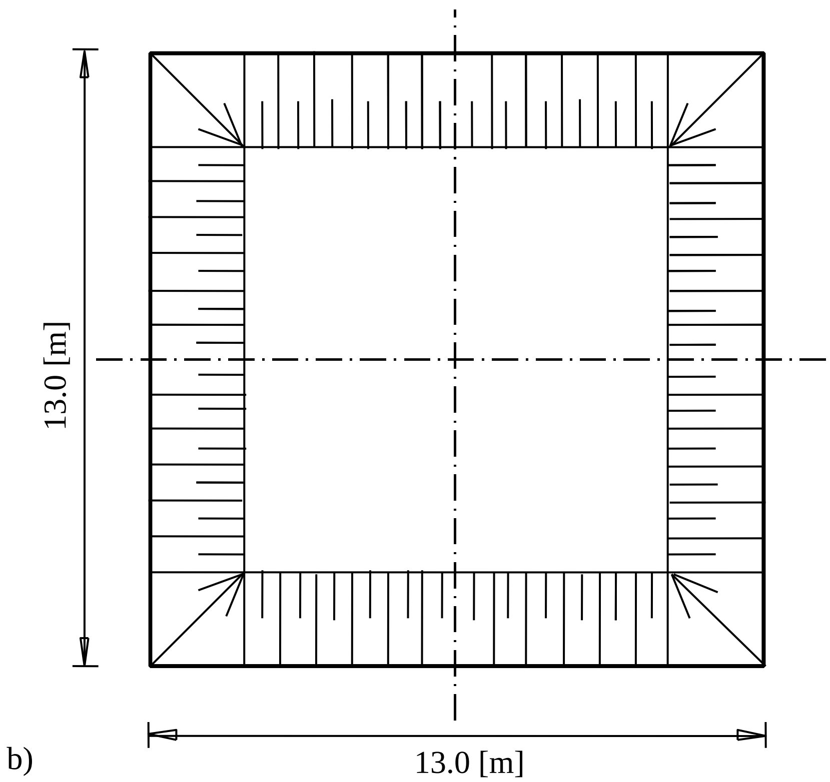

Figure 53 a) Section elevation in soil and the ore heap

b) Plan of the ore heap

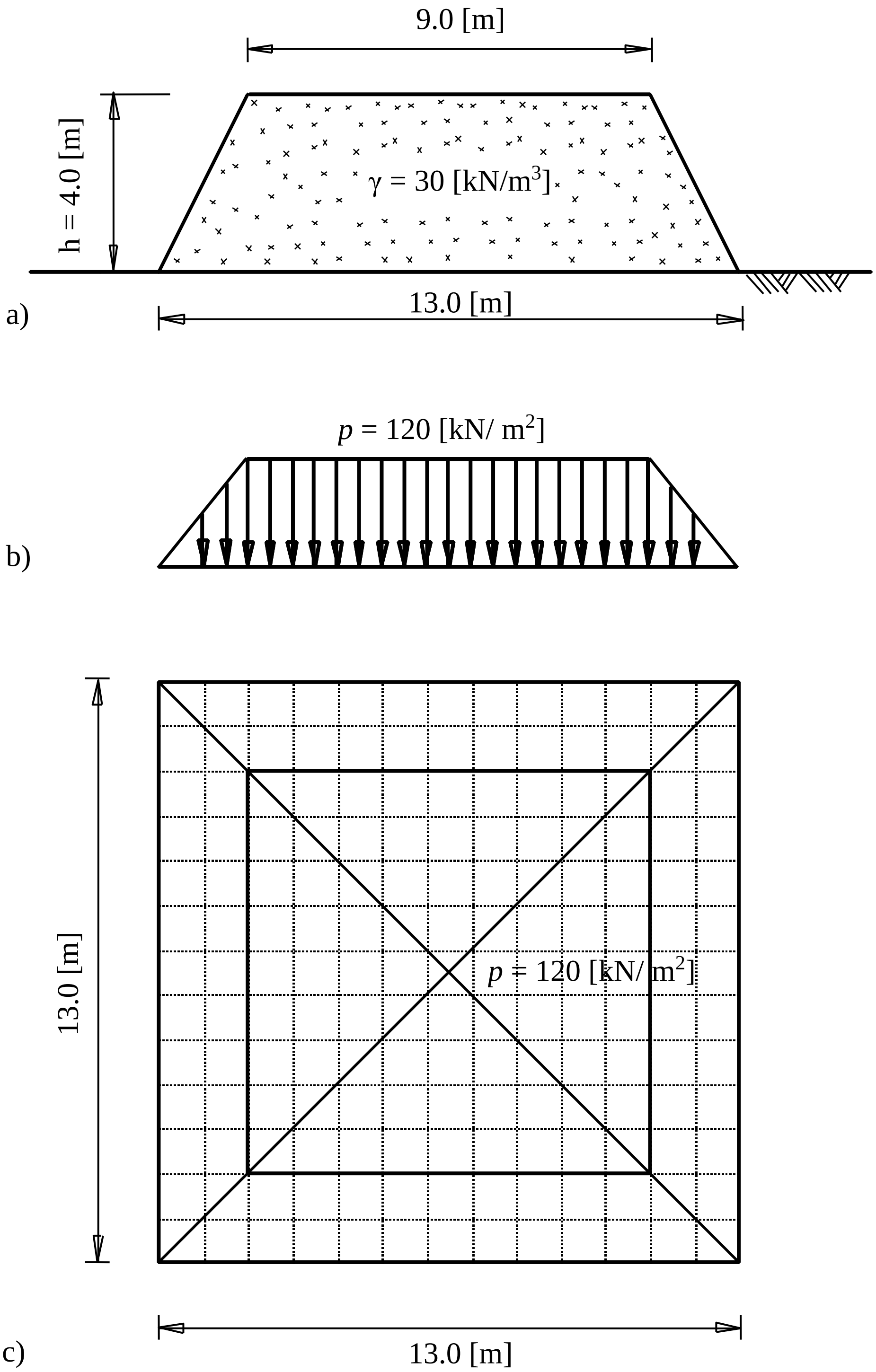

Figure 54 a) Equivalent ore heap mass

b) Pressures on foundation

c) FE-Net

4 Analysis of the foundation

If the foundation is perfectly flexible such as in this example, then the contact stress will be equal to the gravity stress exerted by the foundation on the underlying soil. To carry out the settlement calculation of flexible foundation, the available calculation method "Flexible foundation 9" in *ELPLA* is used to analyze the foundation. A net of equal square elements is chosen. Each element has a side of 1.0 [m] as shown in Figure 54c.

5 Results

Figure 55b shows the contour lines of settlement under the ore heap, while Figure 55a shows minimum and maximum settlement curves. From these figures, it can be concluded that the maximum settlement is s_{max} = 5.78 [cm] at the center of the ore heap while the minimum settlement is s_{min} = 1.25 [cm] at the corners. The settlement difference is Δs = 4.53 [cm], which gives 78 [%] from the maximum settlement.

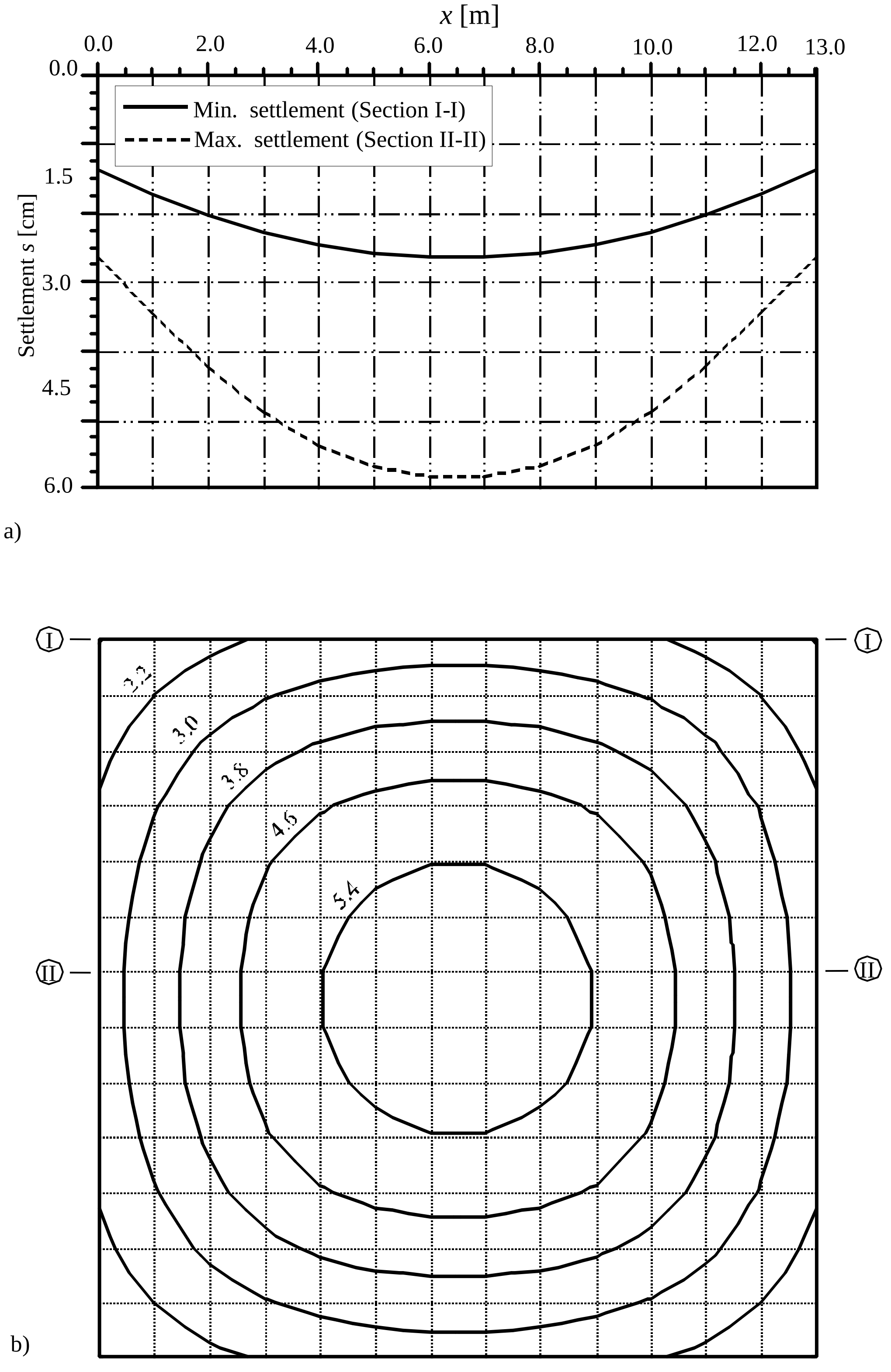

Figure 55 a) Min./ Max. settlement s [cm] at section I and II

b) Contour lines of settlement s [cm]

Example 23: Settlement calculation for a rigid raft subjected to an eccentric load

1 Description of the problem

In many cases, it is required to determine the settlement under an abutment, a bridge pier, a building core or a raft of thick thickness. In these cases, the foundation will be assumed as rigid foundation.

As an example for rigid rafts, consider the rectangular raft of a core from concrete walls shown in Figure 56 as a part of 93.0 [m] structure. The length of the raft is L = 28.0 [m], while the width is B = 25.0 [m]. Due to the lateral applied wind pressure, the raft is subjected to an eccentric vertical load of P = 142000 [kN]. Figure 56 shows section elevation through the raft and subsoil, while Figure 57 shows a plan of the raft, load, dimensions and mesh. It is required to estimate the expected settlement if the raft is considered as perfectly rigid.

2 Soil properties

The raft rests on four different soil layers of stiff plastic clay, middle hard clay, sand and limestone, overlying a rigid base as shown in Figure 56 and Table 33. *Poisson's* ratio is constant for all soil layers and is taken ν_s = 0.0 [-], while unit weight of the soil is γ_s = 13.6 [kN/m^3]. The foundation level of the raft is 11.0 [m] under the ground surface. The level of ground water is 11.0 [m] under the ground surface equal to the foundation level. Therefore, there is no effect for uplift pressure on the raft.

Table 33 Soil properties

Layer No.	Type of soil	Depth of layer under ground surface z [m]	Modulus of compressibility for	
			Loading E_s [kN/ m^2]	Reloading W_s [kN/ m^2]
1	Stiff plastic clay	13	25200	85800
2	Middle hard clay	16	27500	104100
3	Sand	21	31400	133200
4	Limestone	41	44400	209200

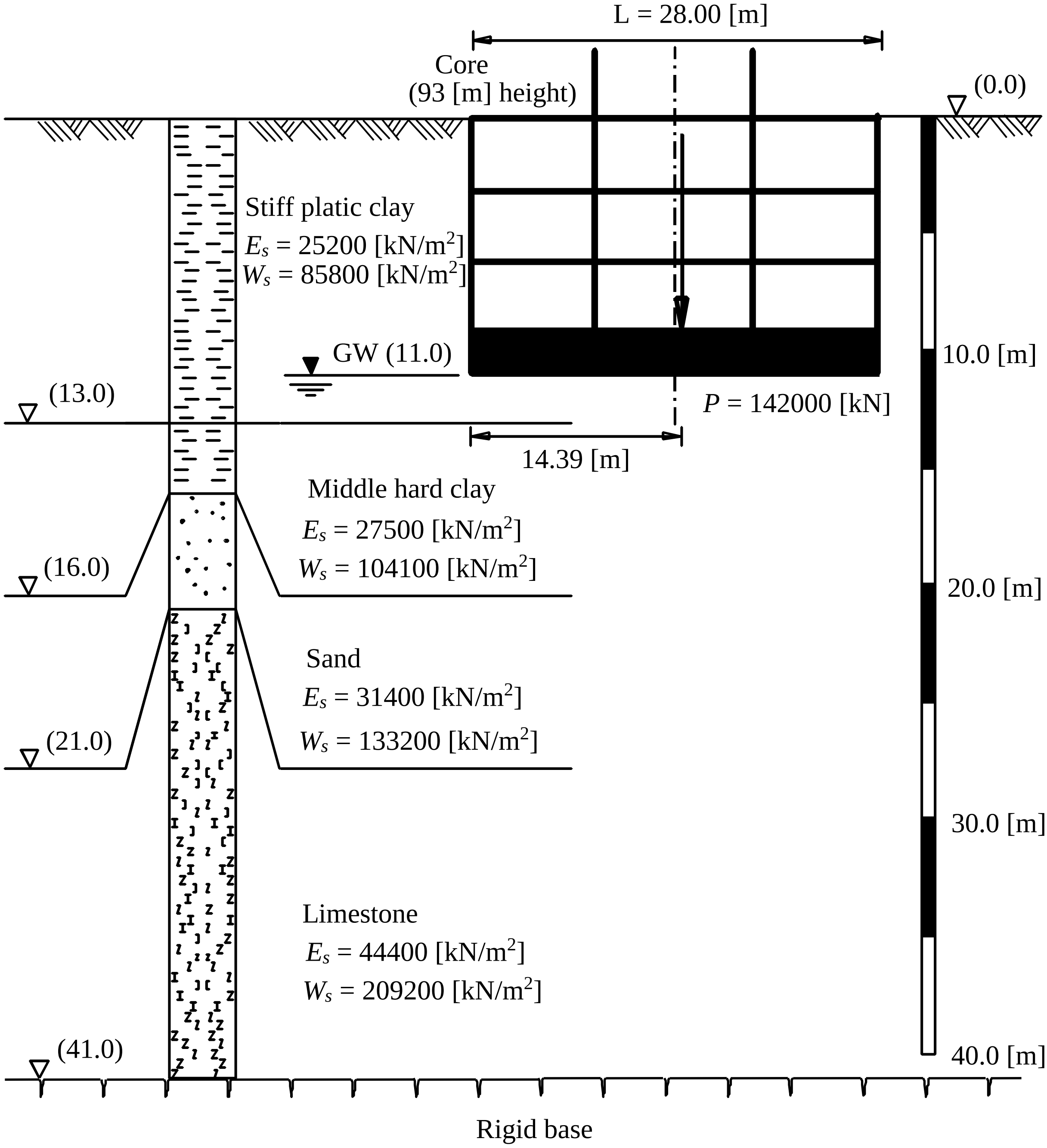

Figure 56 Section elevation through the raft and subsoil

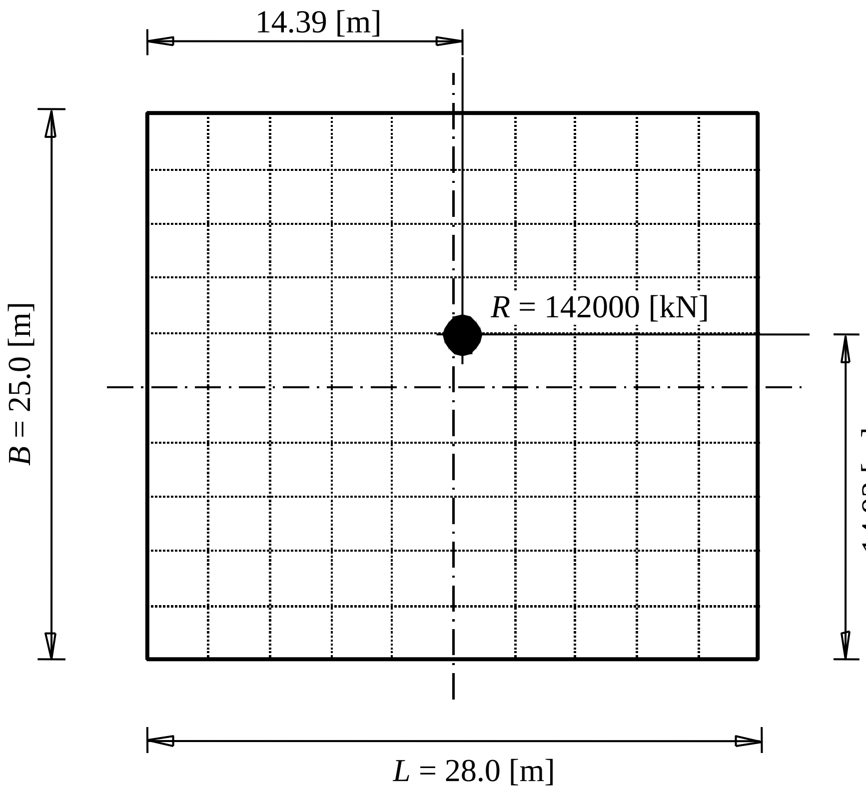

Figure 57 Raft dimensions, load and FE-Net

3 Analysis of the raft

If the raft is perfectly rigid and subjected to an eccentric vertical load, the settlement will be distributed linearly on the bottom of the raft. To carry out the settlement calculation of perfectly rigid raft, the available calculation method "Rigid slab 8" in *ELPLA* is used to analyze the raft. In the analysis of rigid raft, only the settlement is required. Therefore, a coarse finite element net may be used. Here, a coarse net of rectangular elements is chosen. Each element has dimensions of 2.5 [m] × 2.8 [m] as shown in Figure 57.

4 Results

Figure 57b shows the contour lines of settlement under the raft, while Figure 58a shows minimum and maximum settlement curves. From these figures, it can be concluded that the maximum settlement is s_{max} = 6.27 [cm] at the right up corner of the raft, while the minimum settlement is s_{min} = 0.50 [cm] at the left down corner. The settlement difference is Δs = 5.77 [cm], which gives 92 [%] from the maximum settlement.

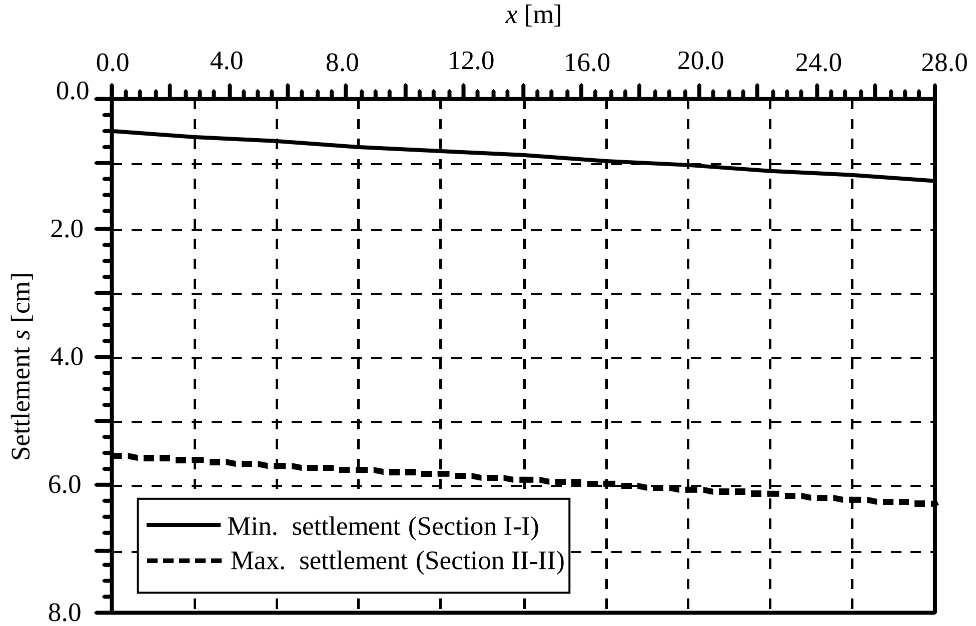

a)

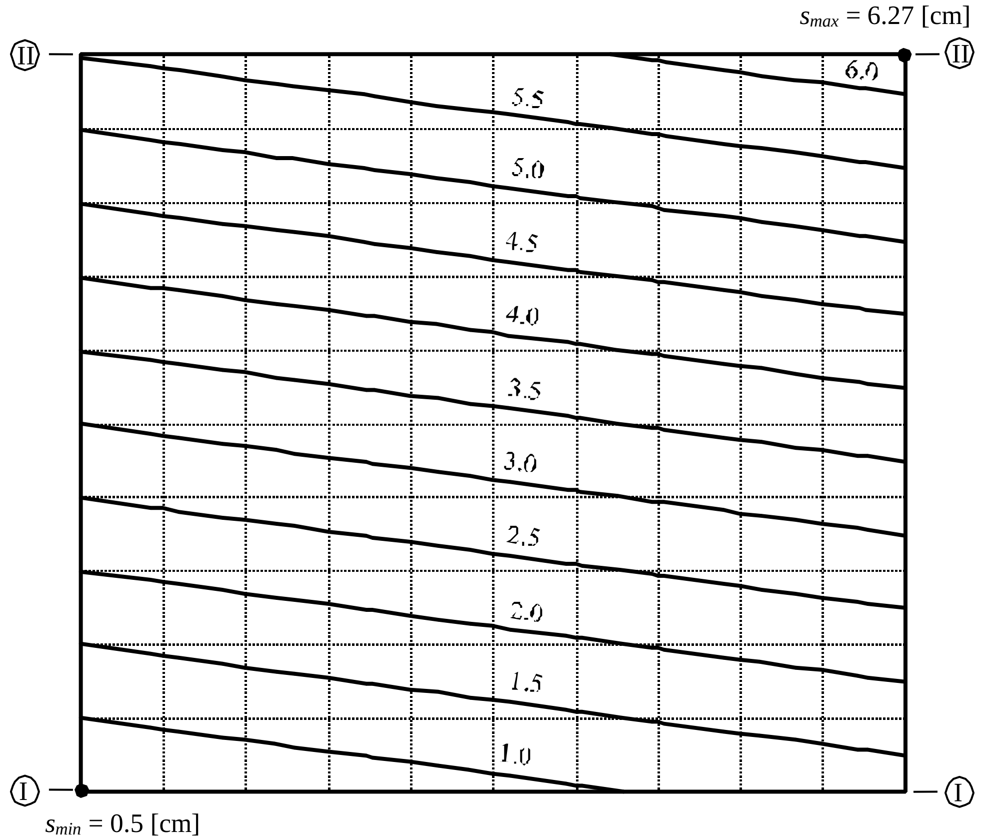

b)

Figure 58 a) Min./ Max. settlement *s* [cm] at section I and II

b) Contour lines of settlement *s* [cm]

Example 24: Verifying deflection of a thin cantilever beam

1 Description of the problem

To verify the mathematical model of *ELPLA* for computing plane stresses, results of a cantilever beam having a thin rectangular cross section introduced by *Timoshenko/ Goodier* (1970), Example 21, page 41, are compared with those obtained by *ELPLA*. The cantilever carries a point load of P = 150 [kN] applied at the end as shown in Figure 59.

2 Cantilever dimensions

The cantilever has the following dimensions:

Cantilever length	L = 6.0	[m]
Cross section depth	h = 1.6	[m]
Cross section width	b = 0.2	[m]

3 Cantilever material

Material of the cantilever has the following parameters:

Young's modulus	E_b	$= 2.0 \times 10^7$	[kN/m^2]
Poisson's ratio	ν_b	= 0.15	[-]
Unit weight	γ_b	= 0	[kN/m^3]

The self-weight of the cantilever is ignored.

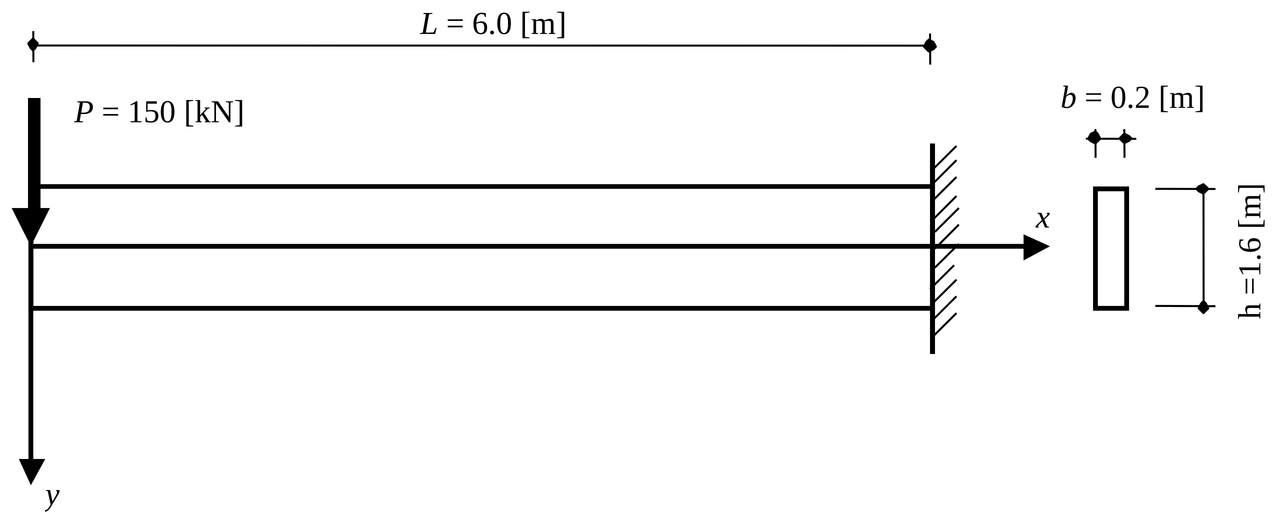

Figure 59 Cantilever beam loaded at the end

4 Analysis and Results

Because the cross section of the cantilever is thin, the cantilever may be considered as a plane stress problem. According to *Timoshenko*/ *Goodier* (1970), the equation of the deflection curve is expressed as:

$$(w)_{y=0} = \frac{Px^3}{6E_bI} - \frac{PL^2x}{2E_bI} + \frac{PL^3}{3E_bI} \qquad (19)$$

where:

w Vertical deflection of the centerline of the cantilever [m]
x Distance of deflection from the free end [m]
P End load [kN]
E_b *Young's* modulus of the cantilever material [kN/m^2]
L Cantilever length [m]
I Moment of inertia of the cantilever cross section [m^4]

Results of *ELPLA* are compared with the exact solution using Eq. 19 in Table 34. From this table, it can be noticed that results of deflection obtained by *ELPLA* are the same as those obtained from Eq. 19. A sufficient accuracy for results obtained by *ELPLA* may be considered at mesh size of 0.2 × 0.2 [m].

Table 34 Comparison of vertical deflection obtained by *ELPLA* and Eq. 19

Distance x [m]	Deflection obtained from Eq. 19	Deflection obtained by *ELPLA*		
		Mesh size		
		0.1×0.1 [m^2]	0.2×0.2 [m^2]	0.3×0.3 [m^2]
0	0.007910	0.008205	0.007895	0.007339
0.6	0.006728	0.006960	0.006709	0.006241
1.2	0.005569	0.005781	0.005572	0.005183
1.8	0.004457	0.004648	0.004480	0.004167
2.4	0.003417	0.003585	0.003455	0.003215
3	0.002472	0.002615	0.002521	0.002346
3.6	0.001645	0.001763	0.001699	0.001582
4.2	0.000961	0.001050	0.001013	0.000944
4.8	0.000443	0.000502	0.000484	0.000452
5.4	0.000115	0.000141	0.000136	0.000127
6	0.0000000	0.0000000	0.000000	0.0000000

Example 25: Verifying forces in piles of a piled group

1 Description of the problem

To verify the mathematical model of *ELPLA* for determining pile forces of pile groups under a pile cap, results of a pile group obtained by *Bakhoum* (1992), Example 5.19, page 592, are compared with those obtained by *ELPLA*.

A pile cap on 24 vertical piles is considered as shown in Figure 60. It is required to determine the force in each pile of the group due to a vertical load of N = 8000 [kN] acting on the pile cap with eccentricities e_x = 1.4 [m] and e_y = 1.8 [m] in both x- and y-directions.

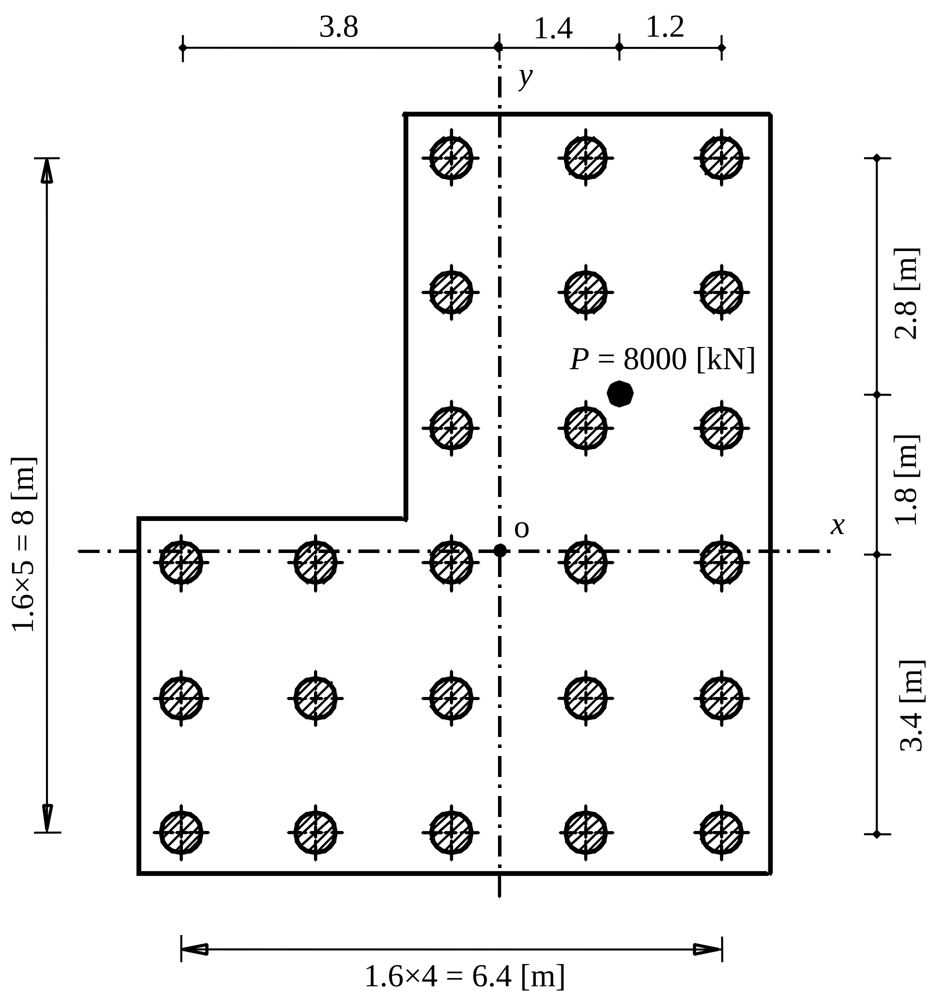

Figure 60 Pile cap dimensions and pile arrangements

The simple assumption model assumes a linear distribution of contact pressure on the base of the foundation. In general case of vertical piles under a pile cap forming linear contact forces, the force in any pile, analogous to *Navier's* solution, can be obtained from

$$P_i = \frac{N}{n} + \frac{M_y I_x - M_x I_{xy}}{I_x I_y - I_{xy}^2} x_i + \frac{M_x I_y - M_y I_{xy}}{I_x I_y - I_{xy}^2} y_i \qquad (20)$$

Where $I_x = \sum_1^n y_i^2$, $I_y = \sum_1^n x_i^2$ and $I_{xy} = \sum_1^n x_i y_i$

and:

P_i	Force in pile *i* [kN]
N	Sum of all vertical applied loads on the pile cap [kN]
x_i	Coordinate of pile *i* from the centroidal axis *x* [m]
y_i	Coordinate of pile *i* from the centroidal axis *y* [m]
M_x	Moment due to *N* about the *x*-axis, $M_x = N\, e_y$ [kN.m]
M_y	Moment due to *N* about the *y*-axis, $M_y = N\, e_x$ [kN.m]
e_x	Eccentricity measured from the centroidal axis *x* [m]
e_y	Eccentricity measured from the centroidal axis *y* [m]
n	Number of piles under the pile cap [-]

2 Hand calculation of pile forces

According to *Bakhoum* (1992), the force in each pile in the pile group can be obtained by hand calculation as follows:

Step 1: Compute moments

$M_x = 8000 \times 1.8 = 14400$ [kN.m]

$M_y = 8000 \times 1.4 = 11200$ [kN.m]

Step 2: Compute properties I_x, I_y and I_{xy}

Determining properties of I_x, I_y and I_{xy} are listed in 0.

Table 35 Properties I_x, I_y and I_{xy}

Pile number	x_i [m]	y_i [m]	x_i^2 [m^2]	y_i^2 [m^2]	$x_i\, y_i$ [m^2]
1	-3.8	-3.4	14.44	11.56	12.92
2	-2.2	-3.4	4.84	11.56	7.48
3	-0.6	-3.4	0.36	11.56	2.04
4	1.0	-3.4	1.00	11.56	-3.40
5	2.6	-3.4	6.76	11.56	-8.84
6	-3.8	-1.8	14.44	3.24	6.84
7	-2.2	-1.8	4.84	3.24	3.96
8	-0.6	-1.8	0.36	3.24	1.08
9	1.0	-1.8	1.00	3.24	-1.08
10	2.6	-1.8	6.76	3.24	-4.68
11	-3.8	-0.2	14.44	0.04	0.76
12	-2.2	-0.2	4.84	0.04	0.44
13	-0.6	-0.2	0.36	0.04	0.12
14	1.0	-0.2	1.00	0.04	-0.20
15	2.6	-0.2	6.76	0.04	-0.52
16	-0.6	1.4	0.36	1.96	-0.84
17	1.0	1.4	1.00	1.96	1.40
18	2.6	1.4	6.76	1.96	3.64
19	-0.6	3.0	0.36	9.00	-1.80
20	1.0	3.0	1.00	9.00	3.00
21	2.6	3.0	6.76	9.00	7.80
22	-0.6	4.6	0.36	21.16	-2.76
23	1.0	4.6	1.00	21.16	4.60
24	2.6	4.6	6.76	21.16	11.96
$\sum$			I_y = 106.56	I_x = 170.56	I_{xy} = 43.2

Step 3: Compute pile force

The force P_i in any pile i at location (x_i, y_i) from the geometry centroid is obtained from

$$P_i = \frac{N}{n} + \frac{M_y I_x \text{-} M_x I_{xy}}{I_x I_y \text{-} I_{xy}^2} x_i + \frac{M_x I_y \text{-} M_y I_{xy}}{I_x I_y \text{-} I_{xy}^2} y_i$$

$$P_i = \frac{8000}{24} + \frac{(11200)(170.56) - (14400)(43.2)}{(170.56)(106.56) - (43.2)^2} x_i + \frac{(14400)(106.56) - (11200)(43.2)}{(170.56)(106.56) - (43.2)^2} y_i$$

$$P_i = 333.333 + 78.988 x_i + 64.421 y_i$$

3 Pile forces by *ELPLA*

The available method "Linear Contact pressure 1@ in *ELPLA* is used to determine the force in each pile in the pile group. A net of equal square elements is chosen. Each element has a side of 1.6 [m]. The pile forces obtained by *ELPLA* are compared with those obtained by *Bakhoum* (1992) in Table 36. It is obviously from this table that pile forces obtained by *ELPLA* are equal to those obtained by hand calculation.

Table 36 Comparison of pile forces obtained by *ELPLA* and Eq. 20

Pile number	*Bakhoum* (1992)						*ELPLA*
	x_i [m]	y_i [m]	N/n [kN]	78.988 x_i [kN]	64.421 y_i [kN]	P_i [kN]	P_i [kN]
1	-3.8	-3.4	333.33	-300.16	-219.03	185.86	-185.85
2	-2.2	-3.4	333.33	-173.77	-219.03	-59.47	-59.47
3	-0.6	-3.4	333.33	-47.39	-219.03	66.91	66.91
4	1.0	-3.4	333.33	78.99	-219.03	193.29	193.29
5	2.6	-3.4	333.33	205.37	-219.03	319.67	319.67
6	-3.8	-1.8	333.33	-300.16	-115.96	-82.79	-82.78
7	-2.2	-1.8	333.33	-173.77	-115.96	43.50	43.60
8	-0.6	-1.8	333.33	-47.39	-115.96	169.98	169.98
9	1.0	-1.8	333.33	78.99	-115.96	296.36	296.36
10	2.6	-1.8	333.33	205.37	-115.96	422.74	422.72
11	-3.8	-0.2	333.33	-300.16	-12.88	20.29	20.29
12	-2.2	-0.2	333.33	-173.77	-12.88	146.68	146.67
13	-0.6	-0.2	333.33	-47.39	-12.88	273.06	273.06
14	1.0	-0.2	333.33	78.99	-12.88	399.44	399.44
15	2.6	-0.2	333.33	205.37	-12.88	525.82	525.82
16	-0.6	1.4	333.33	-47.39	90.19	376.13	376.13
17	1.0	1.4	333.33	78.99	90.19	502.51	502.51
18	2.6	1.4	333.33	205.37	90.19	628.89	628.89
19	-0.6	3.0	333.33	-47.39	193.26	479.20	479.20
20	1.0	3.0	333.33	78.99	193.26	605.58	605.59
21	2.6	3.0	333.33	205.37	193.26	731.96	731.97
22	-0.6	4.6	333.33	-47.39	296.34	582.28	582.28
23	1.0	4.6	333.33	78.99	296.34	708.66	708.66
24	2.6	4.6	333.33	205.37	296.34	835.04	835.04

Example 26: Verifying continuous beam

1 Description of the problem

To verify the mathematical model of *ELPLA* for analyzing continuous beams, results of a continuous beam introduced by *Harry* (1993), Examples 10.2, 10.4 and 10.5, pages 399, 409 and 411, are compared with those obtained by *ELPLA*.

A continuous beam of length L = 35 [m] is chosen as shown in Figure 61. The beam is subjected to a point load of P = 500 [kN] at the center. The beam cross section yields Moment of Inertia I = 0.003 [m^4]. *Young's* modulus of the beam is E_b = 2.0 × 10^8 [kN/m^2].

For the comparison, three different cases are considered as follows:

Case a: Continuous beam with a point load P at the center on supports at points *a*, *b*, *d* and *e*

Case b: Instead of the point load P at the center of the beam, points *a*, *b*, *d* and *e* have the following support settlements: Δ*a* = -2.75 [cm], Δ*b* = -4.75 [cm], Δ*d* = -2.2 [cm] and Δ*e* = -1.0 [cm]

Case c: Points *b* and *d* are supported by elastic springs that have stiffness of $k_{sb} = k_{sd}$ = 3600 [kN/m]

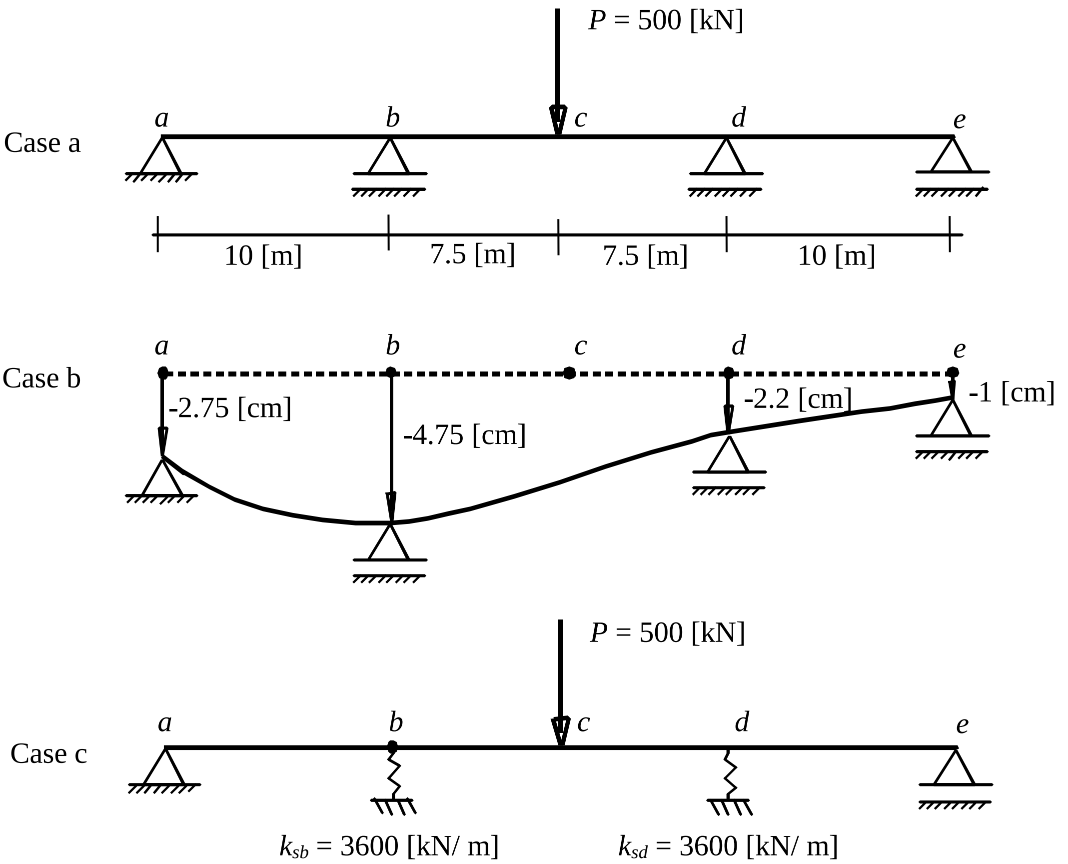

Figure 61 Continuous beam with dimensions and load

2 Comparison of Results

Moments and shear forces for case a obtained by *ELPLA* are compared with those obtained by *Harry* (1993) in Figure 62. Results obtained by *ELPLA* and *Harry* (1993) for case a are the same. Figure 63 compares between moments computed by *Harry* (1993) and *ELPLA* for case b. This figure shows that both results are in a good agreement. For case c, the reaction at the elastic support obtained by *Harry* (1993) and *ELPLA* is equal to 272.9 [kN].

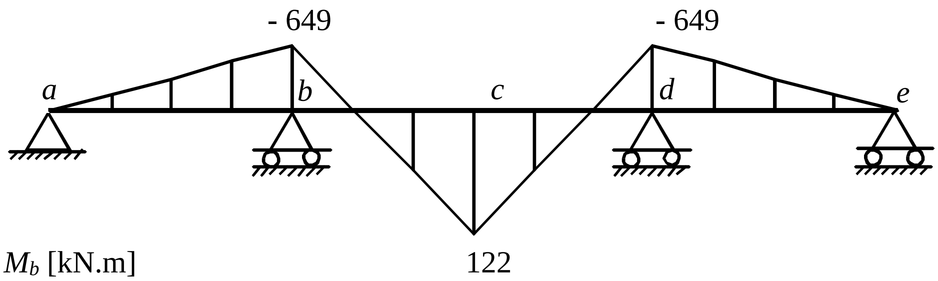

Moments M_b [kN.m]

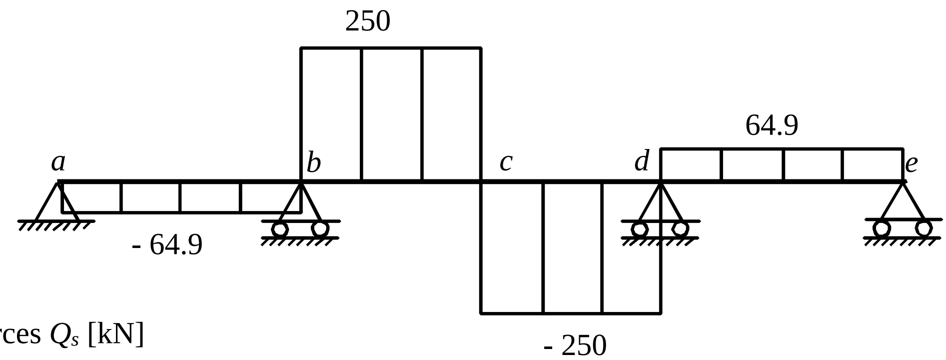

Shear forces Q_s [kN]

Figure 62 Moments and shear forces computed by *Harry* (1993) and *ELPLA* for case a

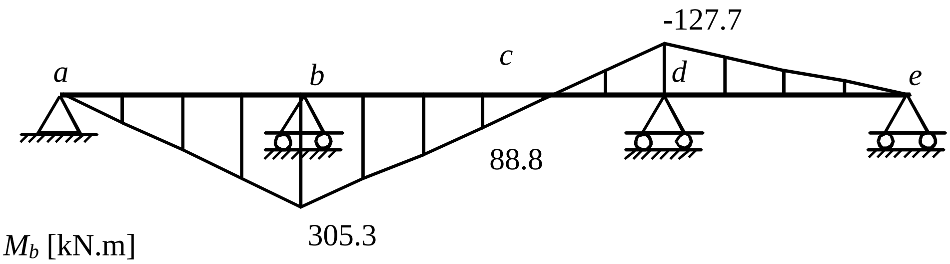

Moment M_b [kN.m]
Harry (1993)

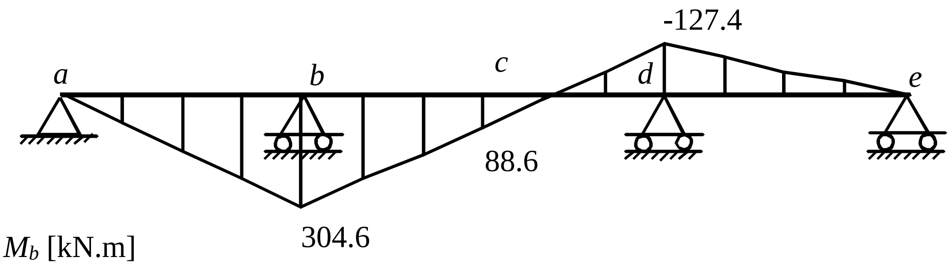

Moment M_b [kN.m]
ELPLA

Figure 63 Comparison of moments computed by *Harry* (1993) and *ELPLA* for case b

Example 27: Verifying moments in an unsymmetrical closed frame

1 Description of the problem

To verify the mathematical model of *ELPLA* for analyzing unsymmetrical closed frames, moments in an unsymmetrical closed frame introduced by *Wang* (1983), Example 15.10.1, page 574 are compared with those obtained by *ELPLA*.

An unsymmetrical closed frame *ABCD* is considered as shown in Figure 64. The frame is subjected to a point load of P = 24 [kN] at the center of the member *BC* and a distributed load of q = 2 [kN/m] on the member *AD.*

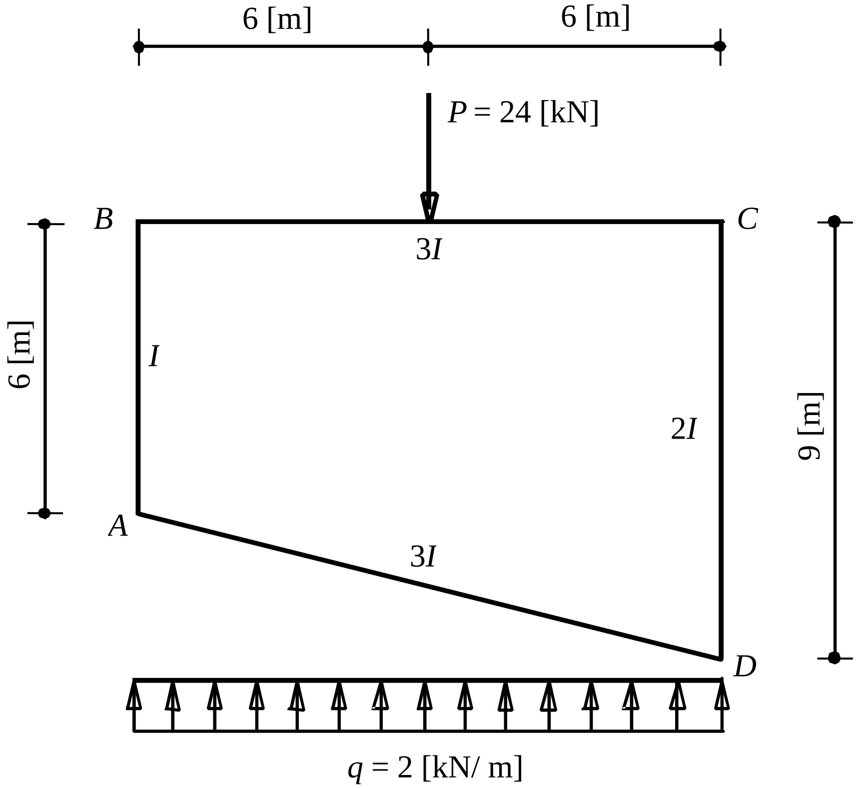

Figure 64 Unsymmetrical closed frame with dimensions and loading

Members have three types of cross sections, which yield moments of Inertia I, $2I$ and $3I$ as shown in Figure 64. Chosen moment of inertia for each type and its corresponding cross section area is listed in Table 37. *Young's* modulus of the frame is assumed to be $E_b = 2.0 \times 10^7$ [kN/m^2].

Table 37 Properties of member types

Member type	Moment of Inertia [m^4]	Cross section area [m^2]
Type 1	0.001	0.032
Type 2	0.002	0.045
Type 3	0.003	0.055

2 Comparison of moments

Moments at points *A*, *B*, *C* and *D* obtained by *ELPLA* are shown in Figure 65 and compared with those obtained by *Wang* (1983) in Table 38. Both moments are in a good agreement.

Table 38 Comparison of moments obtained by *ELPLA* with those obtained by *Wang* (1983)

Point	Moment [kN.m]			
	A	*B*	*C*	*D*
Wang (1983)	-8.50	-14.90	-19.49	-9.89
ELPLA	-8.51	-14.89	-19.47	-9.90

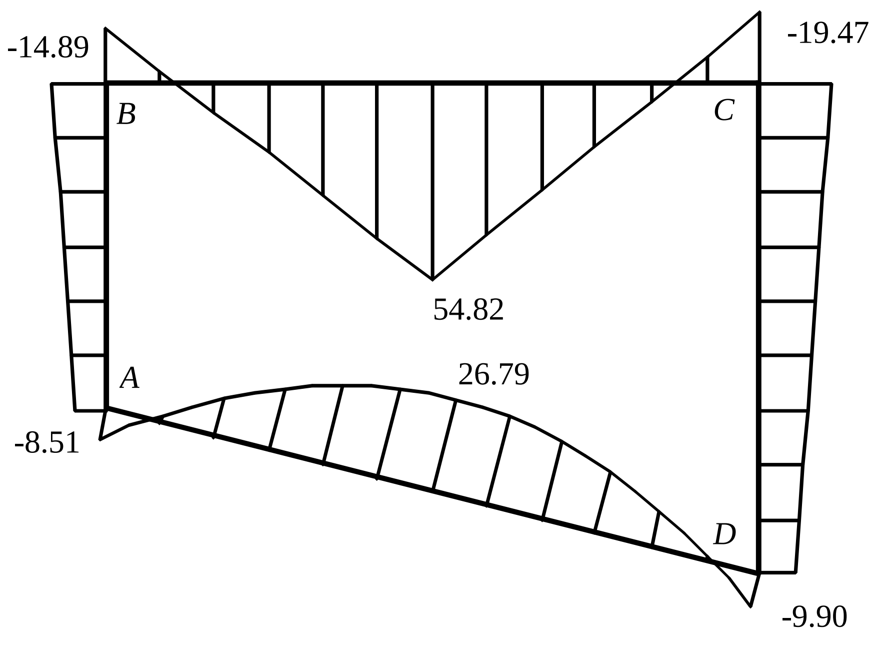

Figure 65 Moments in the unsymmetrical closed frame obtained by *ELPLA*

Example 28: Verifying plane truss

1 Description of the problem

To verify the mathematical model of *ELPLA* for analyzing plane trusses, results of plane truss introduced by *Werkle* (2001), Example 3.1, page 61, are compared with those obtained by *ELPLA*.

A plane truss of 4 nodes and 6 members is considered as shown in Figure 66. Members 5 and 6 are unconnected in their intersection point. The truss is subjected to vertical and horizontal point loads at node 2, each of 10 [kN].

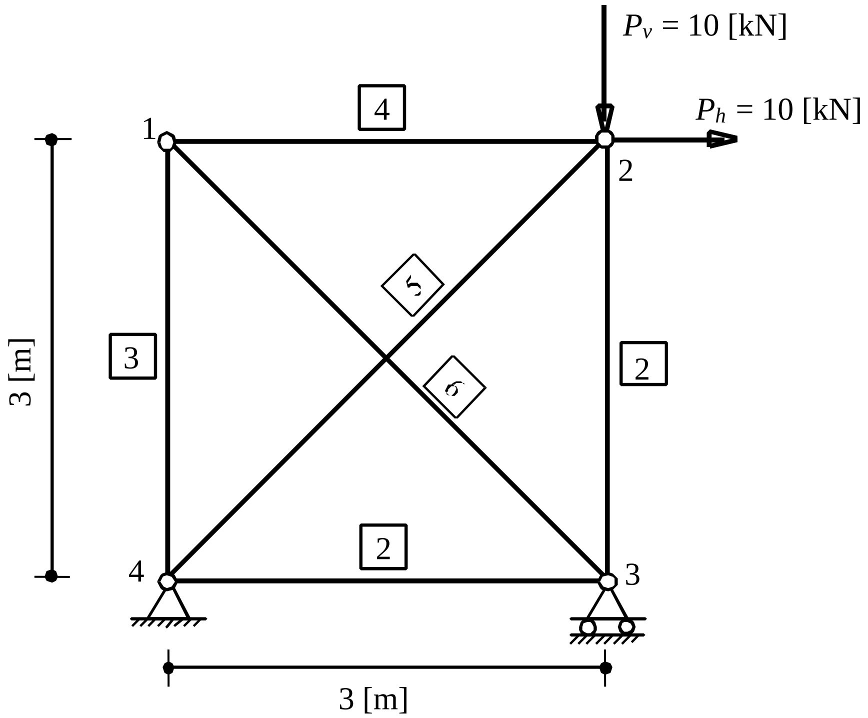

Figure 66 Statical system of plane truss with dimensions and loading

2 Truss properties

The truss has the following properties:

Young's modulus	E_b	= 2.1 × 10^8	[kN/m^2]
Cross-section area of the member	A	= 0.004	[m^2]
Moment of inertia of the member	I	= 0.0016	[m^4]

3 Results

Results obtained by *Werkle* (2001) and *ELPLA* are listed in Table 39 and Table 40. Table 39 shows displacements and reactions in nodes, while Table 40 shows normal forces in members. Both results are the same.

Table 39 Displacements and reactions obtained by *Werkle* (2001) and *ELPLA*

Node	*x*-Displacement [mm]	*y*-Displacement [mm]	*x*-Reaction [kN]	*y*-Reaction [kN]
1	0.086	0.018	-	-
2	0.104	-0.054	-	-
3	0.018	-	-	20
4	-	-	-10	-10

Table 40 Normal forces obtained by *Werkle* (2001) and *ELPLA*

Member	1	2	3	4	5	6
Normal force *N* [kN]	5	-15	5	5	7	-7

Example 29: Influence of *Poisson*'s ratio ν_s

1 Description of the problem

In this example (File q_{e1} with ν_s = 0, q_{e2} with ν_s = 0.2 and q_{e3} with ν_s = 0.5), the influence of *Poisson*'s ratio ν_s on the settlement S of a rectangular raft 10 × 10 [m^2] is studied. Four concentrated loads in the middle of the raft are chosen, each of P = 500 [kN] as shown in Figure 67.

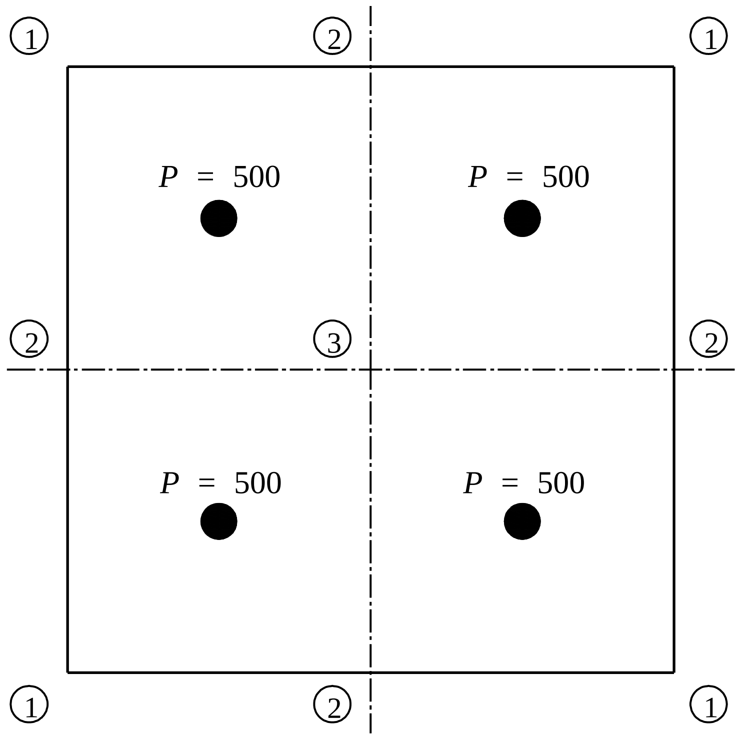

Figure 67 Load locations on the raft

2 Results

Figure 68 shows settlement S [cm] diagram depending on *Poisson*'s ratio ν_s. Accordingly, the settlement of ν_s = 0.0 is the greatest (soil material with free lateral strain), while that of ν_s = 0.5 (material with constant volume) is the smallest. It can be seen that the settlement S at the corner point 1 is always the smallest, while that at the raft center (point 3) is the greatest depending on *Poisson*'s ratio ν_s.

Reference values of *Poisson*'s ratio ν_s for the soil (according to EWB 2003, S. 23):

Material with free lateral strain	$\nu_s = 0.0$
Rock	$\nu_s = 0.1$ to 0.3
Sand	$\nu_s = 0.2$ to 0.35
Clay	$\nu_s = 0.3$ to 0.5
Material with constant volume	$\nu_s = 0.5$

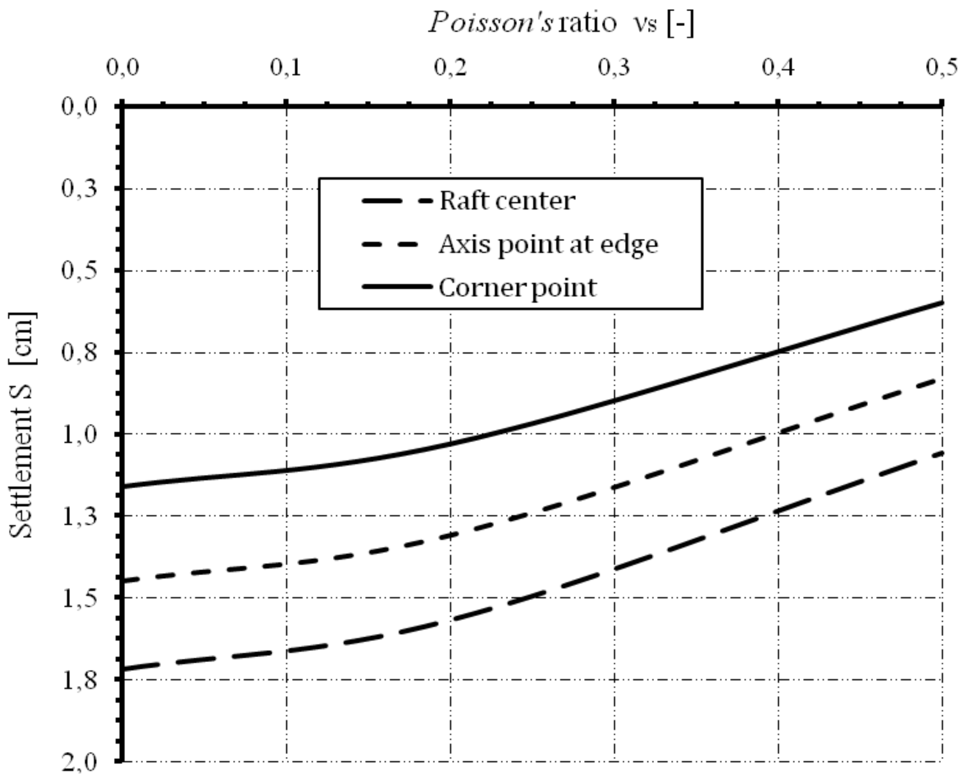

Figure 68 Influence of *Poisson*'s ratio ν_s on the calculation result (Settlement *S* [cm]) for four loads by applying of modulus of compressibility method 7

References

Absi, E. (1970): Étude de problèmes particuliers
Annls Inst. Tech. Bâtim., No. 265, 173-188

Ahlvin, R.G./ Ulery, H.H. (1962): Tabulated Values for Determining the Complete Pattern of Stresses, Strains and Deflections beneath a Uniform Load on a Homogeneous Half Space
Highway Research Board, Bulletin 342

Ahrens, H./ Winselmann, D. (1984): Eine iterative Berechnung von Flächengründungen nach dem Steifemodulverfahren. Finite Elemente Anwendungen in der Baupraxis
Ernst & Sohn, München

Bakhoum, M. (1992): Structural Mechanics
Cairo, Egypt

Bazaraa, A./ Ghabrial N./ Henedy E. (1997): Effect of Boundary Retaining Walls on Raft Behavior
The Third International Geotechnical Engineering Conference, Cairo University, Egypt

Borowicka, H. (1939): Druckverteilung unter elastischen Platten
Ingenieur-Archiv, Band 10, S. 113-125

Bowles, J. (1977): Foundation Analysis and Design
McGraw-Hill, New York

Chow, Y. (1987): Vertical Deformation of Rigid Foundations of Arbitrary Shape on Layered Soil Media
International Journal for Numerical and Analytical Methods in Geomechanics, Vol. 11, 1-15
John Wiley & Sons, Ltd.

Christian, J./ Carrier, W. (1978): Janbu, Bjerrum and Kjaernsli Chart Reinterpreted
Canadian Geotech. J., 15 (1), 124

Czerny, F. (1955): Tafeln für gleichmäßig vollbelastete Rechteckplatten
Bautechnik-Arch., 11
Ernst & Sohn, Berlin

Das, B. (1983): Advanced Soil Mechanics
McGraw-Hill Book Company, Washington, New York, London

DIN 1045, Ausgabe Juli (1988): Bemessung und Ausführung
Stahlbeton- und Spannbetonbau. Beton und Stahlbeton
Beuth Verlag GmbH, Berlin

DIN 1075, April (1981): Betonbrücken. Bemessung und Ausführung
Beuth Verlag GmbH, Berlin

DIN 4017 (1979): Teil 1 Baugrund. Grundbruchberechnungen von lotrecht mittig belasteten Flachgründungen
Beuth Verlag GmbH, Berlin

DIN 4018 (1981): Erläuterungen und Berechnungsbeispiele.
Berechnung der Sohldruckverteilung unter Flächengründungen
Beuth Verlag GmbH, Berlin

DIN 4019 (1974): Teil 1 Baugrund. Setzungsberechnungen bei lotrechter, mittiger Belastung
Beuth Verlag GmbH, Berlin

DIN 4023, März (1984): Baugrund- und Wasserbohrungen.
Zeichnerische Darstellung der Ergebnisse
Beuth Verlag GmbH, Berlin

EWB (2003): Empfehlungen "Wechselwirkungen Baugrund/ Bauwerk bei Fachgründungen"
Beuth Verlag GmbH, Berlin

Fadum, R. (1948): Influence Values for Estimating Stress in Elastic Foundations
Proceedings 2nd International Conference S.M.F.E., Vol. 3, Rotterdam

Falter, B. (1992): Statikprogramme für Personalcomputer, 4. neubearb. u. erw. Aufl.
Werner-Verlag GmbH, Düsseldorf

Fraser, R./ Wardle, L. (1976): Numerical Analysis of Rectangular Rafts on Layered Foundations
Géotechnique 26, No. 4, 613-630

El Gendy, M. (1994): Comparing Examinations of the Influence of Calculation Methods of Basement Slabs
Suez Canal University, Ph.D. Thesis, Egypt

El Gendy, M. (1998): An Iteration Method for Design of Slab on Elastic Foundation
Proc. of the first International Conf. on Civil Engineering, Helewan University, Cairo, Egypt

El Gendy, M. (1998): An analysis for determination of foundation rigidity
Eighth International Colloquium on Structural and Geotechnical Engineering, Ain Shams University, Cairo, Egypt

El Gendy, M. (1999): Effect of Girders on the Raft Rigidity
1st International Conf. for Advanced Trends in Engineering, Minia University, Minia, Egypt

El Gendy, M. (2003): Numerical Modeling of Rigid Circular Rafts on Consolidated Clay Deposits
Int. Workshop on Geotechnics of Soft Soils - Theory and Practice
Vermeer, Schweiger, Karstunen & Cudny (eds.)

Gorbunov-Possadov, M./ Serebrjanyi, R. (1961): Design of Structures on Elastic Foundations
Proceedings of the Fifth International Conference on Soil Mechanics and Foundation Engineering, Vol. 1, 643-648, Paris

Graig, R. (1978): Soil Mechanics, Second Edition
Van Nostrand Reinhold Company, England

Graßhoff, H. (1955): Setzungsberechnungen starrer Fundamente mit Hilfe des kennzeichnenden Punktes
Der Bauingenieur, S. 53-54

Graßohff, H./ Kany, M. (1997): Grundbau-Taschenbuch Teil 3, 5. Auflage
Ernst & Sohn, Berlin, München

Harry, H. (1993): Fundamentals of Structural Analysis
John Wiley & Sons, Inc., New York

Henedy, E. (1987): Raft Foundation Provided with Boundary Retaining Walls
Ph.D. Thesis, Cairo University, Egypt

Janbu, N./ Bjerrum, L./ Kjaernsli, B. (1956): Norwegian Geotechnical Inst. Publication No. 16

Kany, M. (1974): Berechnung von Flächengründungen, 2. Auflage
Ernst & Sohn, Berlin

Kany, M./ El Gendy, M. (1993): Vergleichende Untersuchung über numerische Modelle für die Berechnung von Gründungsplatten
Theorie und Praxis numerischer Modelle in der Bodenmechanik, Sonthofen
Herausgeber: TU Graz

Kany, M./ El Gendy, M. (1995): Computing of Beam and Slab Foundations on Three Dimensional Layered Model
Proc. of the Sixth Intern. Conference on Computing in Civil and Building Engineering, Berlin

Kany, M./ El Gendy, M. (1996): Sicherheitsuntersuchungen bei Flächengründungen nach EC7/ DIN 1054
Forschungsbericht an IFBT, Berlin

Kany, M./ El Gendy, M. (1996): Berechnung von Flächengründungen
Unterlagen zu den TAW-Seminaren, Nürnberg

Kany, M./ El Gendy, M. (1997): Analysis of System of Footing Resting on Irregular Soil
Proceeding of the XIV the International Conference on Soil Mechanics and Foundation Engineering, Hamburg

Kany, M./ El Gendy, M. (1999): Berechnung von großen Systemen starrer Sohlplatten
Bauingenieur, Bd. 74, Nr. 11, S. 471-478

Kany, M./ El Gendy, M. (2000): Einfluss der Bauwerkssteifigkeit auf das Fundamentsystem
2. Kolloquium, Bauen in Boden und Fels, Technische Akademie Esslingen, Ostfildern, Germany

Kany, M./ El Gendy, M. (2002): Berechnung von Fundamenten auf nichtlinearem Baugrund
3. Kolloquium, Bauen in Boden und Fels, Technische Akademie Esslingen, Ostfildern, Germany

Li, H./ Dempsey, J. (1988): Unbounded Contact of a Square Plate on an Elastic Half-Space or a Winkler Foundation
Journal of Applied Mechanics, 55, 430-436

Mikhaiel, S. (1978): Soil Structure Interaction in Multi-Story Buildings
Ph.D. Thesis, Cairo University, Egypt

Newmark, M. (1935): Simplified Computation of Vertical Pressures in Elastic Foundation
University of Illinois Engineering Experiment Station, Circular 24

Rombach, G. (2000): Anwendung der Finite-Elemente-Methode im Betonbau
Ernst & Sohn, Berlin

Scott, C. (1974): An Introduction to Soil Mechanics and Foundations
Applied Science Publishers Ltd, London

Stark, R. (1990): Beitrag zur Numerischen Behandlung des Kontaktproblems beliebig Orthogonal berandeter Fundamentplatten unter Einbeziehung von Grenzzuständen in Boden
Dissertation Uni Innsbruck

Stark, R./ Majer, J. (1988): Soil-Structure Interaction - A possibility for Elastic-Plastic Calculation of Foundation Slabs
Numerical Methods in Geomechanics, volume 2, pp. 1135-1141, Innsbruck

Steinbrenner, W. (1934): Tafeln zur Setzungsberechnung
Straße, S. 121-124

Szilard, R./ Ziesing, D./ Pickhardt, S. (1986): BASIC-Programme für Baumechanik und Statik
Ernst & Sohn, Berlin

Terzaghi, K. (1970): Theoretical Soil Mechanics
John Wiley and Sons, New York

Timoshenko, S./ Goodier, J. (1970): Theory of Elasticity, Third edition
McGraw-Hill, Inc.

Wang, C. (1983): Intermediate Structural Analysis
McGraw-Hill Book Company, New York

Werkle, H. (2001): Finite Elemente in der Baustatik
Frieder Vieweg & Sohn Verlagsgesellschaft mbH, Braunschweig/ Wiesbaden